AN INVESTIGATION INTO AIR STABLE ANALOGUES OF WILKINSON'S CATALYST

By

Serina Naicker

Submitted in fulfilment of the academic requirements for the degree of

Master of Science at the

School of Chemistry

University of KwaZulu-Natal

Durban

South Africa

2010

As the candidate's supervisor I have approved this thesis for submission

_____   _____

Name   Date

_____

Signature

ABSTRACT

Since the discovery of Wilkinson's catalyst and its usefulness in the homogeneous hydrogenation of olefins many investigations have been carried out on trivalent, tertiary phosphine–rhodium complexes.[1] Studies have shown that N-Heterocyclic carbenes as ligands offer increased stability to the complex and possess similar electronic properties as phosphine ligands.[2]

The applications of the traditional catalyst are limited due to the limited stability of its solutions and its susceptibility to attack from the environment i.e. oxygen and moisture. The hydrogenation of olefins and other unsaturated compound is of great importance for the fine chemical and petroleum industries. The aim is to produce more stable and active versions of the traditional catalyst and also to demonstrate their improved stability and activity in catalytic applications.

This study involves the investigation of the effects of ligand modification on Wilkinson type hydrogenation catalysts. Five Rhodium-phosphine complexes **1a**: $Rh(PPh_3)_3Cl$, **1b**: $Rh(PPh_2Me)_3Cl$, **1c**: $Rh(PPh_2Et)_3Cl$, **1d**: $Rh(PPhMe_2)_3Cl$, **1e**: $Rh(PPhMe_2)_3Cl$ have been synthesised and characterised by means of melting point, ^{1}H NMR, ^{13}C NMR, ^{31}P NMR, IR and Mass Spectroscopy. Complexes **1d** and **1e** have also been characterised by means of elemental analysis and single crystal XRD.

Five rhodium-*N*-heterocyclic carbene complexes **2a**: Rh(COD)ImesCl [Imes =1,3-bis(2,4,6-trimethylphenyl)imidazol-2-ylidene] , **2b**: $Rh(COD)(diisopropylphenyl)_2Cl$ **2c**: $Rh(COD)(adamantyl)_2Cl$, **2d**: $Rh(COD)(diisopropyl)_2Cl$ **2e**: $Rh(COD)(ditertbutyl)_2Cl$ have been synthesised and characterised by means of melting point, ^{1}H NMR, ^{13}C NMR, IR and Mass Spectroscopy.

Five rhodium-NHC-CO complexes **3a:** $Rh(CO)_2ImesCl$**, 3b:** $Rh(CO)_2(diisopropylphenyl)_2Cl$, **3c:** $Rh(CO)_2(adamantyl)_2Cl$, **3d:** $Rh(CO)_2(diisopropyl)_2Cl$**, 3e:** $Rh(CO)_2(ditertbutyl)_2Cl$, have been synthesised and characterised by means of ^{1}H NMR, ^{13}C NMR, IR and Mass Spectroscopy.

Complexes **1a, 1d, 1e, 2a, 2b, 2c, 2d, 2e** were tested in the hydrogenation of simple alkenes under mild conditions. For the rhodium-phosphine complexes the catalyst efficiency based on TOF increases in the following order: **1a > 1d > 1e** or $RhCl_3(PPhMe_2)_3$ > $RhCl_3(PPhEt_2)_3$ > $RhCl(PPh_3)_3$. For the rhodium-(COD)-NHC complexes catalyst efficiency based on TOF increases in the following order: **2d > 2b > 2e > 2a > 2c.**

While rhodium-phosphine complexes are far more active than rhodium-(COD)-NHC complexes, the latter seem to be active for a longer time and hence more stable under mild hydrogenation conditions.

PREFACE

The experimental work described in this thesis was carried out in the School of Chemistry, University of KwaZulu-Natal, from April 2008 to March 2010, under the supervision of Dr. Muhammad D. Bala and Prof. Holger B. Friedrich.

These studies represent original work by the author and have not otherwise been submitted in any form for any degree or diploma to any tertiary institution. Where use has been made of the work of others it is duly acknowledged in the text.

DECLARATION 1

PLAGIARISM

I, Serina Naicker, declare that:

1. The research reported in this thesis, except where otherwise indicated, is my original work.
2. This thesis has not been submitted for any degree or examination at any other university.
3. This thesis does not contain other person's data, pictures, graphs or other information, unless specifically acknowledged as being sourced from other persons.
4. This thesis does not contain other person's writing unless specifically acknowledged as being sourced from other researchers. Where other written sources have been quoted, then:
    a. Their words have been re-written but the general information attributed to them has been referenced
    b. Where the exact words have been used, then their writing has been placed in italics and inside quotation marks, and referenced.
5. This thesis does not contain text, graphics or tables copied and pasted from the internet, unless specifically acknowledged, and the source being detailed in the thesis and in the References sections.

_____

Signed

DECLARATION 2

CONFERENCE CONTRIBUTIONS

Parts of this thesis have been presented at conferences or publications as listed below.

1. Poster presentation: *An Investigation into Air Stable Analogues of Wilkinson's catalyst*

   CATSA 2009, Worcester

2. Poster presentation: *An Investigation into Air Stable Analogues of Wilkinson's catalyst*

   CATSA 2008, Parys

_____

Signed

TABLE OF CONTENTS

LIST OF ABBREVIATIONS

Imes	1,3-bis(2,4,6-trimethylphenyl)imidazol-2-ylidene
Ac	Acetate
R	Alkyl or Aryl group
Å	Angstrom
ATR	Attenuated Total Reflectance
X	Br, Cl or I
CHN	Carbon Hydrogen Nitrogen
CO	Carbonyl
Cy	Cyclohexyl
(COD)	1,5-Cyclooctadiene
Cot	Cyclooctatriene
°C	Degrees Celsius
DCM	Dichloromethane
DMSO	Dimethyl Sulfoxide
ee	Enantiomeric Excess
Et	Ethyl
FAB	Fast Atom Bombardment
GC	Gas Chromatography
IR	Infrared
K	Kelvin
L	Ligand
MS	Mass Spectrometry
m/z	Mass to charge ratio
m	Medium
mp	Melting point
MeOH	Methanol
Me	Methyl

M +	Molar mass + 1
NHC	*N*-heterocyclic carbine
NBD	Norbornadiene
NMR	Nuclear Magnetic Resonance
ppm	Parts per million
Ph	Phenyl
π	Pi
py	Pyridine
RT	Room Temperature
σ	Sigma
Δ G°	Standard Gibbs energy
s	Strong
S	Substrate
THF	Tetrahydrofuran
PPh$_3$	Triphenyl phosphine
TOF	Turn Over Frequency
w	Weak
XRD	X-ray Diffraction

LIST OF FIGURES

LIST OF SCHEMES

LIST OF TABLES

ACKNOWLEDGEMENTS

DEDICATION

This work is dedicated to my beloved late Grandmother Kistamma Naicker, Uncle Johnny and Aunt Neela Naidoo who all passed away during the course of my Masters.

1 INTRODUCTION

1.1. CATALYSIS: THE KEY TO SUSTAINABLE CHEMISTRY

The change in energy required for any chemical reaction to occur is called the standard Gibbs energy ($\Delta G°$).[1] A catalyst lowers this activation energy by creating an alternative pathway from reactants to products, thereby increasing the rate of the reaction. The catalyst is not consumed during the reaction nor does it alter the final state of equilibrium.[2] The catalyst can be re-used several times and very small quantities of the catalyst are required in a given process. Catalysis maximises the use of the available resources i.e. minimising waste and at the same time ensuring that there will be resources left over for generations to come. This process can therefore be classified as a sustainable process.[3]
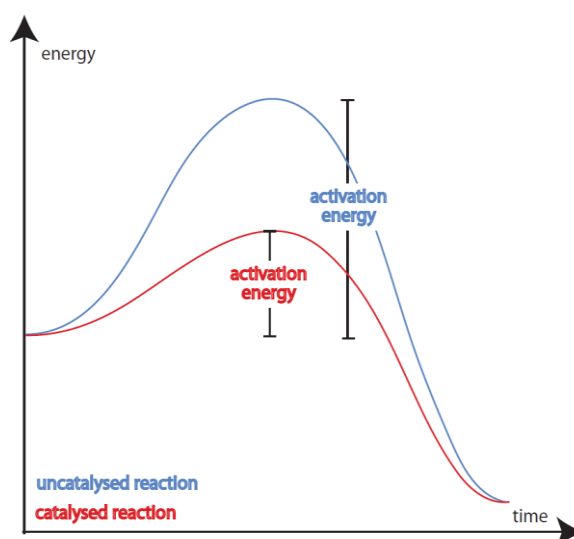
Figure 1.1. Activation energy plot for a hypothetical reaction pathway[4]

A catalyst can be heterogeneous i.e. in a different phase as the reactants or homogeneous i.e. in the same phase as the reactants. In homogeneous catalysis constituents are usually in the liquid phase.[5] Solid heterogeneous catalysts possess many active sites and the desired catalysis may take place at only one of these sites while the other sites may produce undesirable by products. Homogeneous catalysts, with the exception of polynuclear homogeneous catalysts, on the other hand possess one active site and are considered more active and selective than their heterogeneous counterparts. Reactions involving homogeneous catalytic systems are also easier to study using various spectroscopic techniques e.g. IR and NMR due to the simplicity of the active chemical specie. The catalyst can then be optimised and modified depending on the type of catalysis performed.[1]

In spite of the difficulties encountered in separating the desired product from the catalyst and solvent, the high selectivities and activities of homogeneous catalysis make it all the more attractive for industry. For example, the high stability, activity and selectivity of some rhodium catalytic systems far outweigh the high expense of acquiring rhodium metal. Homogeneous catalysts also function under lower temperatures and pressures i.e. mild conditions. This is of great importance as the world is moving toward greener living and conservation of energy. The world is becoming increasingly concerned about environmental issues such as the effects of global warming on limited natural resources and irreversible changes on climate and ecosystems. Therefore catalysis aims to minimise energy consumption and produce less industrial waste.

Catalysis is of intrinsic importance in industry and to our daily living because it is applied in the manufacture of various products e.g. fine chemicals, pharmaceuticals, food items and petroleum products.[6] Industrial applications of homogeneous catalysis include:

- **Hydroformylation/oxo synthesis:** alkenes are treated with hydrogen and carbon dioxide at high pressures to produce aldehydes. Aldehydes are converted to other products for example alcohol and used in the manufacture of detergents

- **Ziegler-Natta Polymerization**: involves the poymerization of 1-alkenes i.e. ethylene and alkenes with a vinyl double bond. These polymers are used in

the manufacture of a wide range of plastic, elastomers and rubber based material.

- **Hydrogenation** which is discussed below.[5]

A good catalyst is both highly efficient and selective. Efficiency is expressed by the turn over frequency or turn over number. It can simply be described as the number of reactant molecules that a single molecule of catalyst can convert to product molecules over a given time period. A highly active catalyst has a fast conversion rate even when it is present in a low concentration and is able to perform many catalytic cycles before it deactivates. Another key point is selectivity. A catalyst is said to be selective when it produces a maximum amount of the desired product and minimal side/by products.[3,5]

1.2. HOMOGENEOUS HYDROGENATION

Hydrogenation is one of the most significant and widely studied form of homogeneous catalysis. In its simplest form hydrogenation involves the conversion of unsaturated compounds to the corresponding saturated analogues mostly using molecular H_2.[7] The hydrogenation of alkenes to alkanes is crucial in the petrochemical industry since crude oil contains many multiple bonded species which first need to be reduced to single bonded species so they can be used as fuel. Hydrogenation is also often the first step in the preparation of numerous other useful products obtained from petroleum. Hydrogenation is also a key step in obtaining target compounds in the pharmaceutical and fine chemical industries.

Complexes used as catalysts are derived from transition metals and lanthanide elements. Transition metals have a unique bonding ability in that they possess partially filled d-orbitals, which enable them to form both σ and π bonds with an olefin (alkene). There is a flow of electron density from metal to the olefin and *vice versa* as seen in **Figure 1.2.**

pi back donation

sigma donation
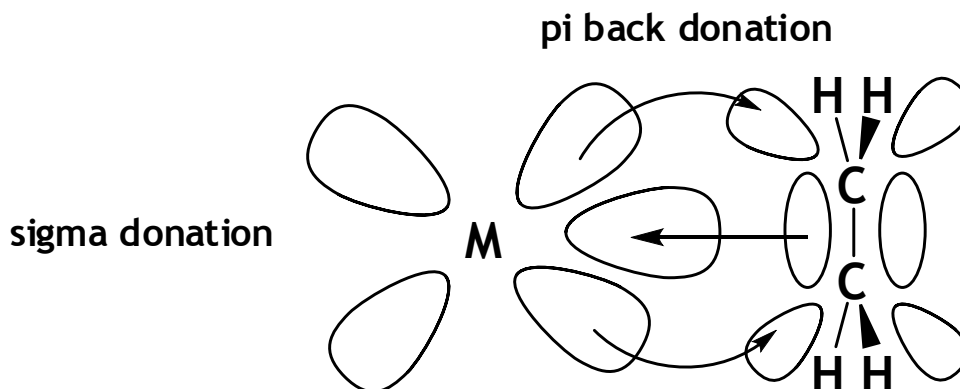
Figure 1.2. Diagrammatic representation of the synergistic bonding (σ and π) that occurs between transition a metal and an alkene [8]

This fortifies the metal-olefin bond such that the olefin is in the correct orientation to react with hydrogen. Transition metal complexes also possess the correct geometry and symmetry to form a bond with molecular hydrogen, thus enabling the transfer of hydrogen to the alkene. Therefore a perfect candidate would be a metal e.g. rhodium that is able to form square planar complexes with strong π acceptor ligands. Four coordinate square planar complexes of Rh(I) have a maximum coordination number of five. If the reaction is accompanied by oxidation six coordination is possible. The metal would be stabilised by the ligand and the complex would possess two vacant sites to which H_2 can easily coordinate to enable the process of hydrogenation. The investigation that follows is centred on the homogeneous hydrogenation of alkenes to the corresponding alkanes by rhodium complexes similar to or related to the iconic Wilkinson's catalyst.

1.3. HOMOGENEOUS HYDROGENATION OF UNSATURATES

The first reported discovery of homogeneous hydrogenation performed by metal complexes was made by Calvin in 1938. He reported the hydrogenation of quinones by copper acetate solutions at 100 °C.[9] Interestingly, rhodium complexes were first used in 1938 by Roelen in hydroformylation reactions[10], also known as the "largest volume reaction catalysed by a homogeneous catalyst".[11]

In the subsequent year the hydrogenation of a series of inorganic and organic compounds by rhodium(III) amine solutions at room temperature were reported by Iguchi. However, rather rapid decomposition of the rhodium occurred in the system.[12] In 1942 he also discovered that solutions of cobalt cyanide selectively reduced conjugated dienes to monoenes in the presence of ethylene linkages.[13,14] Unfortunately these were only soluble in water.[15]

However Sloane reported a range of Ziegler type complexes soluble in organic solvents which permitted the hydrogenation of olefins.[16] Meanwhile Kramer found that a chloroplatinate-trichlorostannate(II) complex proved efficient for the hydrogenation of acetylene and ethylene.[17] It had further been discovered that higher olefins could not be hydrogenated in ethanol[18] unless triphenylphosphine is present e.g. the reduction of the methyl ester of soya bean oil.[19]

Consequently the most vital progress in the field was the discovery of rhodium-tertiary phosphine complexes. In 1963 the discovery of [RhH(CO)(PPh$_3$)$_3$] was reported by Vaska[20] and its activity studies were reported in 1968-1970 by Wilkinson and co-workers.[21,22] It proved to be an efficient catalyst in hydrogenation,[23,24] isomerisation [25] and hydroformylation[26-29] reactions.

1.4. WILKINSON'S CATALYST

In 1964 Wilkinson and co-workers found that ethanol solutions of rhodium and pyridine i.e. Rhpy$_3$Cl$_3$ had the ability to slowly catalyse the hydrogenation of 1-hexene in the presence of H$_2$ at atmospheric pressure. Increased rates were noted at higher pressures.[30] In an effort to further stabilise this type of complex and to improve on its efficiency the pyridine ligands were replaced by ligands possessing stronger π acceptor ability. In 1965 one of the first ligands that were tested was triphenylphosphine in ethanol which produced a rhodium(III) complex. It was later discovered that if excess triphenylphosphine was added to rhodium trichloride in refluxing ethanol a square planar rhodium(I) complex was formed as maroon coloured crystals.

$$RhCl_3(H_2O)_3 \ + \ 4\,PPh_3 \xrightarrow{\text{Ethanol}} RhCl(PPh_3)_3 \ + \ OPPh_3$$

Scheme 1.1. Reaction equation for synthesis of Wilkinson's catalyst

The excess phosphine is oxidised and Rh(III) is reduced to Rh(I). The square planar, 16 electron complex has a rhodium centre coordinated to three sterically demanding triphenyl phosphine ligands.
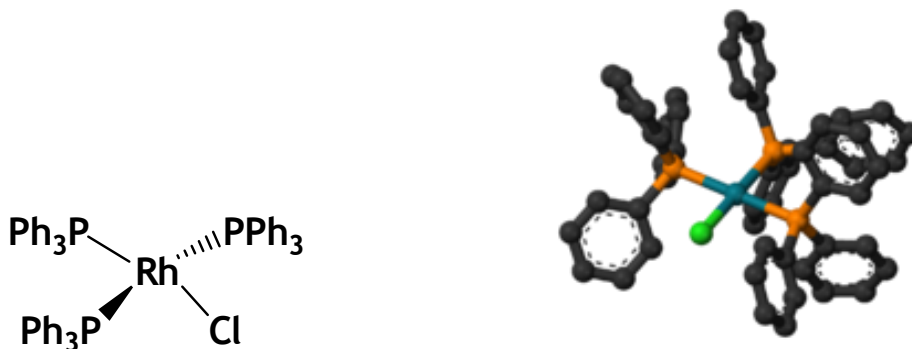
Figure 1.3. 2D and 3D structure of tris(triphenylphosphine)chlororhodium(I)

Horner later reported an alternate synthesis of the complex via displacement of the 1,5-cyclooctadiene ligand in Rh((COD)Cl)$_2$ by triphenylphoshine.[31]

$$(RhCODCl)_2 \ + \ 3PPh_3 \longrightarrow 2RhCl(PPh_3)_3 \ + \ 2COD$$

Scheme 1.2. Reaction equation for alternate synthesis of Wilkinson's catalyst

The discovery of tris(triphenylphosphine)chlororhodium(I) or Wilkinson's catalyst symbolised was a major advancement in homogeneous hydrogenation.[32,33] The complex's extraordinary catalytic abilities were expansively investigated by Wilkinson and co-workers. It was found to be the first highly active homogeneous hydrogenation catalyst capable of reducing both double and triple bonded unsaturates under mild conditions i.e. room temperature and 1 bar pressure even with other groups which are more easily reduced e.g. CHO, NO_2 being present. Terminal alkenes are also hydrogenated with internal alkenes being left untouched.[34]

The currently most established mechanism for the hydrogenation of olefins was first reported by Halpern where H_2 and the alkene are temporarily coordinated to the metal centre before transfer of hydrogen to the alkene occurs. This well known mechanism can be found in most textbooks of Inorganic Chemistry.[34, 35, 6]

1.5. RHODIUM-COMPLEXES AS CATALYSTS IN HOMOGENEOUS HYDROGENATION

1.5.1. RHODIUM CATALYSTS

The triumph of Wilkinson's catalyst stimulated many investigations involving rhodium complexes with various tertiary phosphines. The beginning of a new branch of hydrogenation i.e. enantioselective catalytic hydrogenation was initiated by Mislow[36], Knowles[37] and Horner[38]. They synthesised chiral phosphines and proved that the carbon-carbon double bonds of prochiral molecules could be asymmetrically hydrogenated using rhodium complexes coordinated to tertiary phosphine ligands which are optically active.[13] Monodentate and bidentate phosphine ligands were employed with the belief that the latter yields higher enantiomeric excess (% *ee)* since they are more strongly bonded to rhodium and their conformations have high rigidity.[39,40] One of the most important application of these type of catalysts was established by Knowles and co-workers, in the industrial synthesis of a drug used to treat Parkinson's disease i.e. L-DOPA [41-43] illustrated in Scheme 1.3.
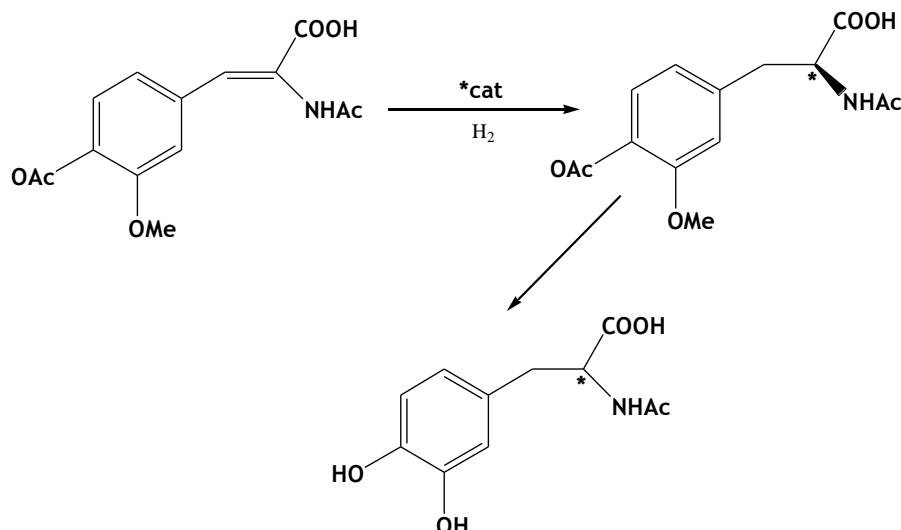
Scheme 1.3. Reduction of the prochiral amide by an optically active Rh catalyst

The notion that diphoshine ligands are more selective than monophoshine ligands has been reconsidered in the past decade with the synthesis of enantiopure monodentate phosphine ligands and the ability of their corresponding rhodium complexes to produce yields equal to and in some cases greater than that of bidentate phoshine ligands.[44-52]

1.5.2.   CATIONIC RHODIUM CATALYSTS

In the late 1960's the synthesis of cationic rhodium complexes of the form: [Rh(diene)(PR$_3$)$_2$]$^+$ were reported independently by a number of groups.[53-56] Osborn and Schrock later found that addition of H$_2$ to these cationic complexes resulted in hydrogenation of the diene and the formation of complexes of the form [RhH$_2$(PR$_3$)$_2$(S)$_2$]$^+$ (S representing the solvent) were formed [57]. Norbornadiene (NBD) or (COD) are generally used for the preparation of catalyst precursors as shown in (Scheme1.4.) below.

$$[\text{Rh(NBD)(PPh}_3)_2]^+ \quad + \quad 3\text{H}_2 \quad \xrightarrow{\text{MeOH}} \quad [\text{RhH}_2(\text{MeOH})_2(\text{PPh}_3)_2]^+ \quad + \quad \text{norbornane}$$

Scheme 1.4. Synthesis of cationic rhodium catalysts

The Rh(III) complexes hydrogenate ketones, alkynes, dienes as well as alkenes under mild conditions similar to Wilkinson's catalyst. The cationic catalysts differed from the traditional Wilkinson's catalyst in that they could be simply synthesised via numerous routes and several donor ligands could be employed. Also phosphine dissociation was not required for catalysis to occur.

1.5.3.   DIRHODIUM CATALYSTS

Dirhodium acetate complexes of the form $[\text{Rh}_2(\text{OAc})_4]$ **(Figure 1.4.)** have also been used for the hydrogenation of alkynes and alkenes.[58,59] The reaction takes place in protonated solvents and occurs at one of the metal sites.[60] Complexes of this form illustrated in have been found to hydrogenate 3-octenol to 3-octanol.
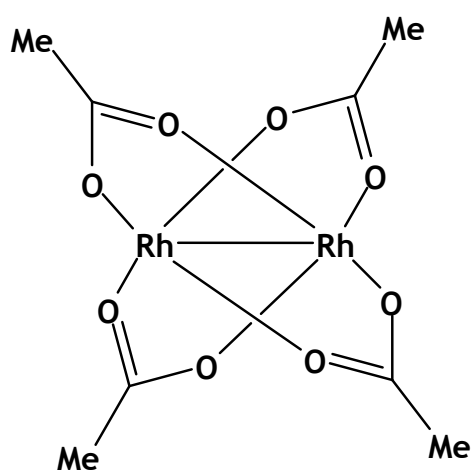
Figure 1.4. Dimeric rhodium catalyst $[\text{Rh}_2(\text{OAc})_4]$[61]

1.5.4.   RHODIUM-TRIARYLPHOSPHINE CATALYSTS

Rhodium-triarylphosphine and to a lesser extent trialkylphosphine complexes also function as effective hydrogenation catalysts.[62]

In this regards, Horner has reported the hydrogenation of 1-hexene using complexes synthesised *in situ* from [Rh(COD)Cl]$_2$, [Rh(C$_2$H$_4$)$_2$Cl]$_2$, [Rh(COT)$_2$Cl]$_2$, or [RhCl(butadiene)$_2$], with the added phosphine being either P(MeOC$_6$H$_4$)$_3$ or PBu$_3$. P(MeOC$_6$H$_4$)$_3$ proved to be the more active of the two phosphines.[31] Coffey found similar results in the reduction of 1-heptene using [RhCl(CO)PR$_3$)$_2$] type catalysts (R = Ph, OPh or Cy/cyclohexyl). The PPh$_3$ complex was found to be the most active while the PCy$_3$ complex was found to be less active than the PPh$_3$ complex but significantly more active than the P(OPh)$_3$ complex. [63-65]

Close to a decade later Heitkamp and co-workers found that the complex [RhH$_2$Cl(PCy$_3$)$_2$] functioned optimally at 100 °C and 1 bar for the hydrogenation alkenes especially (COD).[66] Meanwhile the complex [RhHCl$_2$(P^{t}BuPr$_2$)$_2$] in a basic solution was shown by Masters and co-workers to produce similar activities as that of Wilkinson's catalyst in the hydrogenation of 1-hexene. [67]

1.6. *N*-HETEROCYCLIC CARBENES AS LIGANDS

1.6.1.   DEFINING *N*-HETEROCYCLIC CARBENES

N-heterocyclic carbenes or NHCs are singlet carbenes. The most well known examples of these types of carbenes are diaminocarbenes having the formula (R$_2$N)$_2$C: The R groups are bridged in such a way that the carbon possessing unfilled orbitals becomes part of a heterocycle (Fig. 1.5).[68] NHCs have in the past few decades attracted a lot of attention as ligands for transition metal catalysts and especially as replacement for phosphines. Wanzlick[69] and Ölefe[70] reported the first

NHC based compounds (**1** and **2**). The first isolated stable carbene was reported by Bertrand[70] (**3**) but the actual breakthrough emerged with Arduengo's isolation of 1,3 bis(diadamantyl)imidazol-2-ylidene as a stable NHC (**4**).[72-74]
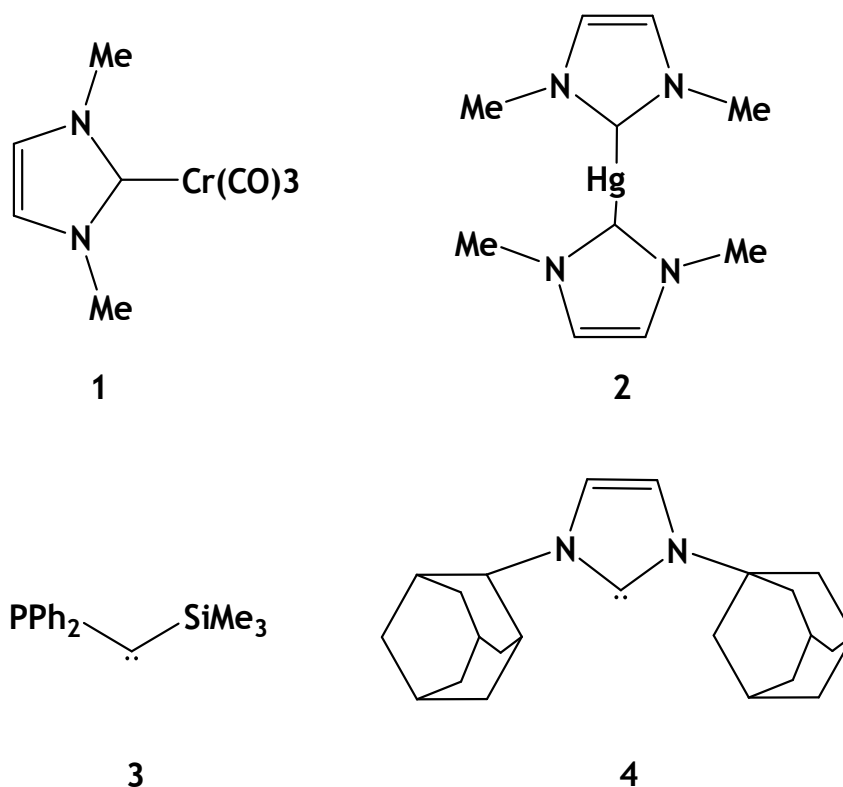
Figure 1.5. Some early Metal-NHC complexes (**1** and **2**) and isolated carbene ligands (**3** and **4**)[11]

Only slight modifications to the structural design of the NHC is required to cause significant changes to its electron donating properties, as well as impart steric constraints on the geometric configuration of the R groups.[73-80] The NHC ligands possess comparable basicity to tertiary phosphine ligands and they have now been firmly established as effective electron donors in the field of homogeneous catalysis.[81-85]
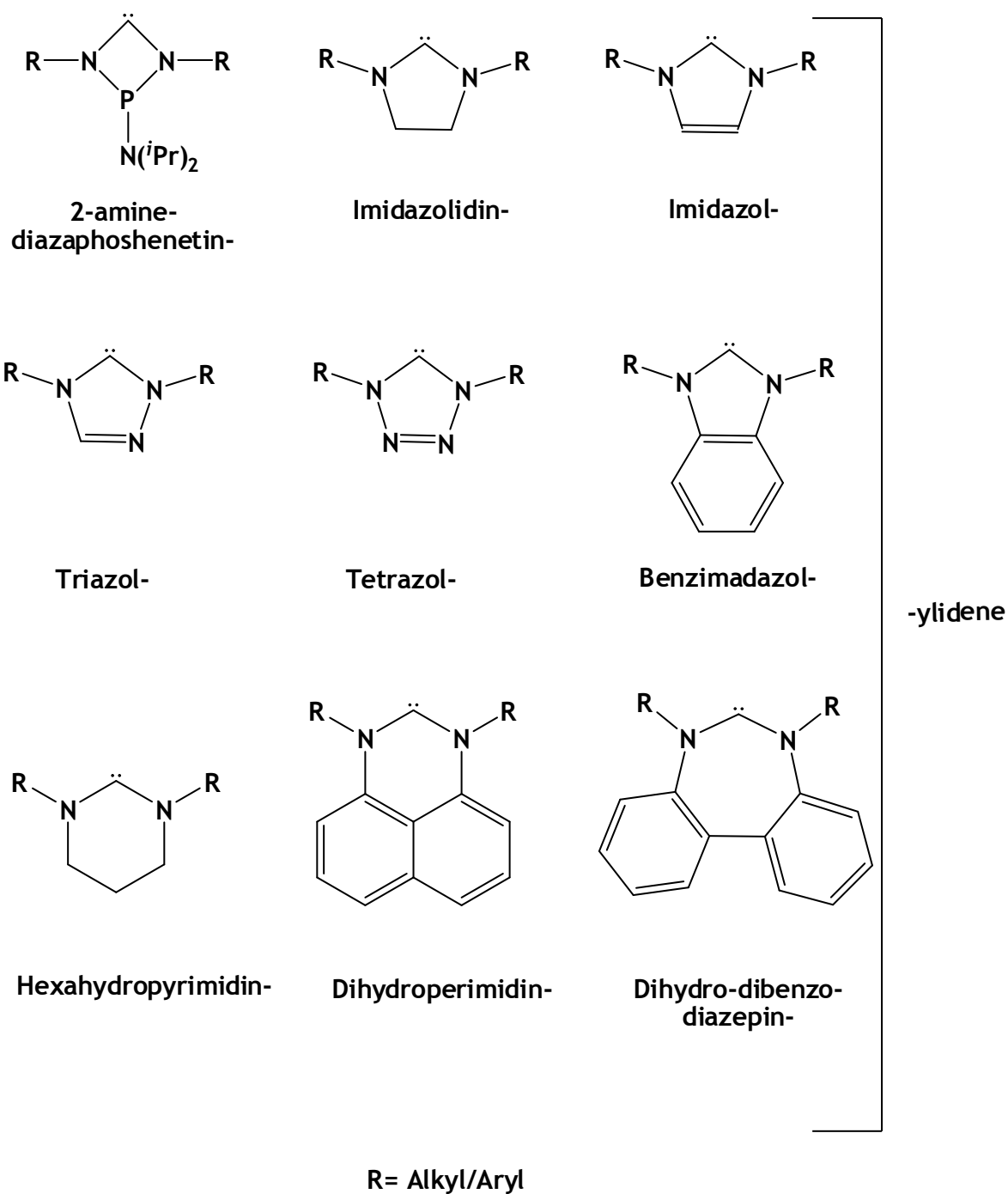
Figure 1.6. Variations of NHCs reported in literature[68]

Numerous NHCs bearing varieties of R groups have since been synthesised and complexed to transition metals. However, this study will concentrate on the 5-

membered ring imidazol- and imidazolidin-based NHCs (Fig 1.6) which are the predominantly encountered versions for transition metal complexing and applications in homogeneous catalysis.

1.6.2.   NHC LIGANDS VERSUS PHOSPHINE LIGANDS

In terms of metal coordination chemistry, NHCs are classified as strong monodentate 2 electron σ donor ligands similar to phosphines, amines and ethers.[86-89] The short metal - carbon bond distance in NHCs results in a partial double bond and increased transfer of electron density between the metal and the NHC ligand. Hence, NHCs possess both a strong σ component as well as a π back bonding component. The π back bonding capability of a ligand may be easily determined using analytical techniques e.g. infrared spectroscopy when IR active ligands such as CO are coordinated to the metal centre. In a metal carbonyl complex with the CO ligand located *trans* to the NHC ligand then the π back bonding capability of the NHC ligand is proportional to the vibrational stretching frequency of the CO group (v_{CO}). The more basic the ligand the lower the v_{CO} stretching wavenumber.[69]

Studies on Nickel(0) complexes by Nolan and co-workers have established that NHCs are superior in their electron donating abilities compared to even the most basic phosphines and in comparison coordinate more strongly to the metal centre.[89] Additionally, thermochemical and structural studies by Nolan on various NHCs and phosphine ligands have confirmed that NHC ligands have far better electron donating ability as compared to similar phosphine ligands with the exception of the bulky adamantyl-NHC ligand.[84] It is worth noting that Herrmann and co-workers on the other hand have determined that NHCs and trialkylphosphines possess comparable bonding abilities.[90]

1.6.3.   NHC COMPLEXES AS CATALYSTS

In an effort to harness the above mentioned properties, NHCs have gradually been used to replace phosphine ligands in well established homogeneous catalysts.[91,92] Typical examples are the Palladium catalyst **5** used in Heck coupling reactions[93,94] and the Ruthenium Grubbs 2nd and 3rd generation catalysts **6** employed in olefin metathesis.[94] The effect of using NHCs as ligands in these systems is observed from the significantly improved efficiency and stability of the catalysts.[99]

5   **6**

R = alkyl, aryl
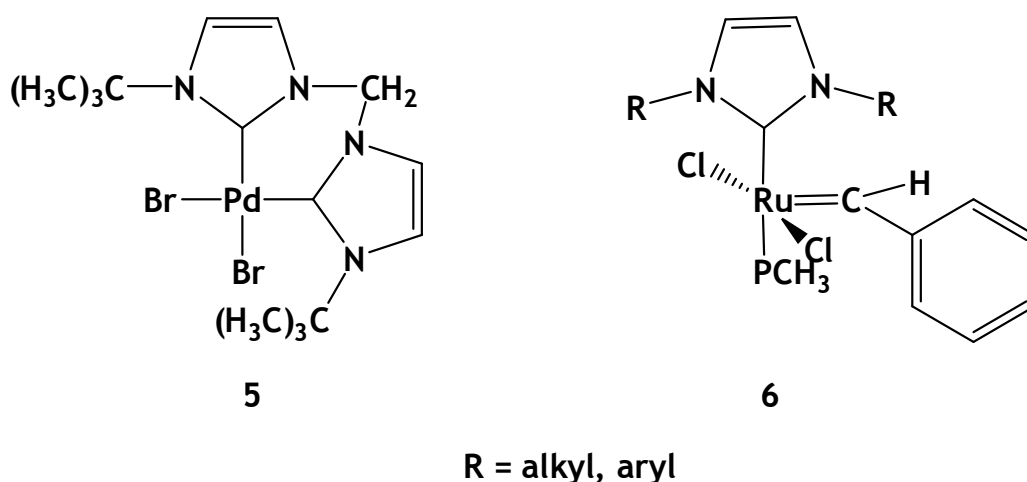
Figure 1.7. Typical metal-NHC complexes employed as catalysts in Heck coupling and olefin metathesis reactions respectively.[80]

The renowned success of Rh(I) and Ir(I) complexes as catalysts in hydrogenation reactions has prompted the investigation of various analogues of Wilkinson's[95] **7** and Crabtree's[96] **8** catalysts.
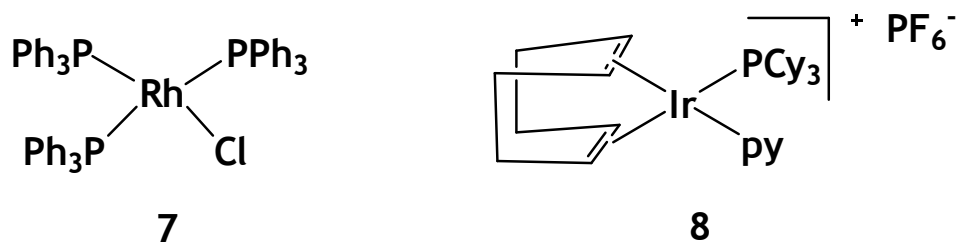
Figure 1.8. Wilkinson's **7** and Crabtree's **8** catalysts. Cy = cyclohexyl

Various homogeneous hydrogenation catalysts of this type have been reported by Nolan and Crudden but only the Rh complexes will be discussed. Nolan investigated the Rh(IMes)(PPh$_3$)$_2$Cl complex and compared its catalytic activity with that of Wilkinson's catalyst under mild conditions.

IMes = 1,3-bis(2,4,6-trimethylphenyl)
imidazol-2-ylidene

9   **10**
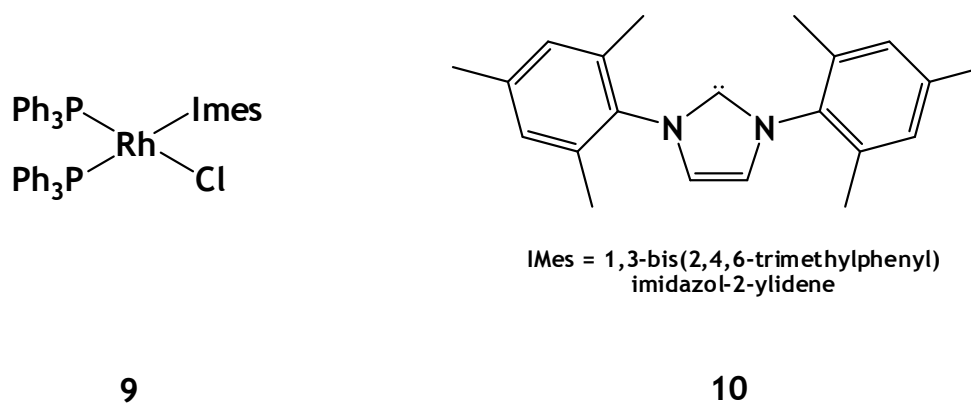
Figure 1.9. Nolan's mixed Rh-phosphine-NHC complex

In the hydrogenation of cyclohexene complex **9** had much lower activity than the traditional Wilkinson's catalyst (Table 1.1) but has the advantage of higher thermal stability.[97]

Table 1.1. Catalytic hydrogenation of cyclohexene using complexes **7** and **9**[97]

Catalyst	Time/hrs	Temperature/ °C	% Yield
Rh(PPh$_3$)$_3$Cl	24	RT	8
Rh(IMes)(PPh$_3$)$_2$Cl	24	RT	9
Rh(PPh$_3$)$_3$Cl	24	45	38
Rh(IMes)(PPh$_3$)$_2$Cl	24	45	18

A few years later Crudden reported the hydrogenation of isosaffrole using complexes **7** and **9** as catalysts. It was found that at room temperature and higher, the addition of a phosphine scavenger (i.e. CuCl) drastically increased the activity of catalyst **9** and produced TOF's higher than that of complex **7** (Table 1.2). [98, 99]

Table 1.2. Catalytic hydrogenation of isosaffrole using complexes **7** and **9**[11]

Catalyst	Temperature/ °C	Additive	TOF/hrs
Rh(PPh$_3$)$_3$Cl	25	-	50
Rh(IMes)(PPh$_3$)$_2$Cl	25	-	2
Rh(PPh$_3$)$_3$Cl	60	-	380
Rh(IMes)(PPh$_3$)$_2$Cl	60	-	36
Rh(PPh$_3$)$_3$Cl	25	CuCl	50
Rh(IMes)(PPh$_3$)$_2$Cl	25	CuCl	90
Rh(PPh$_3$)$_3$Cl	60	CuCl	300
Rh(IMes)(PPh$_3$)$_2$Cl	60	CuCl	430

Also, Herrmann *et al.* have shown that Rh-NHC complexes of the form **11** and **12** are active catalysts for the hydrogenation of simple/aliphatic alkenes in the presence of phosphines.[100]

11

12
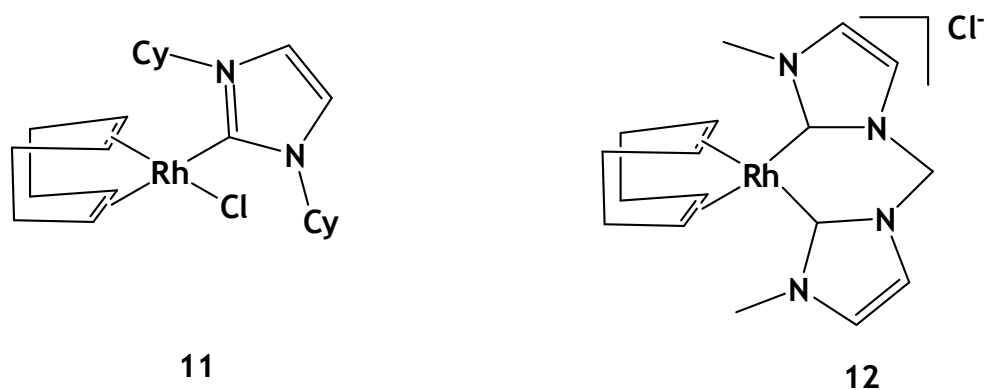
Figure 1.10. Herrmann and Frey's mono and bis Rh-NHC complexes.[100]

A series of bidentate Rhodium-NHC complexes of the form **13** and **14** have been investigated by Messerle which showed significant activity in the hydrogenation of styrene. It was also observed that the greater the steric bulk of the ligand the lower the overall activity of the catalyst. [91,101]

13

14
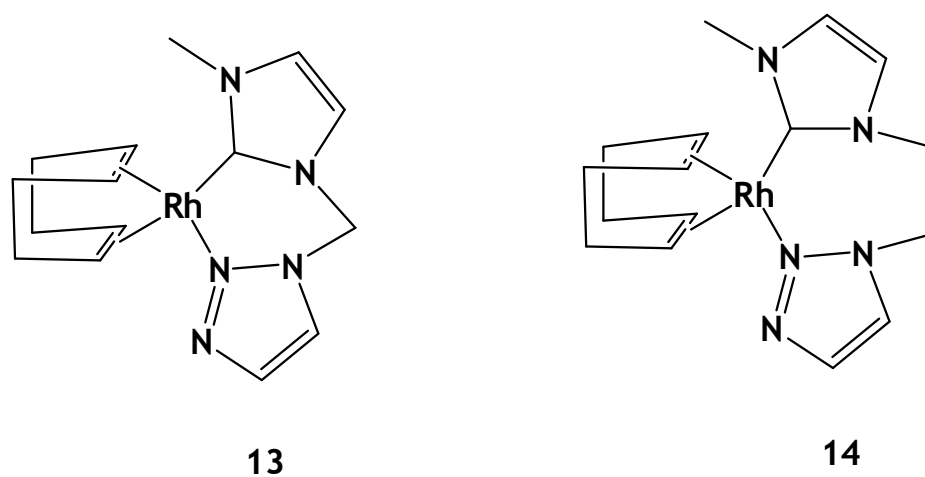
Figure 1.11. Rh-NHC bidentate complexes as hydrogenation catalysts[11]

Vasquez-Serrano investigated the activity of rhodium-(COD)-NHC complexes of the type **15**, **16** and **17** in the absence of phosphines. Significant activity was noted for the hydrogenation of 1-octene in CH_2Cl_2 at 1 atm H_2 and 25 ºC.

15   **16**   **17**
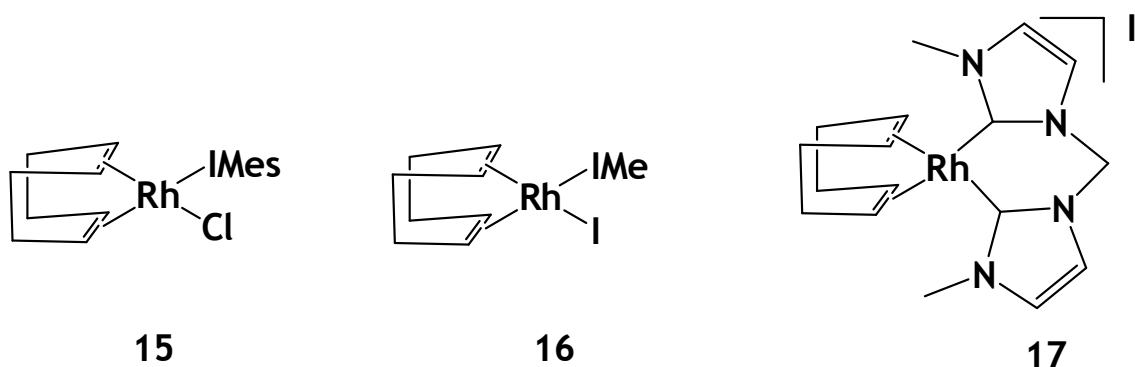
Figure 1.12. Rh-(COD)-NHC complexes as catalysts for the hydrogenation of

1-octene.[102]

The synthesis of Rh-(COD)-NHC complexes can be described as a one pot synthesis. The NHC salt (Figure 1.13) is added to the $(Rh(COD)Cl)_2$ dimer in the presence of a strong base and an appropriate solvent. The synthesis of various Rh-(COD)-NHC complexes was described by Wolf (**18**).

18
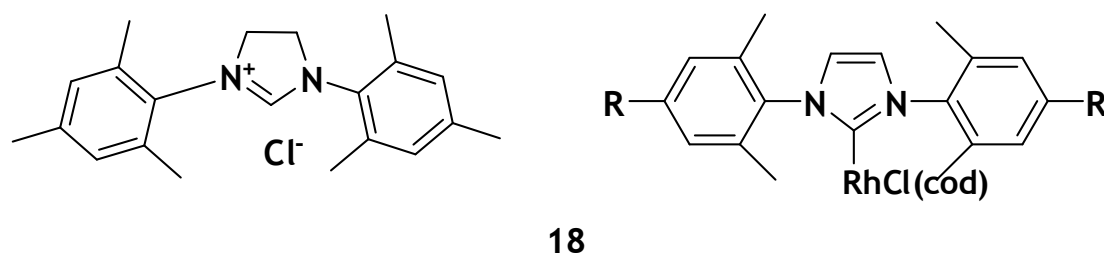
1,3-bis-(2,4,6-trimethylphenyl)
-imidazolinium chloride
(NHC salt)

R = H, Me,
Br, S(O)tol,
NEt_2, $OC_{12}H_{25}$,

Figure 1.13. General form of Rh-(COD)-NHC complexes synthesised by Wolf.[103]

NHCs are more thermally and hydrolytically stable than phosphine ligands[81] and with the ease of synthesis of metal-NHC complexes they are now viewed as a viable substitute for phosphine ligands in an effort to overcome the shortcomings of phosphine ligands such as their rapid oxidation.[96, 104-108] It has become apparent that NHC ligands are not merely imitations of phosphines as there has been mounting evidence that metal-NHC compounds in increasing instances outperform the activity, selectivity and stability of metal-phosphine complexes.[83]

1.7. OVERVIEW OF STUDY

- This study will be investigating the effects of ligand modification on Wilkinson-type hydrogenation catalysts.

- The applications of the traditional catalyst is limited due to the limited stability of its solutions and its susceptibility to attack from the environment i.e. oxygen and moisture.

- The aim of the project is to produce more stable and active versions of the traditional catalyst and also to demonstrate their improved stability and activity in catalytic applications.

- Initially, different phosphine ligands will be complexed to rhodium and then different *N*-heterocyclic carbenes.

- The electronic and steric effects of the different variations will also be monitored.

1.8. REFERENCES

1) C. Masters, *Homogeneous Transition-metal Catalysis-a gentle art*, Chapman and Hall Ltd, 1981.

2) P.W. Atkins and J. de Paula, *Atkins' Physical Chemistry*, 7th ed., Oxford University Press, 2002.

3) G. Rothenburg, *Catalysis: Concepts and Green Applications,* Wiley-VHC, 2008.

4) W. J. Moore, *Physical Chemistry*, 4th ed., Prentice Hall, 1972.

5) D. Shriver and P. Atkins, *Shriver & Atkins Inorganic Chemistry*, 4th ed., Oxford University Press, 2006.

6) G.L. Miessler and D.A. Tarr, *Inorganic Chemistry,* Vol. 3, Prentice Hall, 2004.

7) P.Y. Bruice, *Organic Chemistry*, 4th ed., Pearson Prentice Hall, 2004.

8) U. Pidun, G. Frenking, *Organometallics,* 1995, **14**, 5325.

9) M.Calvin, *J. Am. Chem. Soc.*, 1939, **61**, 2230.

10) O. Roelen, patent, EU, Germany, 1938, 849 548.

11) J.M. Praetorius, C.M. Crudden, *Dalton Trans.*, 2008, 4079.

12) M.Iguchi, *J. Chem. Soc. Japan*, 1939, **60**, 1287.

13) C.J. Elsevier, *Handbook of Homogeneous Catalysis*, Wiley-VHC, 2007, Vol. 1.

14) M.Iguchi, *J. Chem. Soc. Japan*, 1942, **63**, 1752.

15) J.Kwiatek, J.K. Seyler, *J. Org. Chem.,* 1965, **3**, 421.

16) M.F. Sloane, A.S. Matlack, D.S. Breslow, *J. Am. Chem. Soc.,* 1963, **85**, 4014.

17) R.D. Cramer, E.L. Jenner, R.V. Lindsay, jun., U.G. Stolberg, *J. Am. Chem. Soc.,* 1963, **85**, 1691.

18) G.C. Bond, I. Hellyer, *Chem. & Ind.,* 1965, 35.

19) J.C. Bailar, jun., H. Itatani, *Inorg. Chem.,* 1965, **5**, 1618.

20) S.S. Bath, L.Vaska, *J. Am. Chem. Soc.,* 1965, **85**, 3500.

21) D. Evans, G.Yagupsky, G. Wilkinson, *J. Chem. Soc. (A)*, 1968, 2660.

22) M. Yagupsky, C.K. Brown, G. Yagupsky, G. Wilkinson, *J. Chem. Soc. (A)*, 1970, 937.

23) C. O'Connor, G. Yagupsky, D. Evans, G. Wilkinson, *Chem. Commun.*, 1968, 420.

24) C.O'Connor, G. Wilkinson, *J. Chem. Soc. (A)*, 1968, 2665.

25) G. Yagupsky, G. Wilkinson, *J. Chem. Soc. (A)*, 1970, 941.

26) D. Evans, J.A. Osborn, G. Wilkinson, *J.Chem.Soc. (A)*, 1968, 3133.

27) G. Yagupsky, C.K. Brown, G. Wilkinson, *Chem. Commun.*, 1969, 1244.

28)   G. Yagupsky, C.K. Brown, G. Wilkinson, *J. Chem. Soc.*, 1970, 1392.

29)   C.K. Brown, G. Wilkinson, *J. Chem. Soc.*, 1970, 2753.

30)   R.D. Gillard, J.A. Osborn, P.B. Stockwell and G. Wilkinson, *Proc.Chem.* Soc., 1964, 284.

31)   L.Horner, H.Siegel, H.Buthe', *Tetrahedron Lett.*, 1968, 4023.

32)   J.A. Osborn, G. Wilkinson, J.F. Young, *Chem. Commun.*, 1965, 17.

33)   J.A. Osborn, F.H. Jardine, G. Wilkinson, J.F. Young, *J. Chem. Soc.*, 1966, 1711.

34)   C.Daniel, N.Koga, J.Han, X.Y.Fu and K. Morokuma, *J. Am. Chem. Soc.*, 1988, **110**, 3773.

35)   J. Halpern, *Inorg.Chim.Acta.*, 1981, **50**, 11.

36)   O. Korpin, K. Mislow, *J.Am.Chem.Soc.*, 1967, **89**, 4784.

37)   W.S. Knowles, M.J. Sabacky, *Chem. Commun.*, 1968, 1448.

38)   L.Horner, H.Siegel, H.Buthe', *Angew. Chem.*, 1968, 1034.

39)   T.P. Dang, H.B. Kagan, *Chem. Commun.*, 1971, 10.

40)   H.B. Kagan, T.P. Dang, *J.Am.Chem.Soc.*, 1972, **94**, 9429.

41)   W.S. Knowles, M.J. Sabacky, M.D. Vineyard, D.J. Weinkuff, *J. Am. Chem. Soc.*, 1975, **97**, 2567.

42)   W. S. Knowles, *Acc. Chem. Res.*, 1983, **16**, 106.

43)   W. S. Knowles, *Angew. Chem. Int. Ed.*, 2002, **41**, 1998.

44)   H.U. Blaser, C. Malan, B. Pugin, F. Spindler, H. Steiner, M. Stander, *Adv. Synth. Catal.*, 2003, **345**, 103.

45)   F. Guillen, J. Fiard, *Tetrahedron.* Lett., 1999, **40**, 2939.

46)   T. Hayashi, *Acc. Chem. Res.*, 2000, **33**, 354.

47)   F.Lagasse, H.B. Kagan, *Chem. Pharm. Bull.*, 2000, **48**, 315.

48)   I.V. Komarov, A. Bo'rner, *Angew. Chem.*, 2001, **113**, 1237.

49)   M.T. Reetz, T.Sell, A. Mesiselwinkel, G. Mehler, *Angew. Chem. Int. Ed.*, 2003, **42**, 790.

50)   M.T. Reetz, G. Mehler, *Tetrahedron. Lett.*, 2003, **44**, 4593.

51)   M.T. Reetz, G. Mehler, A. Mesiselwinkel, *Tetrahedron: Assymm.*, 2004, **15**, 4593.

52)   J.R. Shapley, R.R. Shrock, J.A.Osborn, *J. Am. Chem. Soc.*, 1969, **91**, 2816.

53)   M.T. Reetz, J.A. Mar, R. Goddard, *Angew. Chem. Int. Ed.*, 2005, **44**, 412.

54)   B.F.G. Johnson, J.Lewis, D.A. White, *J. Am. Chem. Soc.*, 1969, **91**, 5186.

55)   L. M. Haines, *Inorg, Nucl. Chem. Lett.*, 1969, **5**, 399.

56) M. Green, T.A. Kuc, S. Taylor, *Chem. Commun.*, 1970, 1553.

57) R.R. Schrock, J.A. Osborn, *Chem. Commun.*, 1970, 567 .

58) P. Legzdins, G. Rempel, G. Wilkinson, *Chem. Commun.*, 1969, 825.

59) P. Legzdins, R.W. Mitchell, G. Rempel, J.D. Ruddick, G. Wilkinson, *J. Chem. Soc. (A)*, 1970, 3322.

60) B.C. Hui, G.L. Rempel, *Chem. Commun.*, **1970**, 1195.

61) M.C. Simpson, D.J. Cole-Hamilton, *Coord. Chem. Rev.*, 1996, **155**, 163.

62) B. Montelatici, A. van der Ent, J.A. Osborn, G. Wilkinson, *J. Chem. Soc. (A)*, 1968, 1054.

63) R.S. Coffey, patent, UK, 1968, 1121643.

64) R. S. Coffey, *Chem. Abstr.*, 1968, **69**, 139501.

65) W.Strohmeier, W. Rehdher-Stirnweiss, *J. Organomet. Chem.*, 1969, **19**, 417.

66) S. Heitkamp, D.J. Stufkens, K. Vrieze, *J. Organomet. Chem.*, 1978, **152**, 347.

67) C. Masters, W.S. McDonald, G. Raper, B.L. Shaw, *Chem. Commun.*, **1971**, 210.

68) P. de Fremont, N. Marion, S.P. Nolan, *Coord. Chem. Rev.*, 2009, **253**, 862.

69) H.W. Wanzlick, H.J. Schonherr, *Angew. Chem. Int. Ed. Engl.*, 1968, 7.

70) K.Olefe, *J. Organomet. Chem.*, 1968, **12**, 42.

71) A. Igau, H. Gruitzmacher, A. Baceiredo and G. Bertrand, *J. Am. Chem. Soc.*, 1988, **110**, 6463.

72) A.J. Arduengo III, R.L. Harlow, M. Kline, *J. Chem. Soc.*, 1991, **113**, 361.

73) A.J. Arduengo III, H.V.R. Dias, R.L. Harlow, M. Kline, *J. Am. Chem. Soc.*, 1992, **114**, 5530.

74) P. de Fremont, N. Marion, S.P. Nolan, *Coord. Chem. Rev.*, 2009, **253**, **862**.

75) A.J. Arduengo III, *Acc. Chem. Res.*, 1999, **32**, 913.

76) E. Despagnet-Ayoub, R.H. Grubbs, *J. Am. Chem. Soc.*, 2004, **126**, 10198.

77) F.E. Hahn, M.C. Jahnke, *Angew. Chem. Int. Ed.*, 2008, **47**, 3122.

78) P.I. Arnold, S. Pearson, *Coord. Chem. Rev.*, 2007, **251**, 596.

79) D. Pugh, A.A. Danopoulos, *Coord. Chem. Rev.*, 2007, **251**, 610.

80) E. Colacino, J. Martinez, F. Lamaty, *Coord. Chem. Rev.*, 2007, **251**, 726.

81) J.A. Mata, M. Poyatos, E. Peris, *Coord. Chem. Rev.*, 2007, **251**, 841.

82) W.A. Herrmann, C. Kocher, *Angew. Chem. Int. Ed.*, 1997, **36**, 2162.

83) W. A. Herrmann, *Angew. Chem. Int. Ed.*, 2002, **41**, *1290*.

84) S. P. Nolan, *N-Heterocyclic Carbenes in Synthesis*, Wiley-VHC: Weinheim, 2006.

85)   F. Glorius, *N-Heterocyclic Carbenes in Transition Metal Catalysis*, Springer-Verlag: Berlin, 2007.

86)   A.J. Arduengo, G. Bertrand, *Chem.Rev.*, 2009, **108**, 3210.

87)   R.H. Crabtree, *J. Organomet. Chem*, 2006, 5451.

88)   W.A. Herrmann, P.W. Roesky, M. Elison, G.J.R. Artus, K. Ofele, *Organometallics*, 1995, **14**, 1085.

89)   I. Haung, H.-J. Schanz, E.D. Stevens, S.P. Nolan, *Organometallics*, 1999, **18**, 2317.

90)   K.Öfele, W.A. Herrmann, D. Mihalios, M. Elison, E. Herdtwerk, W. Scherer, J. Mink, *Organomet. Chem.*, 1993, **459**, 177.

91)   M.J. Page, J. Wagler, B.A. Messerle, *Dalton Trans.*, 2009, **35**, 7029.

92)   W.A. Herrmann, M. Elison, J. Fisher, C. Kocher, G.R.J. Artus, *Angew. Chem.*, 1995, **34**, 2371.

93)   N. Marion, S.P. Nolan, *Acc. Chem. Res.*, 2008, **41**, 1440.

94)   T.M. Trnka, R.H. Grubbs, *Acc. Chem. Res.*, 2001, **34**, 18.

95)   J.A. Osborn, F.H. Jardine, G. Wilkinson, J.F. Young, *J. Chem. Soc.*, 1966, 1711.

96)   R. Crabtree, *Acc. Chem. Res.*, 1979, **12**, 331.

97)   G.A. Grasa, Z. Moore, K.L. Martin, E.D. Stevens, S.P. Nolan, V. Paquet, H. Lebel, *J. Organomet. Chem.*, 2002, **658**, 126.

98)   D.P. Allen, C.M. Crudden, L.A. Calhoun, R. Wang, *J. Organomet. Chem.,* 2004, **689**, 3203.

99)   D.P. Allen, C.M. Crudden, L.A. Calhoun, R. Wang, A. Decken, *J. Organomet. Chem.,* 2005, **690**, 5736.

100) W.A. Herrmann, G.D. Frey, E. Herdtweck, M. Steinbeck, *Adv. Synth Catal.,* 2007, **349**, 1677.

101) B.A. Messerle, M.J. Page, P. Turner, *Dalton Trans.*, 2006, 3927.

102) D. Vazquez-Serrano, B.T. Owens, J.M. Buriak, *Inorg. Chim. Acta.,* 2006, **359**, 2786.

103) S. Wolf, H. Plenio, *J. Organomet. Chem.,* 2009, **694**, 1487.

104) N. Marion, S. Diez-Gonzalez, S.P. Nolan, *Angew. Chem. Int. Ed.,* 2007, **46**, 2988.

105) D. Enders, O. Niemeier, A. Hensseler, *Chem. Rev.,* 2007, **107**, 5606.

106) R. E. Douthwaite, *Coord. Chem. Rev.,* 2007, **251**, 702.

107) L.H. Gade, S. Bellemin-Laponnaz, *Coord. Chem. Rev.,* 2007, **251**, 718.

108) W.J. Sommer, M. Weck, *Coord. Chem. Rev.,* 2007, **251**, 860.

2 AN INVESTIGATION INTO RHODIUM-TERTIARY PHOSPHINE COMPLEXES

2.1. INTRODUCTION

The discovery of Wilkinson's catalyst and its usefulness in the homogeneous hydrogenation of olefins has spurred on numerous investigations involving trivalent tertiary phosphine–rhodium complexes in the reduction of olefins.[1]

Compounds of the form **1a, 1b, 1c, 1d** and **1e** were synthesised and characterised. The effects of different phosphine ligands on the properties of the complexes were investigated and a comparative study of these complexes was performed in the hydrogenation of alkenes. All complexes have been previously synthesised however an alternative synthetic route is provided for complexes **1b-e**. [38,3,4]
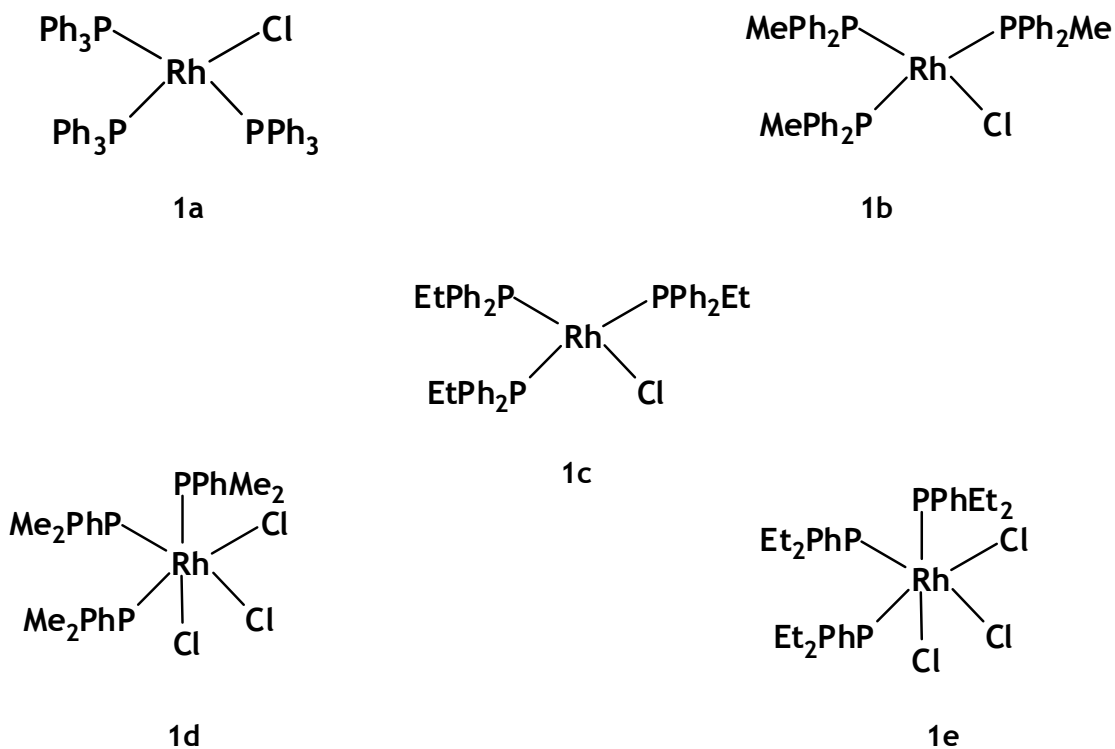
Figure 2.1. Structures of complexes **1a-e**

2.2. SYNTHESIS AND CHARACTERISATION OF RHODIUM – TERTIARY PHOSPHINE COMPLEXES

Complexes **1a-e** were prepared by adding $RhCl_3.3H_2O$ to an excess of the corresponding tertiary phosphine and refluxing in ethanol for 30 minutes. Excess phosphine was added to prevent dimerisation of $RhCl_3.3H_2O$. Compound **1a** precipitated as a maroon coloured solid, while **1b** and **1c** precipitated as yellow-orange solids. In addition, complexes **1d** and **1e** precipitated as yellow-orange solids almost instantaneously with the addition of the phosphine to the rhodium trichloride. The filtered products were washed with ethanol to remove any excess phosphine.

After the original work by Osborn and Wilkinson,[38] the classical Wilkinson's catalyst **1a** has been synthesised by numerous researchers. In order to use **1a** as a reference catalytic system, it was synthesised following the original method of Osborn and Wilkinson and fully characterized to confirm its identity. A melting point of 246-250 °C was obtained which was comparable to the literature melting point of 245-250 °C. Due to the high symmetry of **1a** (Fig. 2.2) the aromatic region in the ^{1}H NMR reveals two proton environments, 7.46 integrating for 30 equivalent protons and 7.38 ppm integrating for 15 equivalent protons.
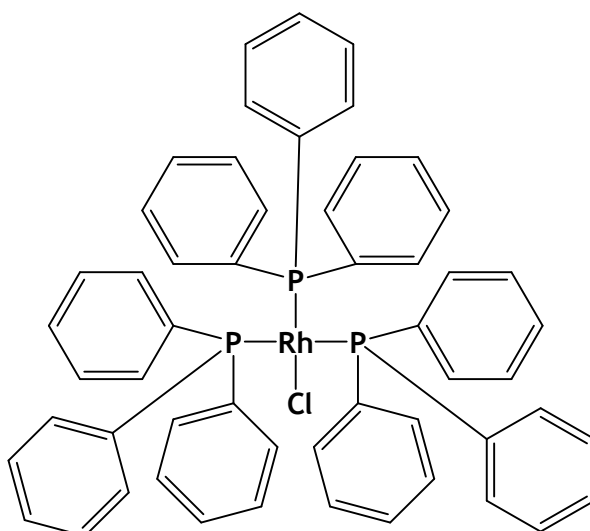
Figure 2.2. Structural representation of Wilkinson's complex **1a**.

This is due to the three phenyl rings attached to each phosphine, two of which are equivalent due the square planar arrangement of the complex. The ^{13}C NMR spectrum of **1a** showed a peak at 133.5 ppm due to the phenyl carbons directly bonded to the phosphines, a peak at 132 ppm due to CH carbons *ortho* and *meta* to the P-C carbon and a final peak appeared at 128.5 due to CH carbons *para* to the P-C carbon.

In the ^{31}P NMR, a doublet of triplets at 48-49 ppm was observed due to the P atom trans to Cl being split to two signals by ^{103}Rh coupling, each of which is further split by the two equivalent phosphines that are trans to each other into three signals. Another signal at 31-32 ppm was a doublet of doublets. This is due to a signal produced by the equivalent P atoms being split into a doublet by Rh. This doublet is split further by the P atoms *trans* to Cl, into a doublet of doublets.

In the IR spectrum a peak of medium intensity arose at 3056 cm^{-1} due to the CH phenyl bonds of the three phenyl rings attached to each phosphorous atom. A weak peak at 1970 cm^{-1} confirms phenyl substitution and a weak peak at 1570 cm^{-1} is due to C=C double bond of the phenyl groups. A strong peak at 692 cm^{-1} arises due to P-phenyl bonds.

Elemental analysis was performed for complex **1a** and the percentages of C and H as calculated for $C_{54}H_{45}ClP_3Rh$ were (C, 70.10), (H, 4.90) and were comparable to the values obtained i.e. (C, 69.78), (H, 4.860).

The *m/z* values obtained from running the FAB mass spectrum of complex **1a**, the corresponding intensities and fragments are shown in Table 2.1. The complex is not very stable to oxidation since the 100 % intensity peak is attributed to PPh$_3$O.

Table 2.1. Summary of mass spectrum data obtained for complex **1a**.

m/z	Intensity/%	Fragment
278.9	100	PPh$_3$O
154	50	M$^+$-2(PPh$_2$)P
626.8	12	M$^+$-Cl-PPh$_3$
888.6	3	M$^+$-Cl
786.4	1	M$^+$-Cl-Rh

Complexes **1b-e** were previously reported by Chatt *et al.*[3] The compounds were synthesised by adding an excess of the respective tertiary phosphine ligand to $RhCl_3.3H_2O$ and boiling in ethanol. Complexes **1b** and **1c** exhibit a four coordinate square planar arrangement of ligands around Rh similar to complex **1a.**

Complex **1b** melted with decomposition above 200 °C.[3] The ^1H NMR, ^{13}C NMR and   is similar to that of complex **1a** with the addition of a singlet at 1.2 ppm, integrating for 6 protons, due to methyl protons that are *trans* to each other and another signal at 2 ppm integrating for 3 protons due to the methyl protons trans to Cl in the ^1H NMR spectrum and a peak at 13 ppm is due to the three methyl carbons in the ^{13}C NMR spectrum.
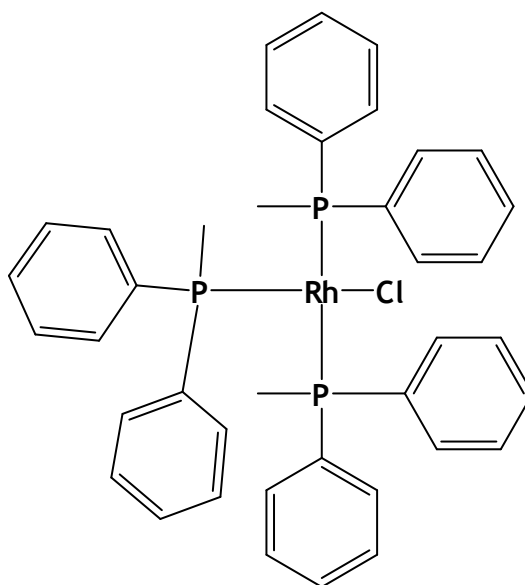
Figure 2.3. Structural representation of complex **1b**.

The ^{31}P NMR revealed a doublet of a multiplet at -2.1 ppm and a doublet of doublets at -4.3 ppm. Since the pattern is similar to that observed for complex **1a,** it is hence logical to conclude coordination in a similar way to the explanation above for the classical Wilkinson's catalyst.

An IR spectrum similar to that of complex **1a** was obtained, including a strong peak at 1434 cm^{-1} due to CH_3 bonds.

Elemental analysis was performed for complex **1b** and the percentages of C and H as calculated for $C_{39}H_{39}ClP_3Rh$ were (C, 63.38), (H, 5.32) and were comparable to the values obtained i.e. (C, 63.00), (H, 4.989).

The *m/z* values obtained from a FAB mass spectrum determination of complex **1b** and corresponding intensities and fragments are shown in Table 2.2.   The complex is not very stable to oxidation since the 100 % intensity peak is attributed to $OPMePh_2$.

Table 2.2. Summary of mass spectrum data obtained for complex **1b**

m/z	Intensity/%	Fragment
216.9	100	$OPMePh_2$
234.9	5	M^+-Rh-2($PMePh_2$)
502.8	3	M^+-Cl-$PMePh_2$
572.7	2	M^+-Ph_2-$PMePh_2$
266.9	1	M^+-Rh-2(PPh_2)

Similar to complex **1b**, a melting point for complex **1c** could not be obtained as the complex decomposed above 200 °C, an observation that is not unusual for these type of complexes.[3]   Both the ^1H NMR and ^{13}C NMR spectrum are similar to those of complexes **1a** and **1b** with the addition of a multiplet at 2.31 ppm integrating for the 6 protons due to ethylene groups and a multiplet at 1.26 ppm integrating for 9 protons due to CH_3 in the ^1H NMR spectrum; and a peak at 23 ppm due to ethylene carbons and a peak at 5.6 ppm due to methyl carbons in the ^{13}C NMR spectrum. The ^{31}P NMR revealed a doublet of multiplets at -2.0 ppm and a doublet of doublets at -4.3 ppm, the explanation of which is the same as for complexes **1a** and **1b.**
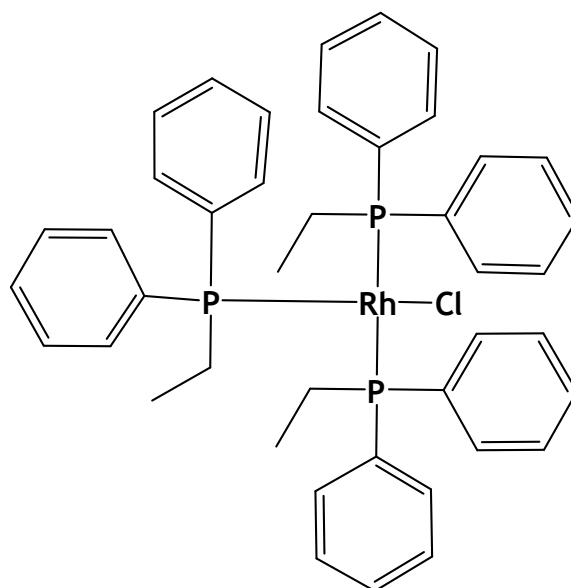
Figure 2.4. Structural representation of complex **1c**

An IR spectrum similar to that of complex **1a** was obtained, including a strong peak at 1437 cm^{-1} due to CH_2 bonds and a medium peak at 1413 cm^{-1} due to CH_3 bonds. Elemental analysis was performed for complex **1c** and the percentages of C and H as calculated for $C_{42}H_{45}ClP_3Rh$ were (C, 64.58), (H, 5.81) and were comparable to the values obtained i.e. (C, 63.22), (H, 5.516).

Complexes **1d** and **1e** were previously synthesized by Intille[4] by dissolving $RhCl_3.3H_2O$ in ethanol and evaporating the mixture twice before re-dissolving the solid in a solution of methylene chloride-ethanol and excess phosphine. This was allowed to stir overnight at room temperature. After the solvent had been allowed to evaporate under vacuum, the precipitate was washed with benzene, dissolved in chloroform, evaporated and washed with benzene again. A simpler method was followed to prepare all the Rh-P complexes as described in Chapter three of this thesis.

A melting point of 216-223 °C was obtained for complex **1d** which agrees with the literature melting point of 218-224 °C followed by decomposition at higher temperatures.[3,4] Both the ^{1}H NMR and ^{13}C NMR spectrum are similar to those of above complexes including a triplet at 1.90 ppm integrating for 12 protons representing four sets of equivalent methyl protons and a doublet at 1.16 ppm integrating for 6

protons representing the two sets of equivalent methyl protons in the ^{1}H NMR spectrum and a signal at 13 ppm is due to the methyl carbons in the ^{13}C NMR spectrum. The ^{31}P NMR showed a doublet of multiplets at 4.5 ppm and a doublet of doublets at -5 ppm, the explanation for which is similar as in the above complexes.
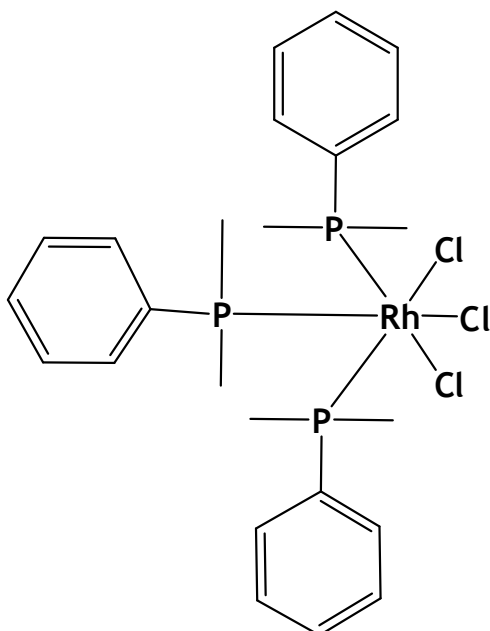
Figure 2.5. Structural representation of complex **1d**

An IR spectrum similar to those of the above complexes was obtained including the presence of a medium intensity peak at 2920 cm^{-1} due to the CH bonds of the methyl and a peak of medium intensity at 1381 cm^{-1} due to the methyl bonds.

Elemental analysis was performed for complex **1d** and the percentages of C and H as calculated for $C_{24}H_{33}Cl_3P_3Rh$ were (C, 46.22), (H, 5.33) and are comparable to the values obtained i.e. (C, 45.81), (H, 4.950).

The *m/z* values obtained from the FAB mass spectrum of complex **1d** and corresponding intensities and fragments are shown in Table 2.3. The complex is not very stable to oxidation since the 100 % intensity peak is attributed to OPMe$_2$Ph.

Table 2.3. Summary of mass spectrum data obtained for complex **1d.**

m/z	Intensity/%	Fragment
154.1	100	$OPMe_2Ph$
449	80	$M^+-Cl-PMe_2Ph$
587	50	M^+-Cl
414	30	$M^+-Cl-Cl-PMe_2Ph$
379	15	$M^+- Cl-Cl-Cl-PMe_2Ph$

A melting point of 184-196 °C was obtained for complex **1e** which agrees with the literature melting point of 183-196 °C and decomposition at higher temperatures was also observed.[3] The broadness of the melting point range (12 °C) indicates the presence of an impurity. Most likely the ligand has been oxidised from PEt_2Ph to $OPEt_2Ph$ which has caused defects in the crystal lattice.[7]

Both the ^1H NMR and ^{13}C NMR spectrum are similar to those of the above complexes with an addition of a multiplet at 1.6 ppm integrating for 12 ethylene protons and a multiplet at 1.09 ppm integrating for 18 methyl protons in the ^1H NMR; and a signal at 14.7 ppm is due to the methylene carbons and a signal at 9.3 due to the methyl carbons in the ^{13}C NMR spectrum. The ^{31}P NMR showed three doublets of multiplets at 17.7 ppm, and a doublet of doublets at 4.3 ppm, the explanation for which is similar as for the previously mentioned complexes.
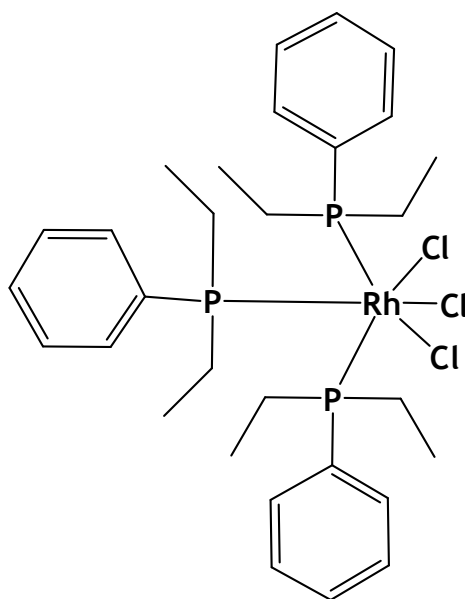
Figure 2.6. Structural representation of complex**1e**.

An IR spectrum similar to those of the above complexes was obtained including the presence of a strong peak at 1433 cm^{-1} due to ethyl bonds and the peak of medium intensity at 1413 cm^{-1} due to the methyl bonds.

Elemental analysis percentage of C and H as calculated for $C_{30}H_{45}Cl_3P_3Rh$ were (C, 50.91), (H, 6.42), which were comparable to the values obtained i.e. (C, 51.28) and (H, 6.432).

The *m/z* values obtained from the mass spectrum of complex **1e** and corresponding intensities and fragments are shown in Table 2.4. The complex is not very stable to oxidation since the 100 % intensity peak is attributed to OPEt$_2$Ph, this was also confirmed by the large melting point range obtained for the complex.

Table 2.4. Summary of mass spectrum data obtained for complex **1e**

m/z	Intensity/%	Fragment
183.2	100	$OPEt_2Ph$
505.2	6	$M^+-Cl-Et_2Ph$
647.5	1.1	M^+-Et_2
663.5	0.9	$M^+- 3(CH_3)$
671.2	0.5	M^+-Cl

2.3. CRYSTAL STRUCTURES OF COMPLEXES 1d AND 1e

Single crystals of complexes **1d** and **1e** were grown from a dichloromethane solution layered with hexane. A summary of the crystal data and selected bond lengths and angles, ORTEP representation showing the numbering scheme and a packing diagram in the unit cell of complex **1d** are presented in **Tables 2.5** and **2.6** and **Figures 2.7** and **2.8** respectively. Similar data parameters and representations for complex **1e** are presented in **Tables 2.7** and **2.8 and Figures 2.9** and **2.10** respectively.

Both complexes crystallized in the monoclinic space group $P2_1/c$ with two molecules in a unit cell and the molecular structures and atom labeling schemes for complex **1d** and **1e** are illustrated in **Figures 2.7** and **2.9** respectively. Unit cell dimensions and thermal parameters are represented in **Table 2.5** below.

The isolated crystalline forms of complexes **1d** and **1e** are Rh(III) complexes possessing octrahedral geometry with three chlorine ligands and three phosphine ligands in a *mer* isomer orientation as confirmed by ^{31}P NMR and the crystal structures (**Figures. 2.7** and **2.9**). It can be seen that in both complexes **1d** and **1e** two chloro groups are *trans* to each other while the third chloro group is *cis* to the other two.

There are no major differences in bond lengths and angles between both complexes but they do differ from that of Wilkinson's catalyst as can be seen in **Table 2.6.**

The angles :P(2)-Rh(1)-P(1), Cl(3)-Rh(1)-P(1) and Cl(3)-Rh(1)-P(3) are similar in all three complexes.

P(1)-Rh(1), P(2)-Rh(1) and P(3)-Rh(1) bond distances are slightly shorter in the Wilkinson's catalyst than in complexes **1d** and **1e**, while the Cl(1)-Rh(1) distance is slightly longer.

Both the P(2)-Rh(1)-Cl(3) and P(2)-Rh(1)-P(3) bond angles are significantly larger in the Wilkinson's catalyst, with the P(1)-Rh(1)-P(3) angle being significantly lower.

In complex **1d** intermolecular and intra molecular interactions occur between alternate H atoms and P atom which are in close contact as seen in **Figure 2.8.**[5]

Table 2.5. Crystal data and structure refinement for **1d** and **1e**

Empirical formula	$C_{24} H_{33} Cl_3 P_3 Rh$ (1d)	$C_{30} H_{45} Cl_3 P_3 Rh$ (1e)
Formula weight	623.67	707.83
Temperature	173(2) K	173(2) K
Wavelength	0.71073 Å	0.71073 Å
Crystal system	Monoclinic	Monoclinic
Space group	P2(1)/c	P2(1)/n
Unit cell dimensions	a = 15.7372(6) Å	a = 10.5259(4) Å
	$\alpha = 90°$	$\gamma = 90°$
	B = 10.2012(4)Å	b = 13.5769(5) Å
	$\beta = 92.2080(10)°$	$\beta = 92.6910(10)°$
	c = 16.6202(6) Å	c = 22.6289(10) Å
	$\gamma = 90°$.	$\gamma = 90°$
Volume	2666.20(17) Å^3	3230.3(2) Å^3
Z	4	4
Density (calculated)	1554 Mg/m^3	1.213 Mg/m^3
Max. and min. transmission	0.9148 and 0.5958	0.8871 and 0.6652
Final R indices [I>2sigma(I)]	R1 = 0.0305, wR2 = 0.0511	R1 = 0.0242, wR2 = 0.0570
R indices (all data)	R1 = 0.0461, wR2 = 0.0549	R1 = 0.0288, wR2 = 0.0589
Largest diff. peak and hole	0.516 and -0.662 e.Å^{-3}	0.373 and -0.916 e.Å^{-3}

Table 2.6. Selected bond lengths [Å] and angles [°] for **1d** , **1e** and Wilkinson's Catalyst

	Complex 1d	Complex 1e	Complex 1a
P(1)-Rh(1)	2.3656(6)	2.3827(4)	2.334 (3)
P(2)-Rh(1)	2.2817(6)	2.3145(4)	2.214 (4)
P(3)-Rh(1)	2.3702(6)	2.4106(4)	2.324 (4)
Cl(1)-Rh(1)	2.3612(6)	2.3607(4)	2.398 (4)
Cl(2)-Rh(1)	2.4216(6)	2.4308(4)	
Cl(3)-Rh(1)	2.3482(6)	2.3575(4)	
P(2)-Rh(1)-Cl(3)	93.15(2)	96.033(14)	156.2 (2)
P(2)-Rh(1)-Cl(1)	87.22(2)	87.236(15)	
Cl(3)-Rh(1)-Cl(1)	178.36(2)	176.565(14)	-
P(2)-Rh(1)-P(1)	96.38(2)	95.603(15)	97.9 (2)
Cl(3)-Rh(1)-P(1)	87.37(2)	86.239(15)	85.2 (2)
Cl(1)-Rh(1)-P(1)	94.17(2)	94.511(15)	
P(2)-Rh(1)-P(3)	96.75(2)	93.466(15)	100.4 (1)
Cl(3)-Rh(1)-P(3)	85.94(2)	84.882(14)	86.1 (2)
Cl(1)-Rh(1)-P(3)	92.43(2)	93.884(15)	
P(1)-Rh(1)-P(3)	165.57(2)	167.917(15)	152.8 (1)
P(2)-Rh(1)-Cl(2)	173.85(2)	174.618(15)	
Cl(3)-Rh(1)-Cl(2)	93.00(2)	89.336(14)	-
Cl(1)-Rh(1)-Cl(2)	86.63(2)	87.390(14)	-
P(1)-Rh(1)-Cl(2)	83.88(2)	85.092(15)	
P(3)-Rh(1)-Cl(2)	83.72(2)	86.626(15)	
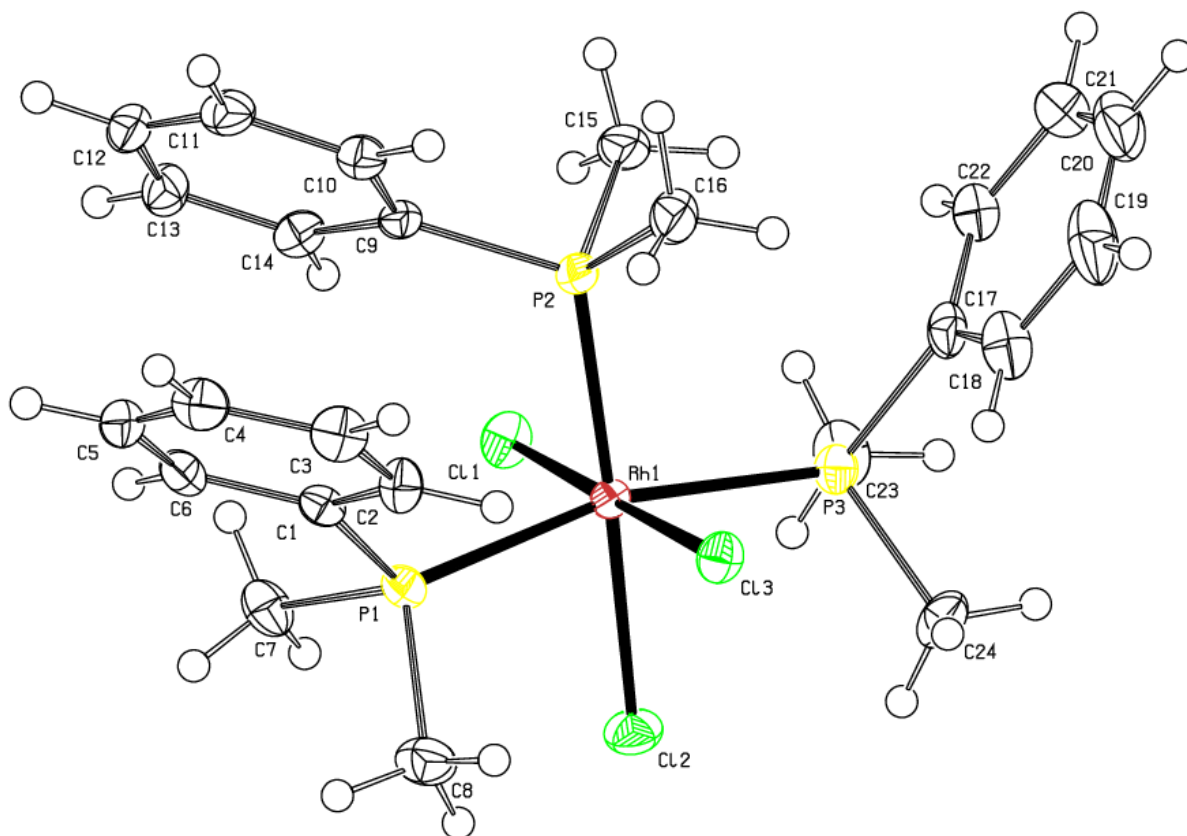
Figure 2.7. ORTEP diagram of crystal structure of **1d** showing the numbering scheme.
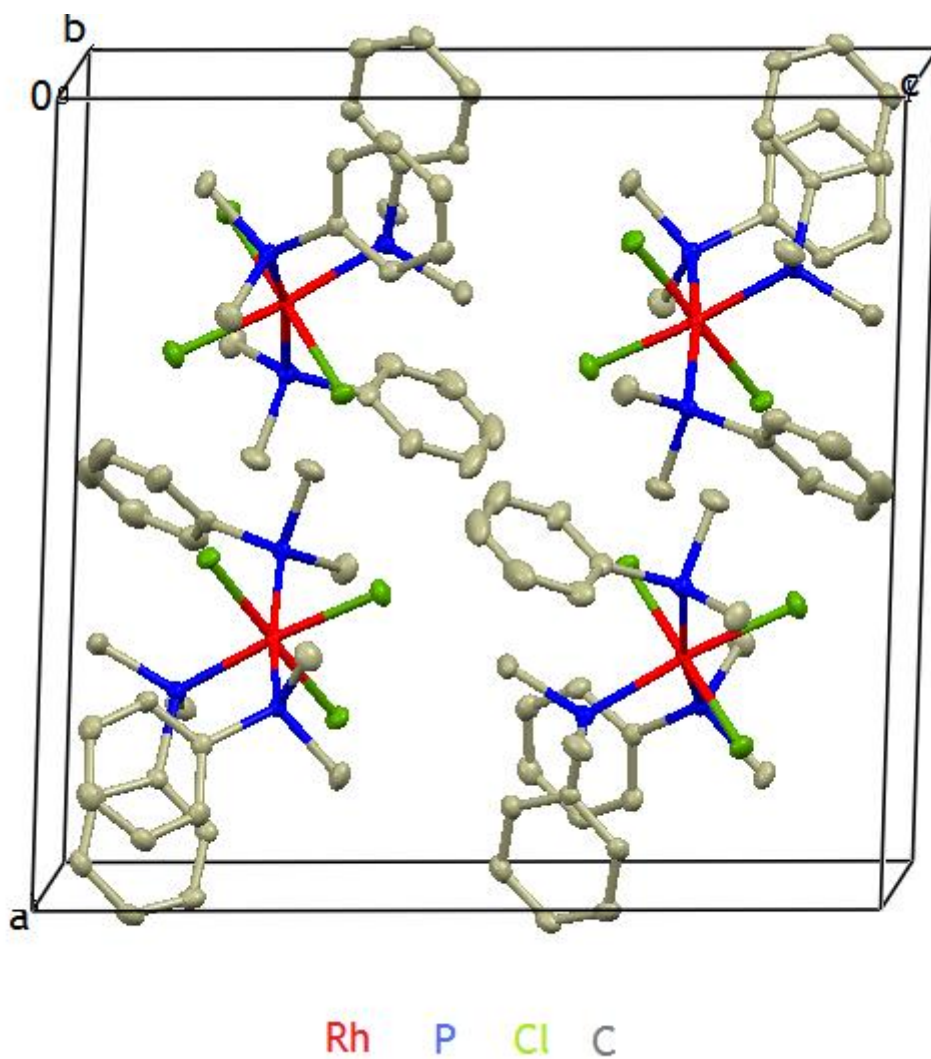
Figure 2.8. Packing diagram of a crystal of **1d**.
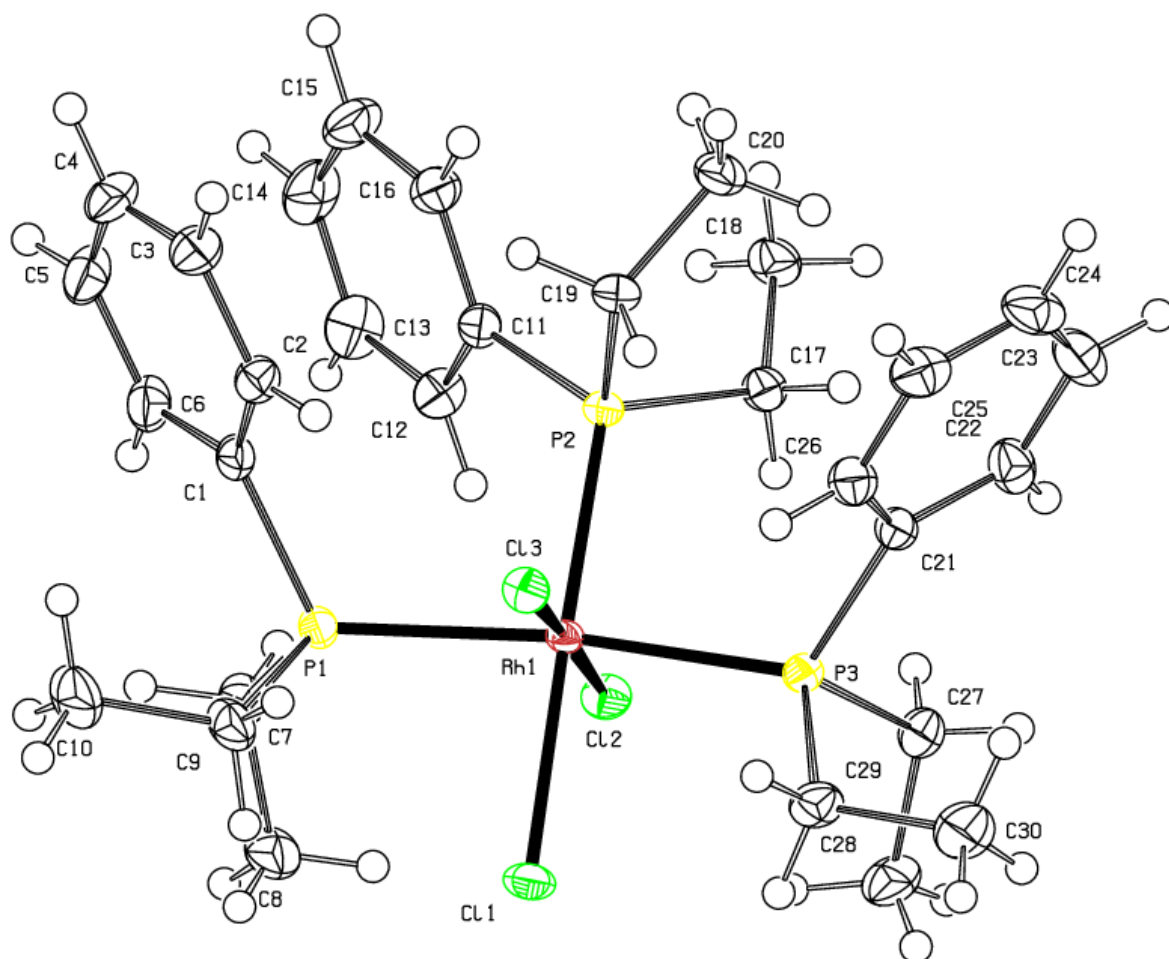
Figure 2.9. ORTEP diagram of a crystal structure of **1e** showing the numbering scheme.
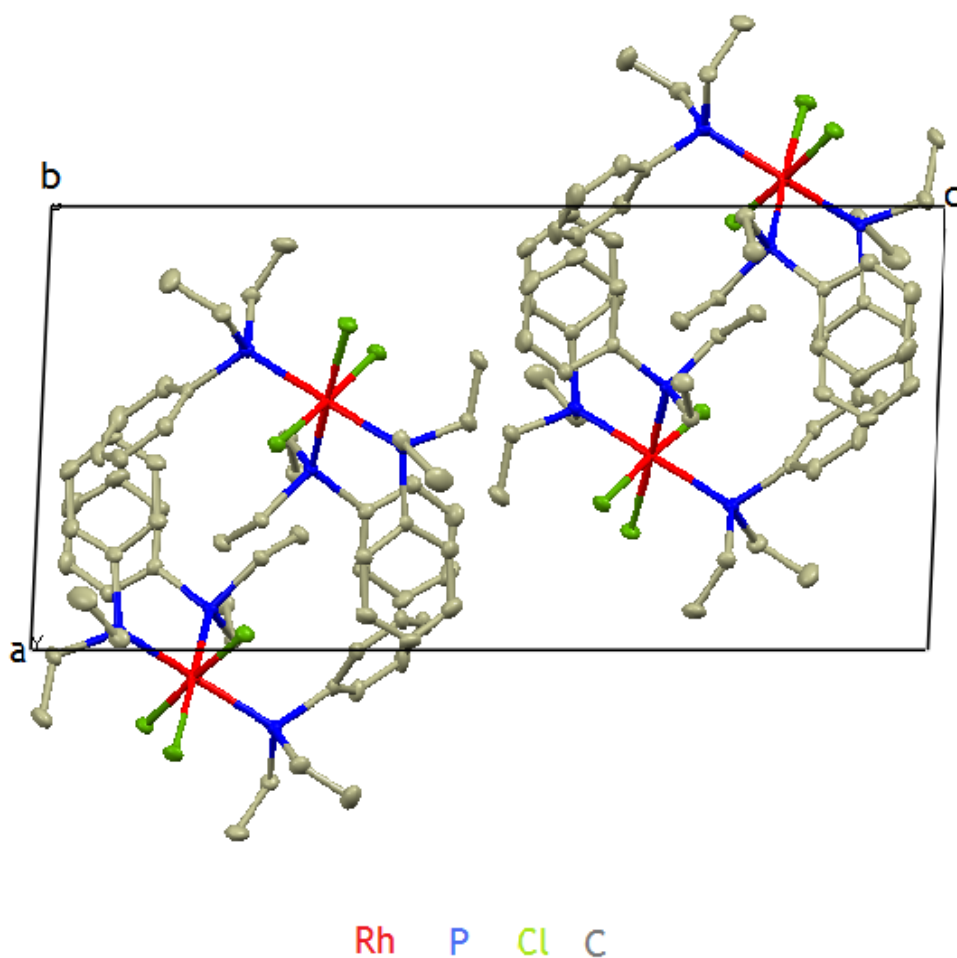
Figure 2.10. Packing diagram of a crystal of **1e**.

These complexes differ from the classical Wilkinson's catalyst due to the fact that the classical Wilkinson's catalyst contains four ligands square planarly coordinated around a Rh(I) centre while complexes **1d** and **1e** contain 6 ligands octahedrally coordinated around a Rh(III) centre.

2.3. REFERENCES

1) C.A. Ogle, T.C. Masterman, J.L. Hubbard, *J. Chem. Soc. Chem. Commum.*, 1990, 1733.
2) J.A. Osborn, F.H. Jardine, G. Wilkinson, J.F. Young, *J. Chem.Soc. (A)*, 1966, 1711.
3) J. Chatt, N.P. Johnson, B.L. Shaw, *Inorg.Chem*, 1963, **705**, 2508.
4) G.M. Intille, *Inorg. Chem.*, 1972, **11**, 695.
5) M.J. Bennet and P.B. Donaldson, *Inorg.Chem,* 1977, **16**, 655.

3 AN INVESTIGATION INTO RHODIUM-NHC COMPLEXES

3.1. SYNTHESIS AND CHARACTERISATION OF RHODIUM-*N*-HETEROCYCLIC CARBENE -(COD) COMPLEXES

3.1.1. INTRODUCTION

Carbene ligands have received substantial attention over the past two decades in the fields of organometallic and coordination chemistry. This stems from their ability to coordinate to both transition metals and main group elements and that they also have comparable electron density to tertiary phosphine ligands, as well as being more stable to oxidation and other environmental influences.[1,2]

In order to study NHC based complexes and compare their properties to those of related phosphine compounds discussed earlier (section 2.1) complexes **2a, 2b, 2c, 2d** and **2e** as illustrated in **Figure 3.1**, were synthesised. The effects of different NHC ligands on the properties of the complexes were investigated and a comparative study between these complexes and complexes **1a-e** was performed in the hydrogenation of various alkenes (section 2.4).
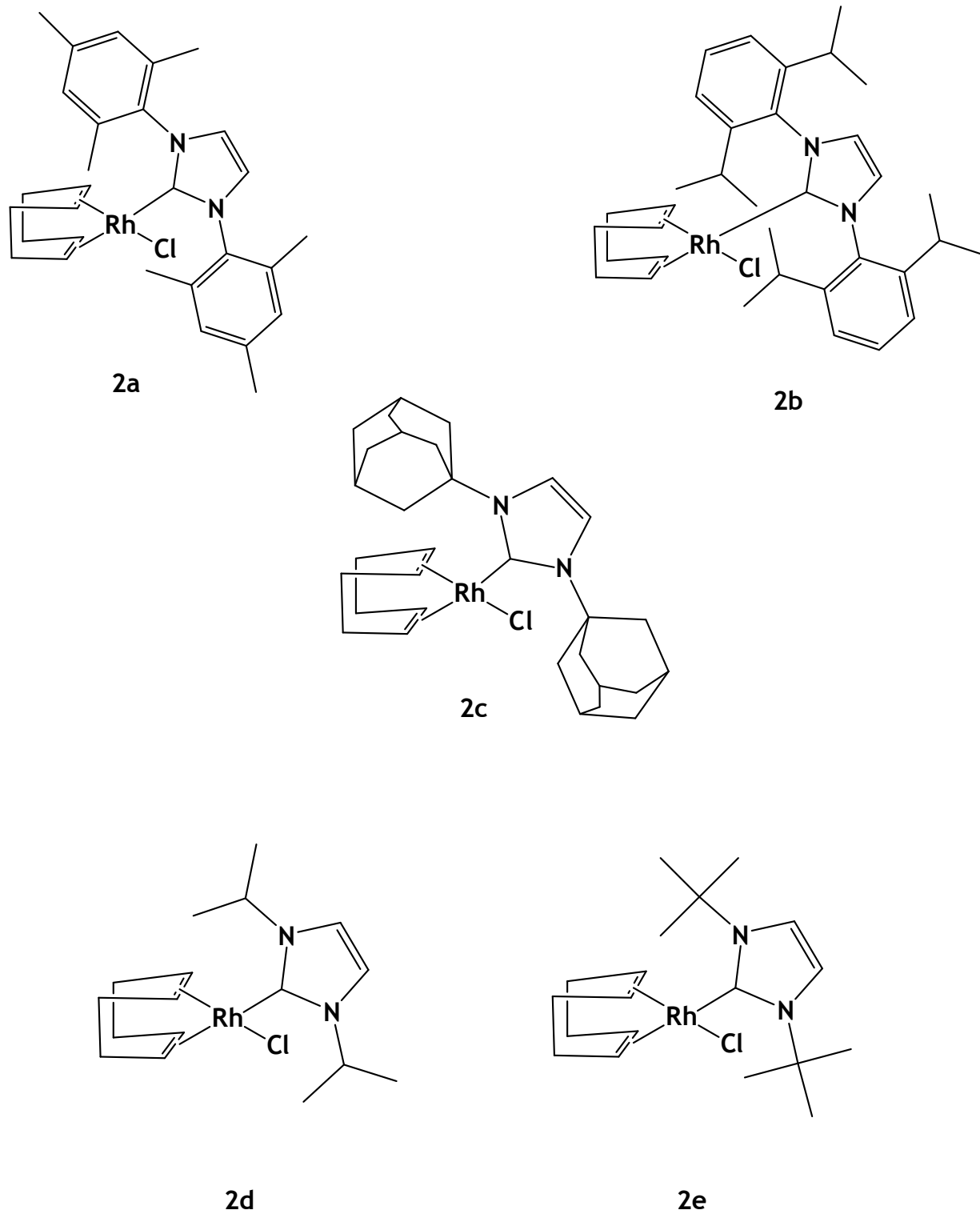
Figure 3.1. Structural Representation of compounds **2a-e**

The first step in the synthesis of the Rh(I) dimer [RhCl(COD)]$_2$ complexes involved the conversion of RhCl$_3$ to a form incorporating the cyclooctadiene (COD) ligand that the free carbene is more reactive towards i.e. the formation of the [RhCl(COD)]$_2$ dimer. **Scheme 2.1** outlines the synthetic route to the dimer where a solution of rhodium trichloride and cyclooctadiene in a water/isopropanol mixed solvent is refluxed. The free carbene radical is generated by the addition of a strong base i.e. NaH which extracts a proton from the carbene salt and forms NaX as illustrated by **Scheme 3.2.** In this method the chloro bridge of the precursor is cleaved to enable coordination of the free carbene. It is specifically used if the acyclic or cyclic carbene has bulky groups in the 1, 3 position e.g. when R= tert butyl groups (Scheme 2.3).[3-10] The synthesis is carried out in one pot to avoid dimerisation of the highly reactive free carbene.

RhCl$_3$
rhodium(III) chloride

+

(1Z,5Z)-cycloocta-1,5-diene

Reflux | **Isopropanol**
H$_2$O
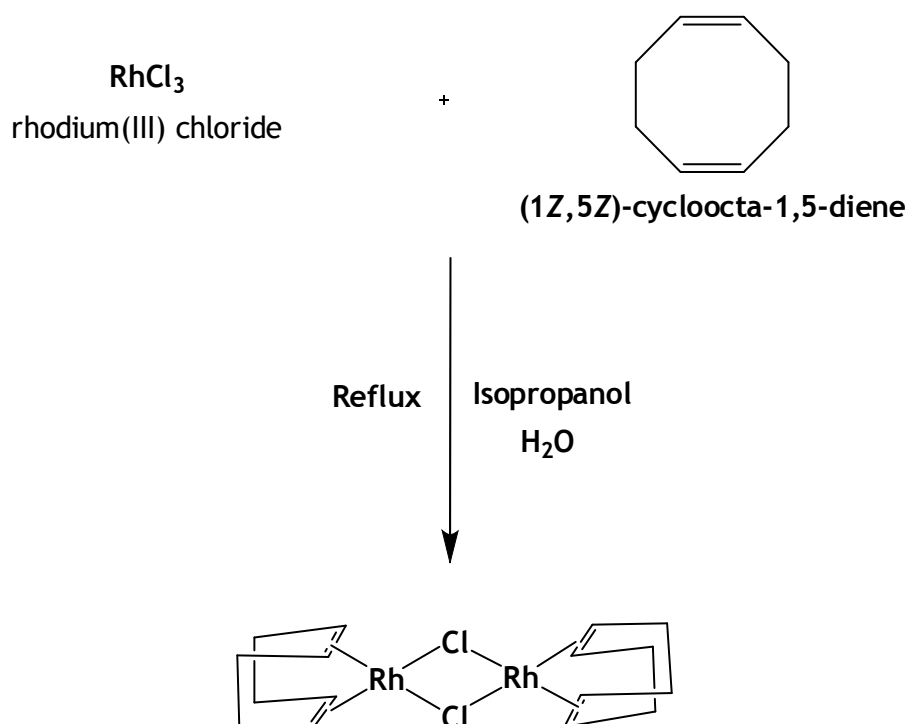
Scheme 3.1. Synthesis of [Rh(COD)Cl]$_2$

Cl^-

1,3-bis-(2,4,6-trimethylphenyl)-imidazolinium chloride

+ NaH

THF | stirring at RT

R—N :: N—R + H_2 + NaCl
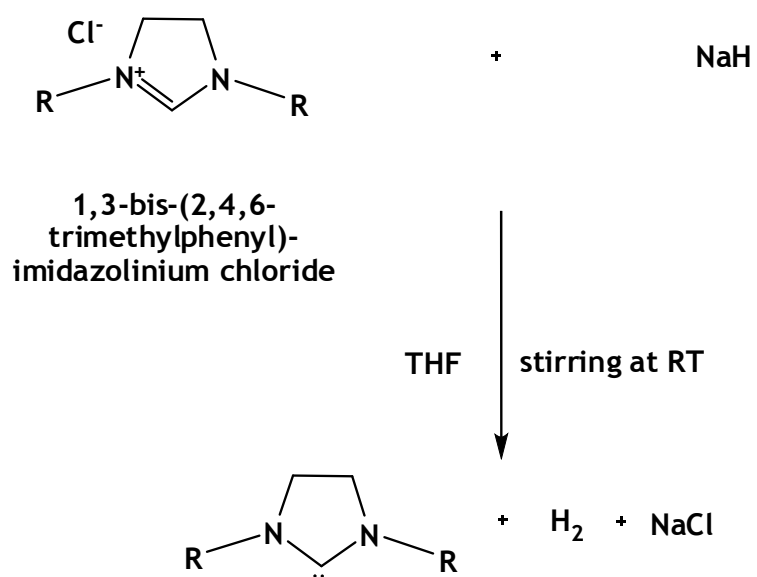
Scheme 3.2. Generation of free carbene

2.2 R—N :: N—R +
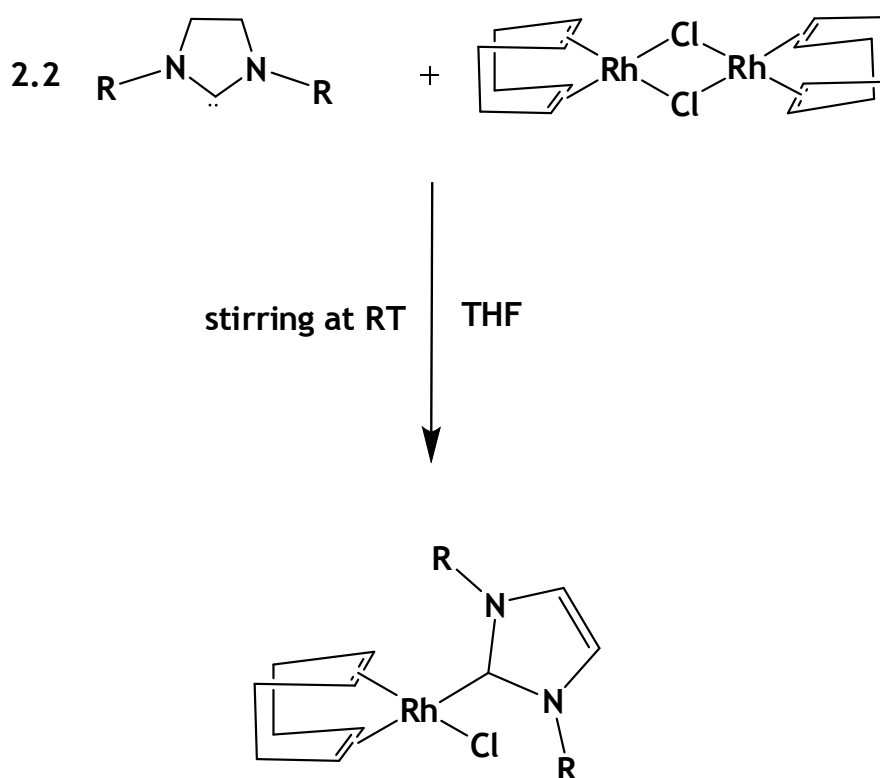
stirring at RT | THF

Scheme 3.3. Synthesis of Rhodium-(COD)-NHC complexes

After stirring at room temperature overnight a yellow solid is formed.

For complex **2a** a melting point of 234-236 ℃ was obtained which is comparable to the literature melting point of 235-235.5 ℃.[11] The ^{1}H NMR spectrum revealed one signal in the aromatic region at 6.92 ppm integrating for 4 protons representing the four phenyl-CH protons (**Figure 3.2**). A signal observed at 4.54 ppm integrated for 2 protons representing the two CH-NHC protons. The signal at 3.71 ppm integrated for 4 protons and was assigned to the four sets of CH-(COD) methylene **f** protons.

Two signals were found at 2.35 ppm and 2.25 the former integrated for 12 protons representing the four sets of equivalent methyl protons and the latter integrated for 6 protons, representing two sets of equivalent methyl protons. A further signal was observed at 2.12 ppm that integrated for 8 protons and was assigned to the remainder of the four sets of equivalent, saturated (CH_2 (COD)) protons.

The ^{13}C NMR spectrum showed a signal at 213.8 ppm representing the carbene carbon (Rh-C). Three signals were seen in the aromatic region. The two signals at 139.5 and 134.2 ppm were due to the phenyl carbons bonded to nitrogens and the peak at 129.3 ppm represented the other phenyl carbons. The important signal at 92.1 ppm is due to NHC carbons. The signal at 55.1 ppm is representative of the (COD) carbons and at 29.9 ppm for the (COD) carbons. The two methyl carbons are represented by a signal at 20.1 ppm and the remaining four methyl carbons are represented by a signal in the spectrum at 17.1 ppm.
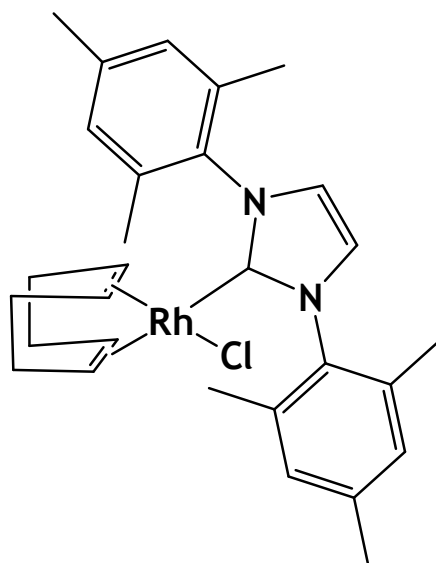
Figure 3.2. Structural representation of complex **2a**.

The IR spectrum revealed a medium intensity peak at 3007 cm^{-1} indicating the presence of CH phenyl bonds and a medium intensity peak at 2815 cm^{-1} representing a non aromatic CH bond stretch. A weak and a medium intensity peak were present at 1625 and 1622 cm^{-1} respectively were assigned to the C=C phenyl bonds. Two strong peaks representing CH$_2$ bonds were observed at 1482 and 1466 cm^{-1}, assigned to the presence of the (COD) moiety. The medium peak at 1383 cm^{-1} was indicative of methyl bonds. An important strong peak occurred at 1259 cm^{-1} due to C-N bonds and another strong peak at 849 cm^{-1} indicating N-phenyl bonds.

The *m/z* values obtained from the mass spectrum of complex **2a** and the corresponding intensities of fragments are shown in **Table 3.1.**

Table 3.1. Summary of mass spectrum data obtained for complex **2a**

m/z	Intensity/%	Fragment
307.3	100	M$^+$- (Rh-Cl-(COD)
517.4	4	M$^+$- 2(CH$_3$)
406.3	3.5	M$^+$-Cl-(COD)
513	1	M$^+$-Cl

For the new complex **2b** a melting point of 233-234 °C was obtained. The ^{1}H NMR spectrum is similar to that of **2a**, including a multiplet at 3.95 ppm integrating for 2 protons representative of the two **f** CH-isopropyl protons and a signal at 1.06 was observed integrating for the equivalent 24 **i** methyl protons (**Figure 3.3**).

The ^{13}C NMR spectrum was similar to that of complex **2a** with the addition of signal at 65.2 which was assigned to the **f** isopropyl carbons and the eight **i** methyl-isopropyl carbons are represented by a signal at 22 ppm.
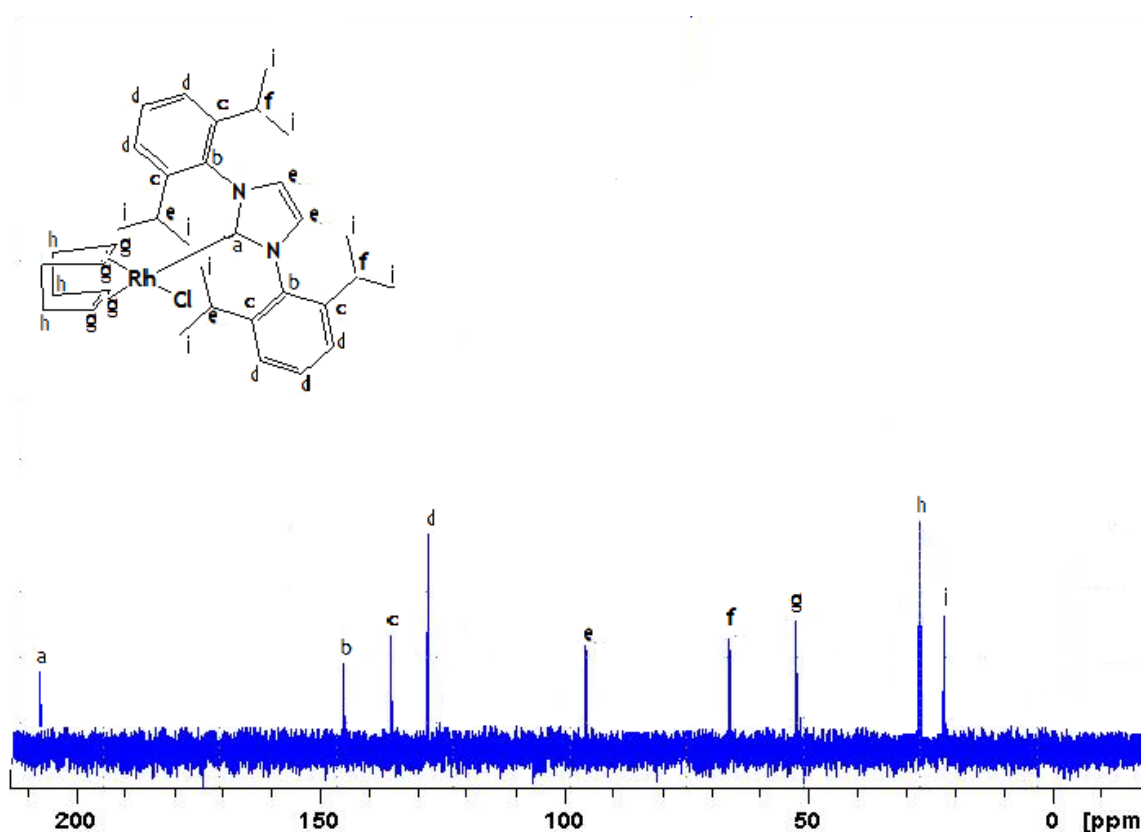
Figure 3.3. Assignment of ^{13}C NMR data for complex **2b**

The IR spectrum is similar to that of complex **2a** and also revealed two strong peaks at 1443 and 1410 cm^{-1} representing ethyl bonds and a medium peak at 1324 cm^{-1} was indicative of methyl bonds.

The *m/z* values obtained from the mass spectrum of complex **2b** and the corresponding intensities and fragments are shown in **Table 3.2.**

Table 3.2. Summary of mass spectrum data obtained for complex **2b**

m/z	Intensity/%	Fragment
601.5	100	M$^+$- 2(CH$_3$)
487.4	96	M$^+$-Ph(isopropyl)$_2$-CH$_3$
391.5	95	M$^+$-Rh-Cl-(COD)
207.1	55	M$^+$-NHC-Cl
281.1	40	M$^+$-Rh-Cl-(COD)-7(CH$_3$)

A melting point of 227-231°C was obtained for the new complex **2c**. The ^{1}H NMR spectrum was similar to that of complexes **2a** and **2b** with the exclusion of phenyl peaks. The multiplet present at 3.77 ppm integrates for 4 protons representing four sets of CH-(COD) protons and the signal at 3.56 integrates for 6 protons representing the 6 sets of equivalent CH-adamantyl protons (**Figure 3.4.**). The singlet at 2.45 ppm integrating for 12 protons represents the 6 sets of ethyl-adamantyl protons and the singlet close by at 2.34 ppm integrates for 8 protons and is representative of 4 sets of ethyl-(COD) protons. The next signal at 1.82 ppm integrates for 12 protons and represents the last 6 sets of ethyl-adamantyl protons.

The ^{13}C NMR spectrum showed a signal at 212.4 ppm representing the carbene carbon (Rh-C).The signal at 129.3 ppm was is due to the CH-NHC carbons and the signal at 51.1 ppm is representative of the CH-(COD) carbons. A signal observed at 40.6 ppm represents CH-adamantyl carbons and the signal at 31.4 ppm represents the ethyl-adamantyl carbons. The last two signals occurred at 28.1 and 27.1, the former is due to ethyl-(COD) carbons and the latter is due to ethyl-adamantyl carbons.

#
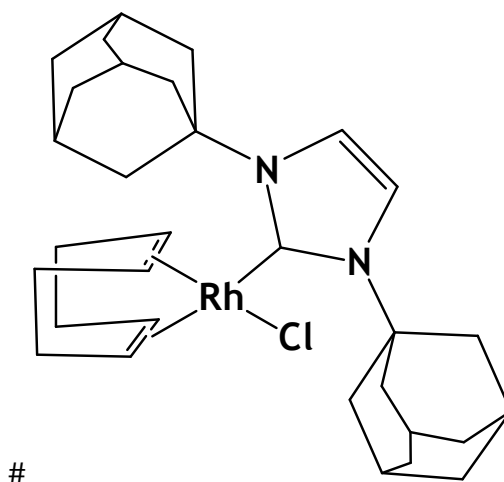
Figure 3.4. Structural representation of complex **2c**

The IR spectrum was similar to above complexes with the exception of methyl bonds.

The *m/z* values obtained from the mass spectrum of complex **2c** and corresponding intensity and fragment are shown in **Table 3.3.**

Table 3.3. Summary of mass spectrum data obtained for complex **2c**

m/z	Intensity/%	Fragment
337.5	100	M$^+$-Rh-Cl-(COD)
207.1	35	M$^+$-NHC-Cl

For complex **2d** a melting point of 222-223°C which agreed with the literature melting point of 221.5-222 °C.[11] The ^{1}H NMR spectrum revealed one signal at 4.86 ppm integrating for 2 protons representing the two CH-NHC protons (**Figure 3.5**). The multiplet at 3.45 ppm integrates for 2 protons and is representative of the two CH-isopropyl protons. A multiplet signal at 2.34 ppm integrating for 4 protons represents four sets of CH-(COD) protons.

Two signals at 1.98 and 1.5 ppm, the former integrating for 8 protons, represents four sets of equivalent ethyl-(COD) protons and the latter integrating for 12 protons represents the four sets of equivalent methyl protons.

The ^{13}C NMR spectrum showed a signal at 210.6 ppm representing the carbene carbon (Rh-C). A signal at 117.8 ppm was present due to the CH-NHC carbons and the signal at 66.7 represents the CH-isopropyl carbons. The signal 52.2 ppm is representative of the CH-(COD) carbons and the signal observed at 25 represents the ethyl-(COD) carbons. The 8 methyl-isopropyl carbons are represented by a signal at 22.5 ppm.
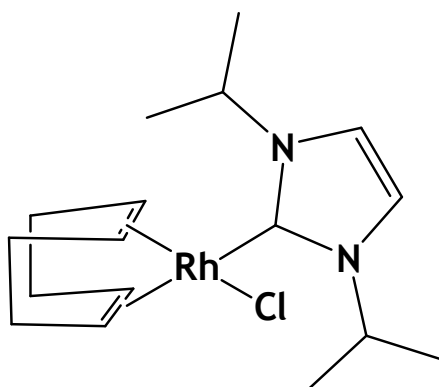
Figure 3.5. Structural representation of complex 2d

The IR spectrum was similar to that of complex **2b** with the exclusion of CH phenyl bonds.

The *m/z* values obtained from the mass spectrum of complex **2d** and corresponding intensities and fragments are shown in **Table 3.4.**

Table 3.4. Summary of mass spectral data obtained for complex **2d**

m/z	Intensity/%	Fragment
254.2	4	M$^+$-Rh-Cl-(COD)
153.3	100	M$^+$-NHC
363.5	7	M$^+$- 2(CH3)
289.3	3.5	M$^+$-(COD)
339.6	1	M$^+$-Cl-CH$_3$

A melting point of 220-222 °C was obtained for the new complex **2e**. The ^{1}H NMR spectrum revealed one signal at 4.49 ppm integrating for 2 protons representing the two CH-NHC protons (**Figure 3.6**). The multiplet at 3 ppm integrates for 4 protons representing four sets of CH-(COD) protons. Two signals at 2.1 and 1.41 ppm the former integrating for 8 protons, representing four sets of equivalent ethyl-(COD) protons and the latter integrating for 18 protons representing the six sets of equivalent methyl protons, were observed.

The ^{13}C NMR spectrum showed a signal at 211.2 ppm representing the carbene carbon (Rh-C). There was an important signal at 129 ppm due to the CH-NHC carbons and the signal at 64.1 represents the C-di*tert*butyl carbons. The signal at 50.2 ppm is representative of the CH-(COD) carbons and the signal observed at 28.1 represents the ethyl-(COD) carbons. The 6 methyl carbons are represented by a signal at 27 ppm.
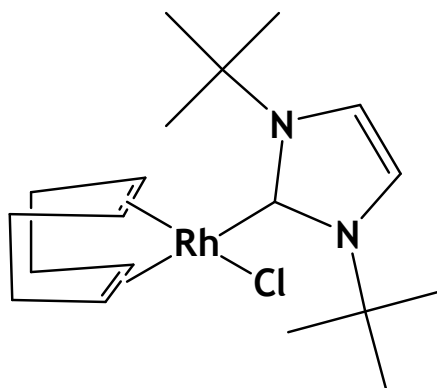
Figure 3.6. Structural representation of complex 2e

The IR spectrum was similar to that of complex **2d** including a medium peak at 1374 cm^{-1} occurring due to methyl bonds of the di*tert*butyl group.

The *m/z* values obtained from the mass spectrum of complex **2e** and corresponding intensity and fragment are shown in **Table 3.5.**

Table 3.5. Summary of mass spectrum data obtained for complex **2e**

m/z	Intensity/%	Fragment
183.2	100	M$^+$-Rh-Cl-(COD)
326.9	10	M$^+$-Cl-4(CH$_3$)
207	35	M$^+$- (COD)- 2(tertbutyl)
221	15	M$^+$-(COD)-Cl-4(CH$_3$)
281	20	M$^+$-Cl-(COD)

None of the MS data obtained for the rhodium-(COD)-NHC complexes contained any oxidized forms of the NHC ligands therefore the rhodium-(COD)-NHC complexes are less readily oxidised than the rhodium-phosphine complexes and are therefore more stable in air.

3.2. SYNTHESIS AND CHARACTERISATION OF RHODIUM-CO-*N*-HETEROCYCLIC CARBENE COMPLEXES

3.2.1. INTRODUCTION

The CO substituted complexes, **3a, 3b, 3c, 3d, 3e** as shown in **Figure 3.7** were synthesised. The effects of different NHC ligands on the properties of the complexes were investigated. The presence of the CO ligand enabled a comparative study of the complexes in terms of the basicity of the coordinated NHC ligands by using simple IR techniques.

3a

3b

3c

3d

3e
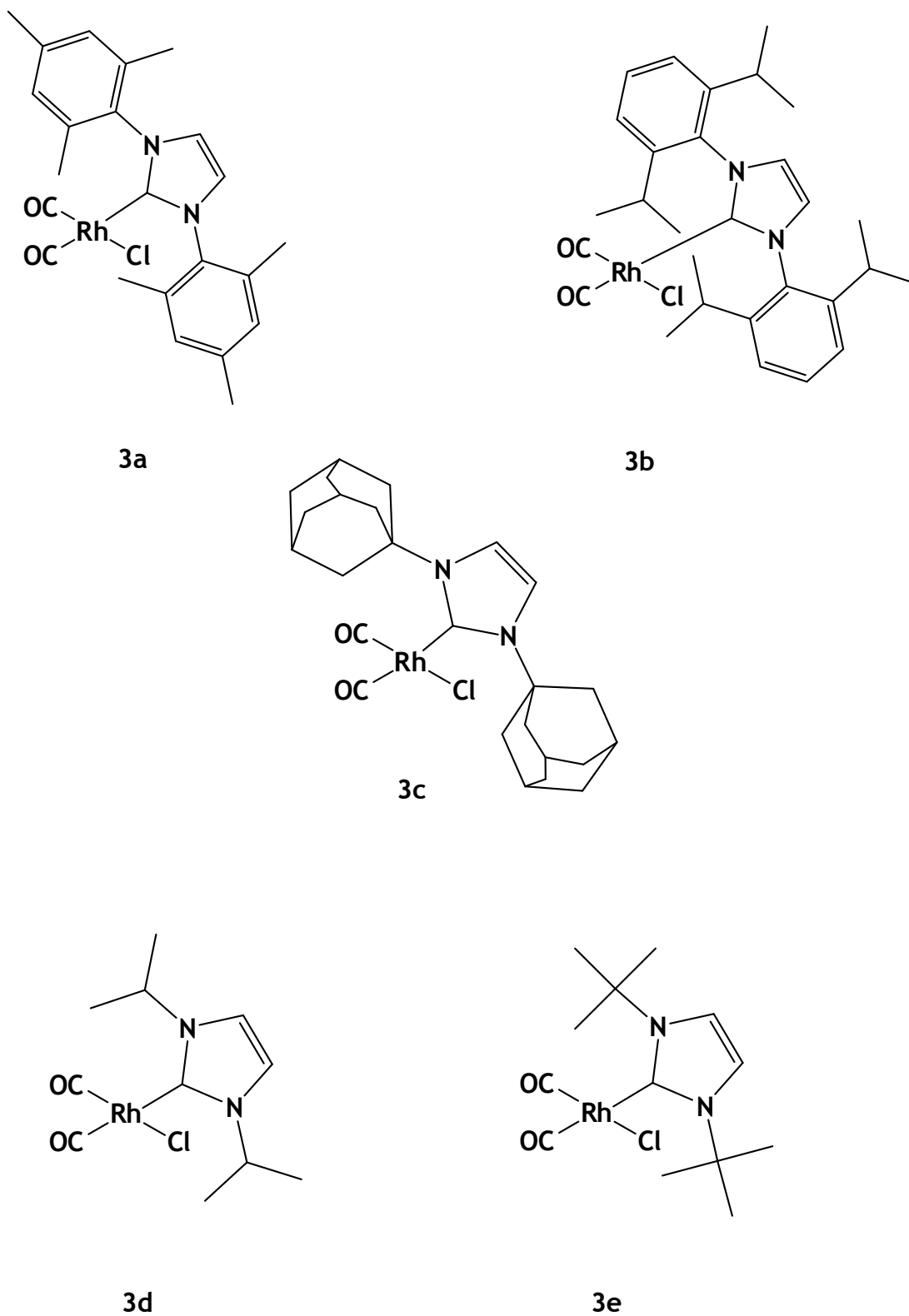
Figure 3.7. Structural Representation of compounds **3a-e**

Carbon monoxide (CO) was bubbled through a solution of each rhodium-(COD)-NHC complex in dichloromethane at room temperature (**Scheme 3.4.**). The product was formed within 15 minutes which was evident from a colour change from yellow to a lighter shade of yellow. Since NHC is a strong donor and CO is a strong acceptor, CO can completely displace the (COD) ligand in a short time.
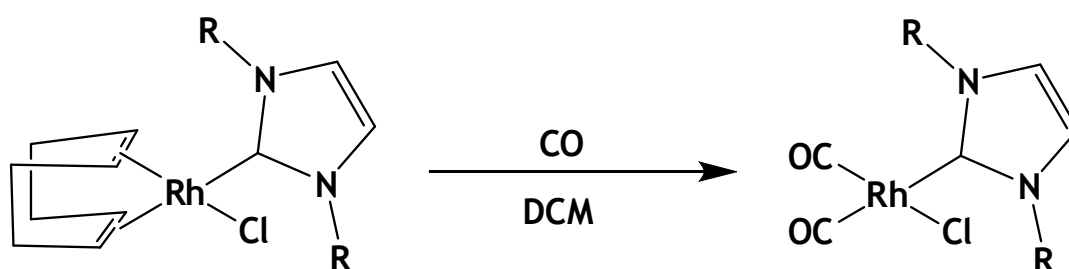
Scheme 3.4. Synthesis of rhodium-CO-NHC complexes

Both NMR and IR spectrum indicate the cis conformation of the CO ligands in all complexes i.e. with CO trans to the NHC ligand. Two CO signals appear in the ^{13}C NMR spectrum between δ = 145 and 170 ppm.[3] The IR spectrum contains two intense ν(CO) bands indicating that the two CO ligands are not equivalent and are *cis* to each other. The CO NMR peaks and CO stretching frequencies are tabulated in **Table 3.6.**

Table 3.6. Selected IR and NMR Data

Complex	ν (CO) sym	ν (CO) assym	^{13}C δ ppm: (CO)
3a	2067	1998	168.1, 159.2
3b	2067	1986	166.5, 146.2
3c	2161	1989	162.3, 159.2
3d	2162	1982	165.3, 146.1
3e	2162	1983	166, 147.3

The ^{1}H NMR spectrum for complex **3a** revealed one signal in the aromatic region at 6.93 ppm integrating for 4 protons representing the four CH phenyl protons (**Figure 3.8**). A signal at 4.41 ppm is present integrating for 2 protons representing the two CH-NHC protons. Two signals at 2.34 and 2.25 ppm, the former integrating for 12 protons representing the four sets of equivalent methyl protons and the latter integrating for 6 protons, representing two sets of equivalent methyl protons, were also observed. The fact that the methyl groups are equivalent indicates that complex is symmetrical.

The ^{13}C NMR spectrum showed a signal at 211.2 ppm representing the carbene carbon (Rh-C). Two peaks were observed due to both CO groups at 168.1 and 159.2 ppm which confirms that CO groups are cis orientated. Three signals were observed in the aromatic region. The two signals at 139.7 and 134.2 ppm represents the phenyl carbons bonded to the nitrogens and the one at 129.2 ppm represents the CH phenyl carbons. A signal at 92 ppm is due to the CH-NHC carbons. The signal at 20 ppm is representative of two sets of methyl carbons and the remaining four methyl carbons are represented by the last signal in the spectrum at 17 ppm.
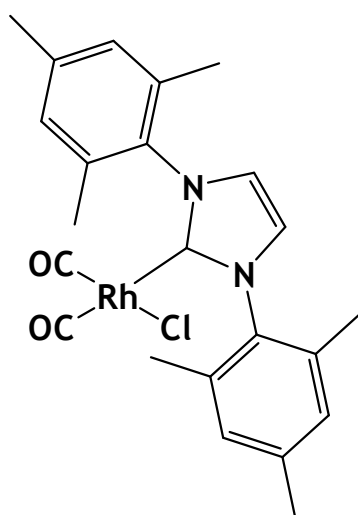
Figure 3.8. Structural representation of complex **3a**

The IR spectrum revealed a medium intensity peak at 3034 cm^{-1} due to the CH aromatic bonds and a medium peak at 2919 cm^{-1} due to CH non aromatic bonds. The important peaks to note are due to the Rh-CO bonds, present at 2067 and 1998 cm^{-1}. A weak to medium peak were present at 1627 cm^{-1} due to C=C aromatic bonds. Two stong peaks due to ethyl bonds at 1484 and 1464 cm^{-1} were observed. The medium peak at 1380 cm^{-1} was indicative of methyl bonds. An important strong peak occurred at 1262 cm^{-1} due to the C-N bond and another strong peak at 852 cm^{-1} was due to N-phenyl bonds.

The *m/z* values obtained from the mass spectrum of complex **3a** and corresponding intensity and fragment are shown in **Table 3.7.**

Table 3.7. Summary of mass spectrum data obtained for complex **3a**

m/z	Intensity/%	Fragment
207	100	M$^+$- Cl - 2(CO) - 2(PhMe$_3$)
307.2	98	M$^+$-NHC
326.9	40	M$^+$- 2(CO) -PhMe$_3$
340.9	25	M$^+$-CO -PhMe$_3$-CH$_3$
281	65	M$^+$-2CO-PhMe$_3$-Me$_3$

The ^{1}H NMR spectrum for complex **3b** is similar to that of complex **3a** including two signals at 3.33 and 1.37 ppm, the former integrating for 4 protons representing the four sets of equivalent CH-isopropyl protons and the latter integrating for 24 protons, representing four sets of equivalent methyl protons (**Figure 3.9**). The fact that the methyl protons are equivalent tells us that the carbene ligand is symmetrical.

The ^{13}C NMR spectrum was similar to that of complex **3a** with the addition of the signal at 67.8 ppm which is representative of the four sets of CH-isopropyl carbons and the four sets methyl carbons are represented by the last signal in the spectrum at 25.8 ppm.
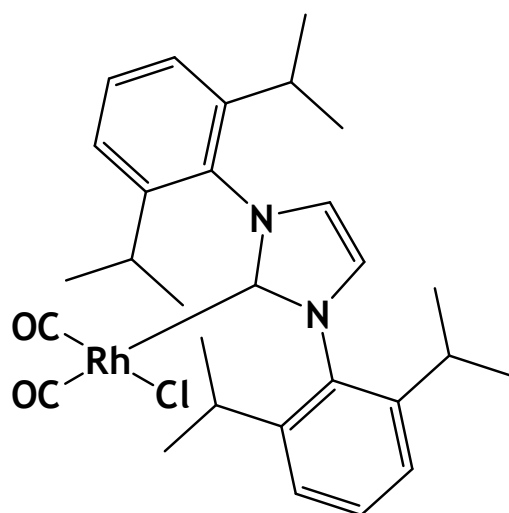
Figure 3.9. Structural representation of complex **3b**

The IR spectrum is similar to above complex **3a** including a medium peak at 1384 cm^{-1} which was indicative of methyl bonds.

The *m/z* values obtained from the mass spectrum of complex **3b** and corresponding intensity and fragment are shown in **Table 3.8.**

Table 3.8. Summary of mass spectrum data obtained for complex **3b**

m/z	Intensity/%	Fragment
489.1	100	M$^+$- Cl - 2(CO)
154	98	M$^+$-Cl-NHC
387.2	70	M$^+$- Cl-Rh-2CO
232.1	35	M$^+$-(diisopropylphenyl)-CO
549	25	M$^+$-Cl

For complex **3c** the ^{1}H NMR spectrum revealed a signal at 4.16 ppm integrating for 2 protons representing the two CH-NHC **a** protons (**Figure 3.10**). The multiplet present at 2.24 ppm integrates for 6 protons, representing the 6 sets of equivalent CH-

adamantyl **b** protons. The singlet at 2.14 ppm, integrating for 12 protons, represents the 6 sets of ethyl-adamantyl **c** protons. The last signal at 1.71 ppm integrates for 12 protons and represents the last 6 sets of ethyl-adamantyl **d** protons.

The ^{13}C NMR spectrum is similar to that of the above complexes i.e. **3a** and **3b** including a signal at 34.2 ppm representing CH-adamantyl **b** carbons and the signal at 32.5 ppm representing the **c** ethyl-adamantyl carbons. The last signal occurred at 28.4 ppm and is due to ethyl-adamantyl **d** carbons.
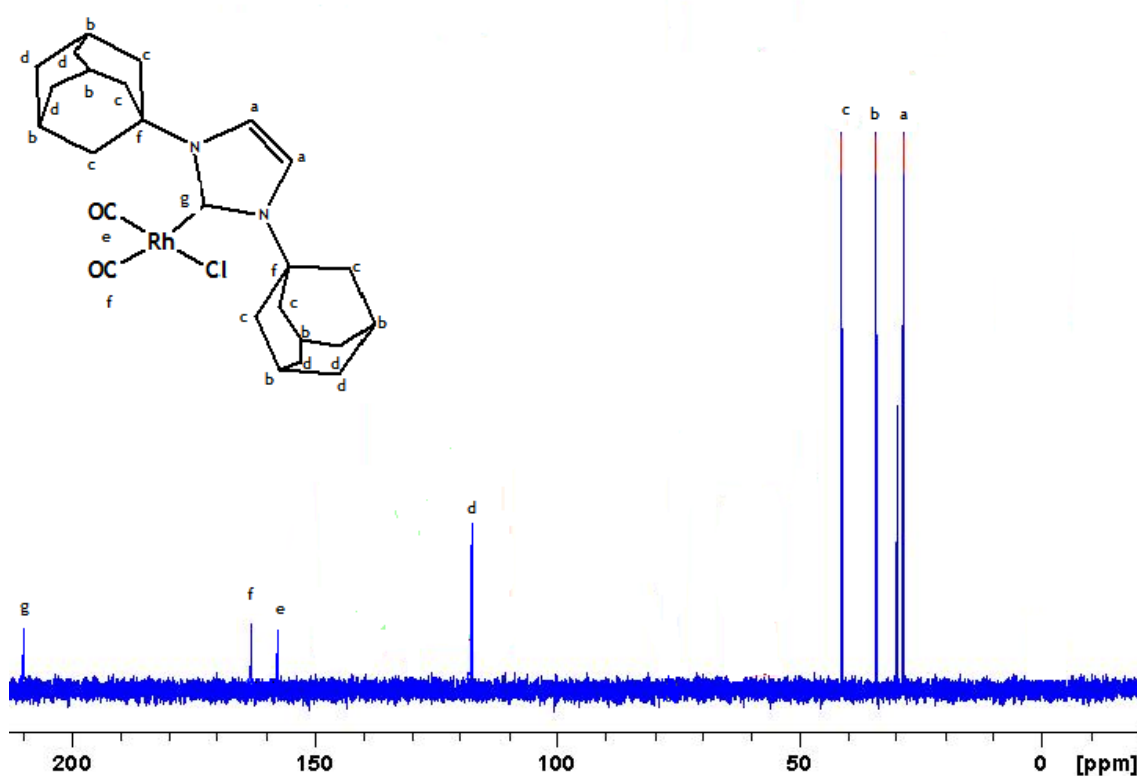
Figure 3.10. Assignment of ^{13}C NMR data for complex **3c**

The IR spectrum was similar those of complexes **3a-c**. The m/z values obtained from the mass spectrum of complex **3c** and corresponding intensities and fragments are shown in **Table 3.9.**

Table 3.9. Summary of mass spectrum data obtained for complex **3c**

m/z	Intensity/%	Fragment
337.1	100	M$^+$- Cl – Rh-2(CO)
154	30	M$^+$-Cl-NHC

The ^{1}H NMR spectrum for complex **3d** was similar to those of **3a-c** including two signals at 3.52 and 1.9 ppm, the former integrating for 4 protons representing the four sets of equivalent CH-isopropyl protons, and the latter integrating for 24 protons, representing four sets of equivalent methyl protons (**Figure 3.11**).

The ^{13}C NMR spectrum was similar to complexes **3a-c**. In addition, the signal at 53.1 ppm is representative of the four sets of CH-isopropyl carbons and the four sets of methyl carbons are represented by the last signal in the spectrum at 25.8 ppm.
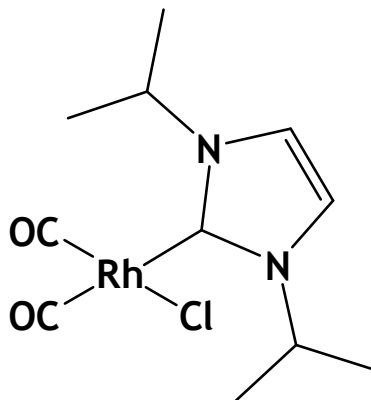
Figure 3.11. Structural representation of complex **3d**

The IR spectrum revealed a weak intensity peak at 3144 cm^{-1} due to the CH aromatic bonds and a medium peak at 2980 cm^{-1} due to CH non aromatic bonds. The important peaks to note are due to the Rh-CO bonds present at 2062 and 1982 cm^{-1}. A medium peak was present at 1637 cm^{-1} due to C=C aromatic bonds. A strong peak due to ethyl

bonds at 1466 cm^{-1} was observed. The medium peak at 1374 cm^{-1} was indicative of methyl bonds and an important strong peak occurred at 1033 cm^{-1}, due to the C-N bonds.

The ^{1}H NMR spectrum for complex **3e** was similar to those of the above carbene complexes, including a signal at 1.38 ppm integrating for 18 protons, representing six sets of equivalent methyl protons.

The ^{13}C NMR spectrum was also similar to those of the above carbene complexes (**3a-3d**), including a signal at 63.5 ppm which is representative of the two sets of C-di*tert*butyl carbons and the six sets of methyl carbons are represented by the next signal in the spectrum at 27.2 ppm.
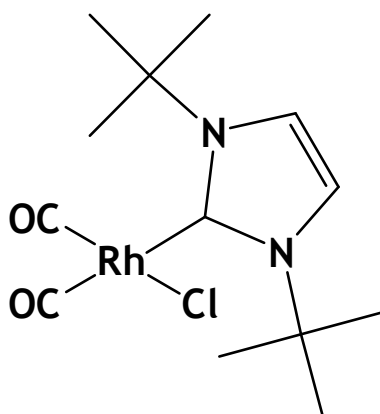
Figure 3.12. Structure of complex **3e**

The IR spectrum was similar those of the above carbene complexes. In addition a medium peak at 1380 cm^{-1} was indicative of methyl bonds.

The *m/z* values obtained from the mass spectrum of complex **3e** and corresponding intensity and fragment are shown in **Table 3.10.**

Table 3.10. Summary of mass spectrum obtained for complex **3e**

m/z	Intensity/%	Fragment
183.2	100	M^+-Rh-Cl-(COD)
289	15	M^+-CO-2(CH_3)
203.1	9	M^+- CO- 2(tertbutyl)

3.3. REFERENCES

1)   W. A. Herrmann, *Angew. Chem. Int. Ed.,* 2002, **41**, 1290.

2)   J.M. Praetorius, C.M. Crudden, *Dalton Trans.,* 2008, 4079.

3)   G.D. Frey, C.F. Rentzsch, D. von Preysing, T. Scherg, M. Muhlhofer, E. Herdtwerk, W.A. Herrmann, *J. Organomet. Chem.,* 2006, **691**, 5725.

4)   W.A. Herrmann, M. Elison, J. Fisher, C. Kocher, G.R.J. Artus, *Chem. Eur. J.,* 1996, **2**, 772.

5)   P. Bazinet, G.P.A. Gap, D.S. Richeson, *J. Am. Chem. Soc.,* 2003, **125**, 13314.

6)   Y.Zhang, D. Wang, K. Whurst, M.R. Buchmeiser, *J. Organomet. Chem.,* 2005, **690**, 5728.

7)   W.A. Herrmann, L. J. Goossen, M. Spiegler, *Organometallics,* 1998, **17**, 2162.

8)   A.R. Chianese, R.H. Crabtree, *Organometallics,* 2005, **24**, 4432.

9)   S. Gastgir, K.S. Coleman, A.R. Cowley, M.L.H Green, *Organometallics,* 2006, **25**, 300.

10)   M. Denk, P. Sirsch, W.A. Herrmann, *J. Organomet. Chem.,* 2002, **649**, 219.

11)   I.Özdemir, S. Demir, B. Cetinkaya, *J. Mol. Cat(A).,* 2004, **215**, 45.

4 CATALYTIC TESTING OF COMPLEXES IN HYDROGENATION REACTIONS

4.1. INTRODUCTION

Complexes **1a, 1d, 1e, 2a, 2b, 2c, 2d** and **2e** were tested as catalysts for the hydrogenation of alkenes to alkanes under mild conditions using a simple hydrogenation apparatus (see **Figure 5.1.** in the experimental section for details). The hydrogenation scheme is shown in **Scheme 4.1.,** while the substrates reported in this study are shown in **Figure 4.1.**
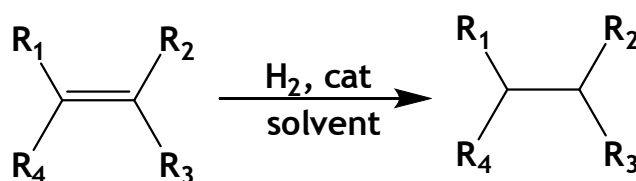
Scheme 4.1. Hydrogenation Scheme
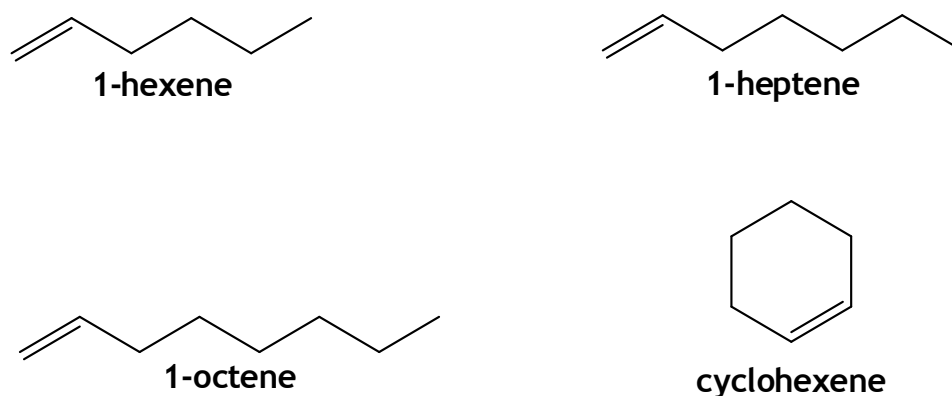
Figure 4.1. Substrates used for the hydrogenation studies

The procedure involved the bubbling of hydrogen gas through the solvent mixture for 30 minutes to ensure that the solvent becomes saturated with hydrogen. A small amount of the complex was introduced to the pear shaped flask and when dissolved complex **1a** produced a red solution which immediately turned orange on addition of the alkene. Also, solutions of complexes **1d, 1e, 2a, 2b** and **2c** originally yellow turned a lighter shade of yellow on addition of the alkene. The 100 ml syringe attached to the apparatus was filled with hydrogen so the exact amount of hydrogen consumed by the reaction could be determined.

4.2. HYDROGEN CONSUMPTION AND TOF STUDIES

Plots of hydrogen consumption in milliliters against time in seconds were plotted for all complex-substrate combinations (Experimental Section, **figures 5.6-5.7**). The R^2 values or correlation coefficients of the plots are shown in **Table 4.1.** all of which in summary indicates that all the reactions followed pseudo first order kinetics since the R^2 values are close to one.

Table 4.1. R^2 values of plots of hydrogen consumption/ml against time/s for all complex-substrate combinations

Substrate	1a	1d	1e	2a	2b	2c
1-hexene	0.9412	0.8815	0.8697	0.9673	0.9931	0.9784
1-heptene	0.9832	0.9646	0.9098	0.9428	0.9693	0.9416
1-octene	0.9568	0.9918	0.9660	0.9335	0.9922	0.9549
cyclohexene	0.9065	0.9921	0.9939	0.9846	0.9743	0.9698

The reaction mixture was analysed by GC. The presence of only the corresponding alkane peak and solvent peak in the chromatograph confirmed that all of the alkene was hydrogenated with no side products being produced. The rate of the reaction or

turnover frequency was calculated using **Equation 4.1**. The results are tabulated in **Tables 4.2.** and **4.3.** and illustrated in **Figure 4.2.** and **4.3.** for the purpose of clarity.

$$TOF = \frac{Moles\ of\ Product}{Moles\ of\ Catalyst} / Hour$$

Equation 4.1. Equation for the computation of turnover frequency

Table 4.2. Turnover rates of hydrogenation for rhodium-phosphine complexes

Substrate	1a	1d	1e
1-hexene	9560	7314	8184
1-heptene	9593	7339	8212
1-octene	10407	7962	8909
cyclohexene	11532	8823	9872
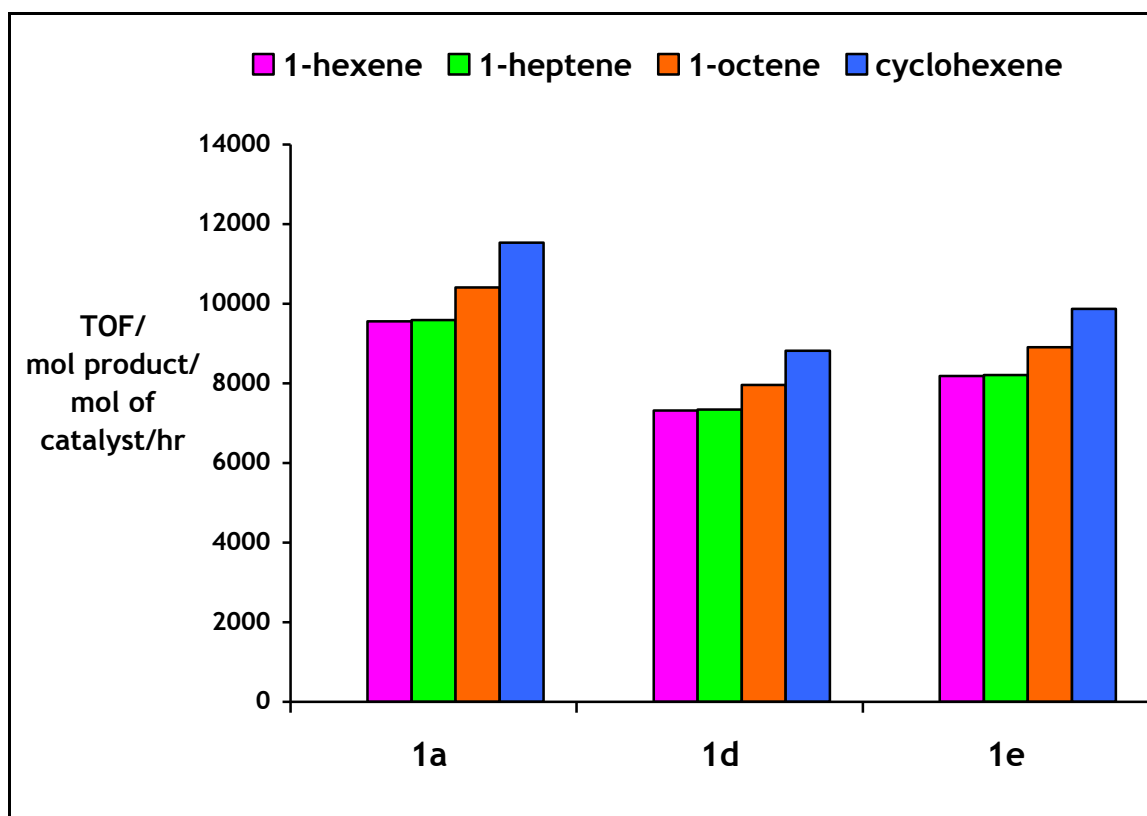
Figure 4.2. Graph showing TOFS for different rhodium-phosphine catalyst-substrate combinations

Table 4.3. Turnover rates of hydrogenation for rhodium-(COD)-NHC complexes

Substrate	2a	2b	2c	2d	2e
1-hexene	424	475	376	500	441
1-heptene	294	325	245	38	332
1-octene	172	186	123	257	136
cyclohexene	42	49	36	55	51
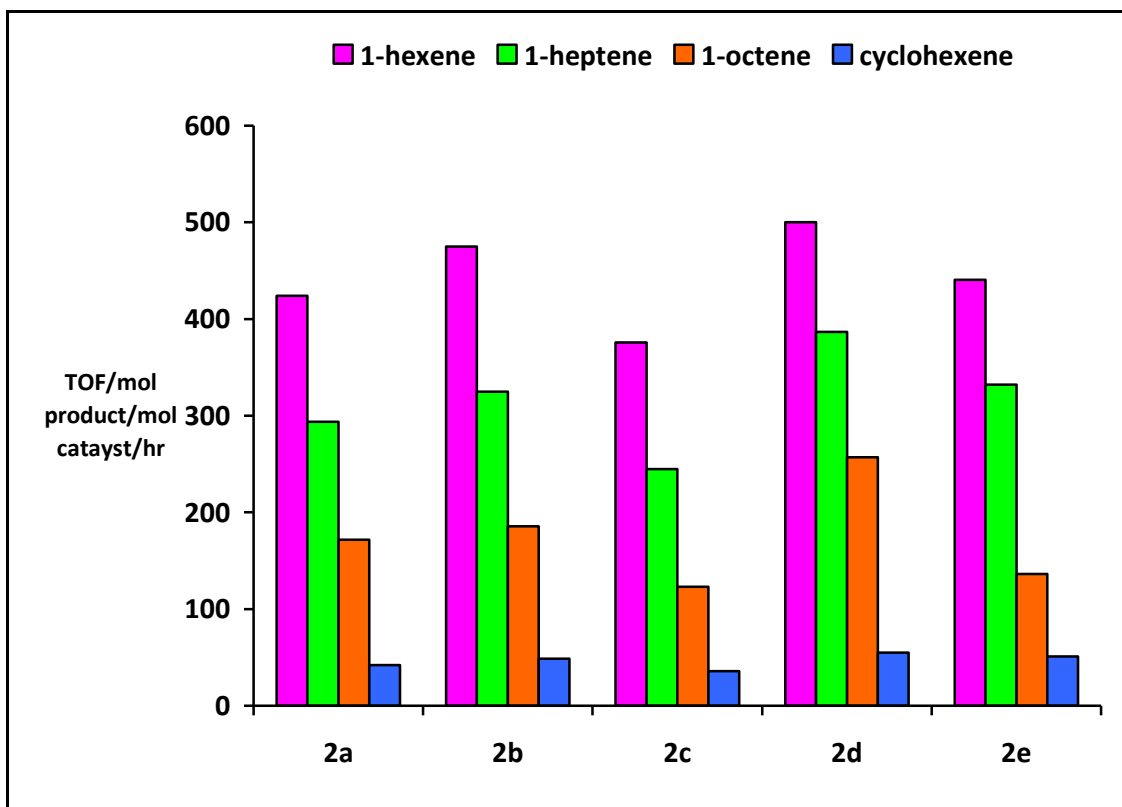
Figure 4.3. Graph showing TOFS for different rhodium-(COD)-NHC catalyst-substrate combinations

From the above data it is evident that the rate of hydrogenation increases in the following order for the carbene based complexes tested: 1-hexene > 1-heptene > 1-octene > cyclohexene. For this set of complexes it is therefore safe to argue that the higher the chain length of the alkene, the slower was the rate of hydrogenation. This is opposite the trend observed for the phosphine based complexes. For these complexes the catalyst efficiency based on TOF also increases in the following order: **1a > 1e > 1d** or RhCl(PPh$_3$)$_3$> RhCl$_3$(PPhEt$_2$)$_3$ > RhCl$_3$(PPhMe$_2$)$_3$. This relationship is explained by **1e** having the highest electron donating ability or greater *trans* influence than **1d**. Higher catalytic activity is accompanied by an increase in electron donor ability of the ligand.

Roodt *et al.*[1] have reported numerous RhClCO(L$_2$) complexes with L$_2$ denoting different phosphine ligands, analysed by IR spectroscopy. Higher stretching

frequencies of CO indicated stonger a CO bond therefore a weaker Rh-C bond and a stronger Rh-L bond. Hence, the ligand dissociation in those complexes would occur at a faster rate, consequently so does the rate of hydrogenation.[1] The movement of electron density in a metal-CO complex is illustrated in **Figure 4.4.**Transition metal complexes give rise to stable metal carbonyls because thay thave partially filled d-orbitals of correct symmetry to overlap with CO antibonding orbitals.
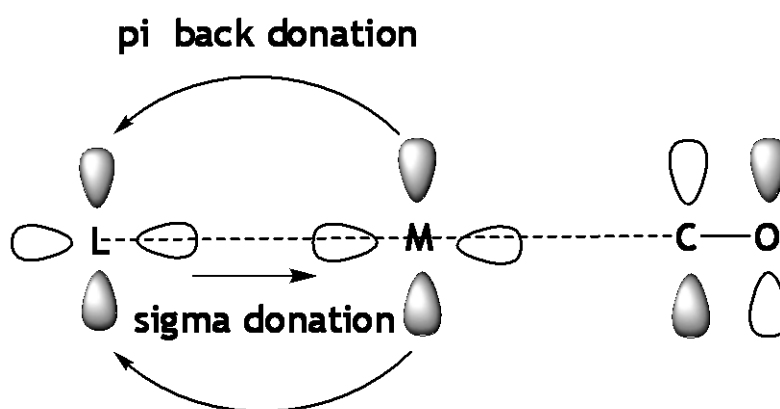
Figure 4.4. Illustration of movement of electron density in a metal-ligand-CO complex[2]

For the rhodium-(COD)-NHC complexes catalyst efficiency based on TOF increases in the following order: **2d > 2b > 2e > 2a > 2c**. This agrees with the CO vibrational frequencies contained in **Table 4.4.** for the corresponding CO analogues, since the *trans* influence or electron donor ability increases in a similar order. Also it is evident that both sterics and electronics play a role in the catalytic activity, since complex **2b** is bulkier but less electron donating than **2e** and hence more active than **2e**.

Table 4.4. Selected IR data for rhodium-CO-NHC complexes

Complex	ν (CO) assym
3a	1998 (1996)
3b	1986 (1997)
3c	1989
3d	1982
3e	1983

Figures 4.5 - 4.8 illustrates the behaviour of catalyst activity over time. It is evident that the activity of rhodium-phosphine complexes (**1a**, **1d** and **1e**) level off or remain constant over time while the activity of rhodium-NHC complexes (**2a-e**) continue to increase.
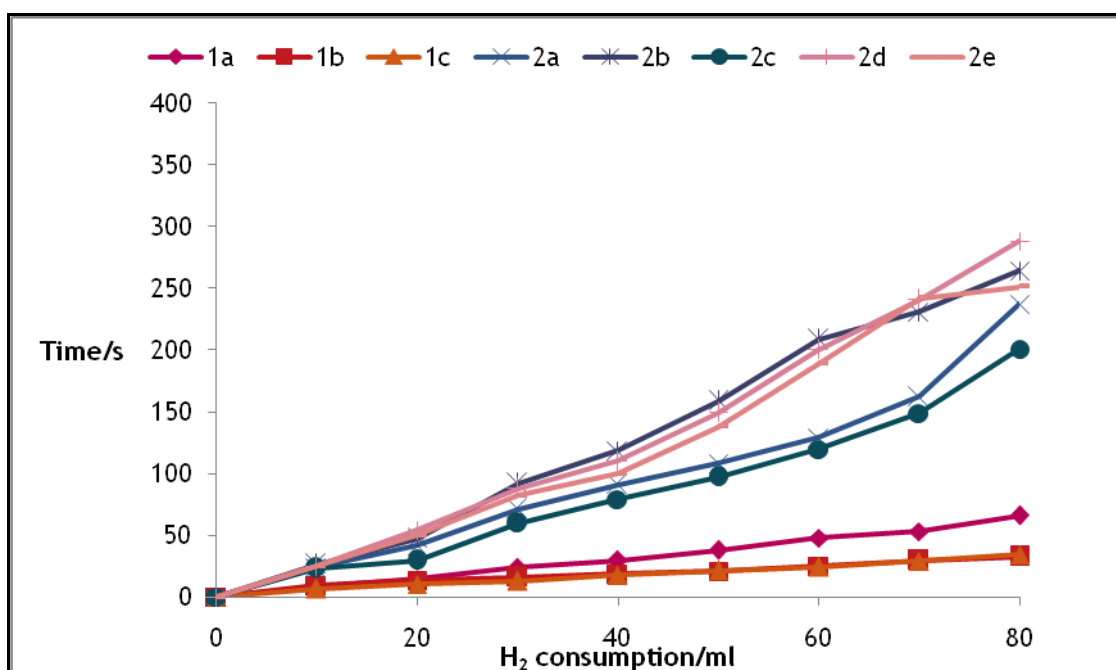
Figure 4.5. Graph of time against H_2 consumption for tested complexes for the conversion of hexene to hexane.
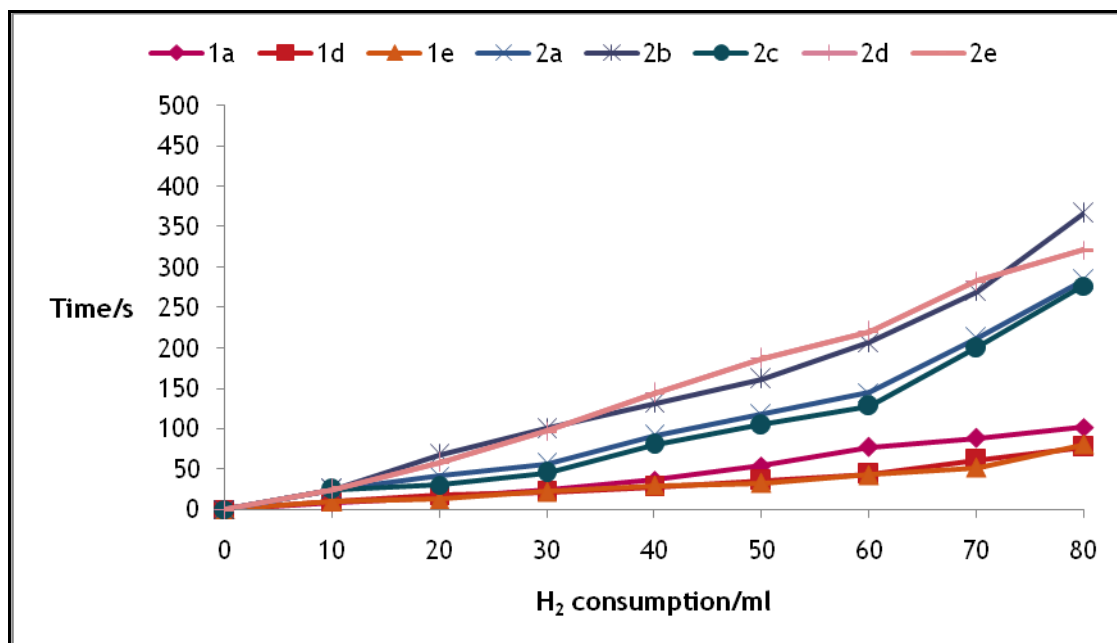
Figure 4.6. Graph of time against H_2 consumption for tested complexes for the conversion of heptene to heptane.
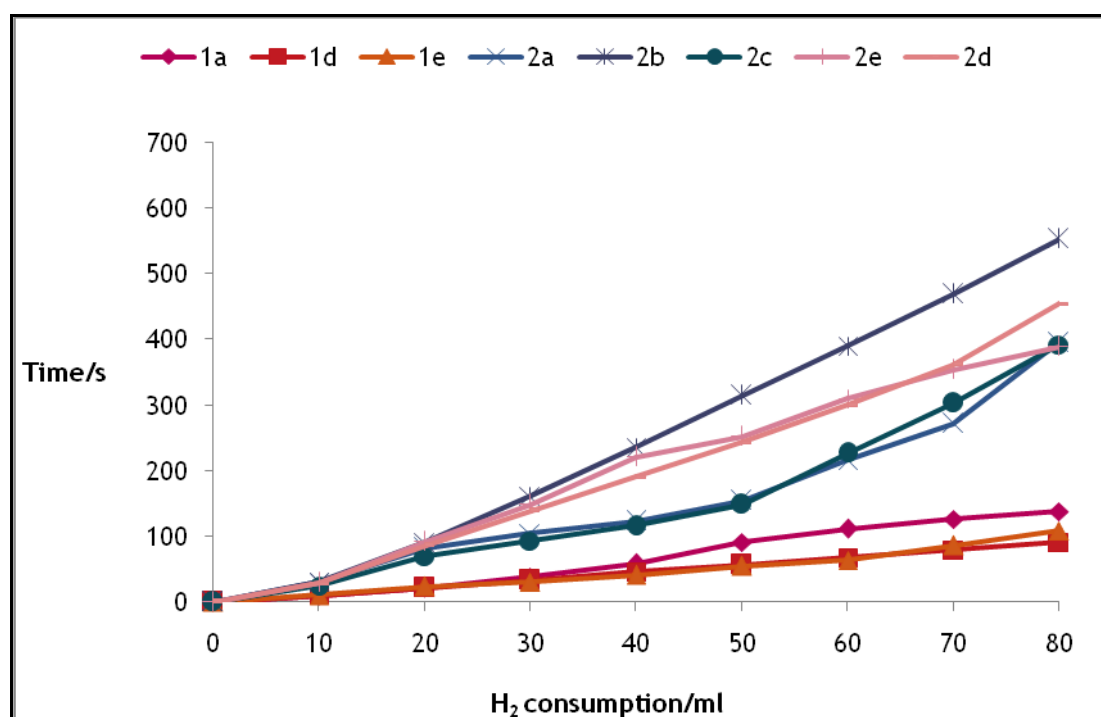
Figure 4.7. Graph of time against H_2 consumption for tested complexes for the conversion of octene to octane.
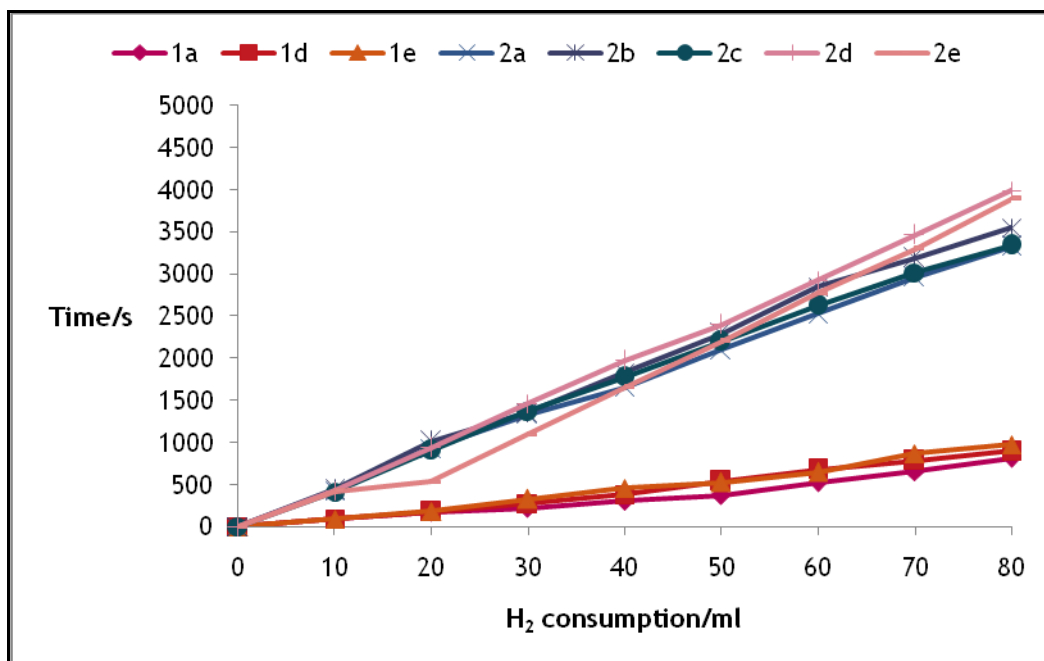
Figure 4.8. Graph of time against H_2 consumption for tested complexes for the conversion of cyclohexene to cyclohexane.

From the subsequent findings it is evident that rhodium-phosphine complexes are far more active than rhodium-(COD)-NHC complexes, the latter seem to be active for a longer time and hence more stable under mild hydrogenation conditions. The stability of the rhodium-(COD)-NHC complexes is also confirmed by the MS data in that it showed no presence of any oxidised species.

4.5. REFERENCES

1)   A. Roodt, S. Otto, G. Steyl, *Coord. Chem. Rev.,* 2003, **245**, 121.

2)   A. Brink, MSc Dissertation, University of Free State, 2007.

5 EXPERIMENTAL

All complexes were synthesised using standard Schlenk techniques under nitrogen atmosphere and using solvents dried in accordance with standard procedures and stored over molecular sieves (4 A). All synthesized complexes were characterized via infrared spectroscopy (IR), nuclear magnetic resonance spectroscopy (NMR), fast atom bombardment mass spectrometry (FAB-MS) and chemical analysis i.e. CHN elemental analysis. The structures of two complexes (**1d** and **1e**) were determined using diffraction techniques i.e. single crystal X-ray diffraction spectroscopy

5.1. REAGENTS

The phosphines and *N*-Heterocyclic carbenes were supplied by Sigma-Aldrich. $RhCl_3.3H_2O$ was obtained from *NEXT* Chimica. NaH, absolute ethanol (99%), hexane, THF, DCM and toluene were supplied by Merck.

5.2. INSTRUMENTS

All NMR spectra were obtained using a Bruker 400 MHz NMR spectrometer. Infrared spectra were recorded on Perkin Elmer attenuated total reflectance (ATR) spectrophotometer. Gas chromatographic analysis was carried out on Perkin Elmer Autosystem XL with a Flame Ionisation Detector. Low resolution mass spectrometry was conducted using a VG70SE FAB-MS. Elemental Analyses were carried out using a LECO elemental analyser.

5.3. GAS CHROMATOGRAPHY COLUMN CONDITIONS

Oven temperature	350 ℃	Mobile phase	Nitrogen
Detector temperature	200 ℃	PONA Column length	50 m
Injector temperature	250 ℃	PONA Column diameter	320 μm

5.4. GENERAL PROCEDURE FOR THE SYNTHESIS OF RHODIUM-PHOSPHINE COMPLEXES

All Rhodium phosphine complexes were synthesised by adding rhodium trichloride trihydrate ($RhCl_3 \cdot 3H_2O$) (1 g, 3.8 mmol) to an excess of the respective tertiary phosphine (0.95 mmol) (1:4 molar ratio) dissolved in absolute ethanol. The mixture was refluxed for 30 minutes and allowed to cool to room temperature. After cooling, the precipitate was filtered using a cannula, washed with absolute ethanol and dried overnight under vacuum. Physical data is shown in **Table 5.1**.

Table 5.1. Identification of rhodium-phosphine complexes.

Complex	Phosphine ligand	Colour	% yield	Melting point/ °C
1a	Triphenylphosphine	Maroon	85	246-250
1b	Methyldiphenylphosphine	Yellow-orange	75	216-223
1c	Ethyldiphenylphosphine	Yellow-orange	70	184-196
1d	Dimethylphenylphosphine	Yellow-orange	66	decomposed > 200
1e	Diethylphenylphosphine	Yellow-orange	62	decomposed > 200

1a: **^{1}H NMR (CDCl$_3$) (δ, ppm):** 7.46 (m, 30H, CH phenyl), 7.38 (m, 15H, CH phenyl);

^{13}C NMR (CDCl$_3$) (δ,ppm): 133.5(C phenyl) , 132 (CH phenyl), 128.5 (CH phenyl);

^{31}P NMR (CDCl$_3$) (δ,ppm): 48 (dt,) 30.9 (dd);

IR (v, cm^{-1}): 3056 (m, CH phenyl), 1970 (w, ph substitution), 1570 (w, C=C phenyl), 692 (s, P-phenyl);

Elemental Anal. % calculated for C$_{54}$H$_{45}$ClP$_3$Rh: (C, 70.10), (H, 4.90) **Found:**(C, 69.78), (H, 4.860);

MS (FAB, *m/z* (%)): 278.9 (100%) [PPh$_3$O], **154** (50%) [M$^+$-2(PPh$_2$)P], **626.8** (12)[M$^+$- Cl - PPh$_3$], **888.6** (3) [M$^+$- Cl], 786.4(1) [M$^+$- Cl- Rh].

1b: **^{1}H NMR (CDCl$_3$)** (δ,ppm): 7.75(m,12H, CH phenyl), 7.53 (m,18H, CH phenyl), 2 (s, 9H, CH$_3$);

^{13}C NMR (CDCl$_3$) (δ,ppm): 130.7 (C phenyl), 129.5 (CH phenyl), 128.2 (CH phenyl), 16 (CH$_3$);

^{31}P NMR (CDCl$_3$) (δ,ppm): -2.1(dm), -4.28 (dd)**;**

IR (v, cm^{-1}): 3053 (m, CH phenyl), 2915 (m, CH), 1572 (w, C=C phenyl), 1434 (s, CH$_3$), 692 (s, P-phenyl);

Elemental Anal. % calculated for C$_{39}$H$_{39}$ClP$_3$Rh:(C, 63.38), (H, 5.32) **Found:** (C, 63.00), (H, 4.989);

MS (FAB, *m/z* (%)):216.9 (100%) [OPMePh$_2$], 234.9 (5 %) [M$^+$- Rh - 2(PMePh$_2$)], 502.8 (3%) [M$^+$- Cl - PMePh$_2$], 572.7 (2%) [M$^+$- Ph$_2$ - PMePh$_2$], 266.9 (1%) [M$^+$- Rh - 2(PPh$_2$)].

1c: **^{1}H NMR (CDCl$_3$)** (δ,ppm): 7.76(m,12H, CH phenyl), 7.52 (m,18 H, CH phenyl), 2.31(m,6H,CH$_2$), 1.26 (m, 9H, CH$_3$);

^{13}C NMR (CDCl$_3$) (δ,ppm): 131.7 (C phenyl), 130.9 (CH phenyl), 128.7(CH phenyl), 23(CH$_3$), 5.6 (CH$_3$)**;**

^{31}P NMR (CDCl$_3$) (δ,ppm): -2(dm), -4.3 (dd);

IR (v, cm^{-1}) 3057 (m, CH phenyl), 2937 (m,CH), 1592 (w, C=C phenyl), 1437 (s, CH$_2$), 1413 (m, CH$_3$), 717 (s, P-phenyl);

Elemental Anal. % calculated for C$_{42}$H$_{45}$ClP$_3$Rh: (C, 64.58), (H, 5.81) **Found:** (C, 63.22), (H, 5.516).

1d: **^{1}H NMR (CDCl$_3$)** (δ, ppm): 7.51(m,5H, CH phenyl), 7.1(m,5H, CH phenyl), 6.88 (m,5H, CH phenyl), 1.9(t,12H,CH$_3$), 1.16 (d, 6H, CH$_3$);

^{13}C NMR (CDCl$_3$) (δ, ppm): 132.9 (C phenyl), 131.8 (CH phenyl), 129 (CH phenyl), 128.2 (CH phenyl), 13(CH$_3$);

^{31}P NMR (CDCl$_3$) (δ, ppm): 4.5 (dm), -5 (dd);

IR (v, cm^{-1}) 3034 (m, CH phenyl), 2920 (m,CH), 1998 (ph substitution) 1627 (m, C=C phenyl), 1381 (m, CH$_3$), 805 (m, P-phenyl).

Elemental Anal. % calculated for C$_{24}$H$_{33}$Cl$_3$P$_3$Rh : (C, 46.22), (H, 5.33) **Found:** (C, 45.81), (H, 4.950).

MS (FAB, *m/z* (%)):154.1 (100) [OPMe$_2$Ph], 449 (80) M [$^+$-Cl-PMe$_2$Ph], 587 (50) [M$^+$-Cl], 414 (30) [M$^+$-Cl-Cl-PMe$_2$Ph], 379 (15) [M$^+$- Cl-Cl-Cl-PMe$_2$Ph]

1e: **^{1}H NMR (CDCl$_3$)** (δ,ppm): 7.54(m,5H,CH phenyl), 7.1(m,10H,CH phenyl), 1.6(m,12H,CH$_2$), 1.09 (m, 18H, CH$_3$);

^{13}C NMR (CDCl$_3$) (δ,ppm): 130.6 (C phenyl), 129.6 (CH phenyl), 128.5 (CH phenyl), 128.2 (CH phenyl), 14.7(CH$_3$) 9.3 (CH$_2$);

^{13}P NMR (CDCl$_3$) (δ,ppm): 17.7(dm), 4.3 (dd)**;**

IR (v, cm^{-1}): 3045 (m, CH phenyl), 2933 (m, CH) 1998v (phenyl substitution), 1571 (w, C=C phenyl), 1433 (s, CH$_2$), 1413 (m, CH$_3$) 697 (s, P-phenyl).

Elemental Anal. % calculated for C$_{30}$H$_{45}$Cl$_3$P$_3$Rh : (C, 50.91), (H, 6.42), **Found:** (C, 51.28), (H, 6.432).

MS (FAB, *m/z* (%)):183.2 (100) [OPEt$_2$Ph], 505.2 (6) [M$^+$-Cl-Et$_2$Ph], 647.5 (1.1), M$^+$-Et$_2$, 663.5 (0.9) [M$^+$- 3(CH$_3$)], 671.2 (0.5) [M$^+$-Cl]

5.5.   COLLECTION OF SINGLE CRYSTAL DATA

A small amount of complex **1d** and **1e** was dissolved seperately in DCM. The solution was concentrated under nitrogen and layered with hexane. As the solvent evaporated single crystals grew and were analysed using single crystal X-ray diffraction analysis.

Intensity data were collected on a Bruker APEX II CCD area detector diffractometer with graphite monochromated Mo K_α radiation (50kV, 30mA) using the APEX 2 data collection software. The collection method involved ω-scans of width 0.5° and 512 x 512 bit data frames. Data reduction was carried out using the program *SAINT+* and face indexed absorption corrections were made using *XPREP*.

The crystal structure was solved by direct methods using *SHELXTL*. Non-hydrogen atoms were first refined isotropically followed by anisotropic refinement by full matrix least-squares calculations based on *F^2* using *SHELXTL*. Hydrogen atoms were first located in the difference map, then positioned geometrically and allowed to ride on their respective parent atoms. Diagrams and publication material were generated using SHELXTL, PLATON and ORTEP-3. [1-5]

Selected crystal and structural refinement data are presented in **Table 3.4.** and the balance of the data are presented in the appendix section.

5.6. SYNTHESIS OF (Rh(COD)Cl)$_2$

Rhodium trichloride trihydrate (RhCl$_3$.3H$_2$O) (1 g, 3.8 mmol) was dissovled in 15 ml of distilled water and 31.2 ml isopropanol. Then, 1,5-cyclooctadiene ((COD)) (5.7 ml,46.4 mmol) was added to the above solution and refluxed for six hours. The yellow-orange crystals formed were washed with 1:5 (methanol:water), filtered by means of a filter cannula and dried overnight under vacuum.

5.6.1. GENERAL PROCEDURE FOR THE SYNTHESIS OF RHODIUM-NHC COMPLEXES

All rhodium-(COD)-NHC complexes were synthesied by dissolving (Rh(COD)Cl)$_2$ (0.02 mmol) in THF. NaH (0.044 mmol) was added to this mixture along with an excess of the NHC salt (0.044mmol). The mixture was then allowed to stir overnight at room temperature. The precipitate was purified by means of cannula filtration, washed with hexane and dried overnight under vacuum. Physical Data is shown in **Table 5.2**.

Table 5.2. Identification of rhodium-NHC complexes.

Complex	NHC ligand	Colour	% yield	Melting point/°C
2a	1,3-bis-(2,4,6-trimethylphenyl)-imidazol-2-ylidene	Yellow	60	234-236
2b	1,3-bis-(2,6-diisopropylphenyl)-imidazol-2-ylidene	Yellow	57	233-234
2c	1,3-bis(1-adamantyl)-imidazol-2-ylidene	Yellow	55	227-231
2d	1,3-diisopropyl-imidazol-2-ylidene	Yellow	50	222-223
2e	1,3-di-tert-butyl-imidazol-2-ylidene	Yellow	52	220-222

2a: ^{1}H NMR (CDCl$_3$) (δ,ppm): 6.92 (s, 4H, CH phenyl), δ 4.54 (s, 2H, CH-NHC), 3.71 (s, 4H, CH (COD)), 2.35 (s,12H, CH3), 2.25 (s, 6H, CH$_3$), 2.12 (s, 8H, CH$_2$ (COD));

^{13}C NMR (CDCl$_3$) (δ,ppm): 213.8 (Rh-C), 139.5(C, phenyl) 134.2 (C, phenyl), 129.3 (CH, phenyl), 92.1 (CH, NHC), 55.1(CH, (COD)), 29.9 (CH$_2$, (COD)), 20.1 (CH$_3$), 17.1 (CH$_3$);

IR (v, cm^{-1}): 3007(m, CH aromatic), 2815 (m,CH), 1625, 1622 (w,m C=C aromatic), 1482,1466 (s, CH$_2$), 1383v (m, CH$_3$), 1259 (s, C-N), 849 (s, N-phenyl);

MS (FAB, m/z (%)):307.3 (100) [M$^+$-Rh-Cl-(COD)], 517.4 (4) [M$^+$- 2(CH$_3$)], 406.3 (3.5) [M$^+$-Cl-(COD)], 513 (1) [M$^+$-Cl], 154.1(1) [M$^+$-Cl-PhMe$_3$].

2b: ^{1}H NMR (CDCl$_3$) (δ,ppm): 7.36 (s, 6H, CH phenyl), δ 4.45 (s, 2H, CH-NHC), 3.93 (m, CH), 3.17 (s, 4H, CH (COD)), 1.38 (s, 8H, CH$_2$ (COD)), 1.06 (s,12H, CH$_3$);

^{13}C NMR (CDCl$_3$) (δ,ppm): 213.2 (Rh-C), 145.1(C, phenyl) 135.7 (C, phenyl), 127.9 (CH, phenyl), 124.1 (CH, phenyl), 95.6 (CH, NHC), 65.2(CH-isopropyl), 52.7 (CH,(COD)), 27.1(CH$_2$-(COD)), 22 (CH$_3$-isopropyl);

IR (ν, cm^{-1}): 3100 cm^{-1} (m, CH aromatic), 2961 (m,CH), 1660, 1587 (w,m C=C aromatic), 1443,1410 (s, CH$_2$), 1324 (m, CH$_3$), 1261 (s, C-N), 802 (s, N-phenyl);

MS (FAB, *m/z* (%)):601.5 (100) [M$^+$- 2(CH$_3$)], 487.4 (96) [M$^+$-Ph(isopropyl)$_2$-CH$_3$], 391.5 (95) [M$^+$-Rh-Cl-(COD)], 207.1 (55) [M$^+$-NHC-Cl], 281.1 (40) [M$^+$-Rh-Cl-(COD)-7(CH$_3$)].

2c: ^{1}H NMR (CDCl$_3$) (δ,ppm): 212.4 (Rh-C), 5.59 (s, 2H, CH-NHC), 3.77 (s, 4H, CH (COD)), 3.56 (m,6H, CH-adamantyl), 2.45 (s, 12H, CH$_2$-adamantyl), 2.34 (m, 8H, CH$_2$-(COD)), 1.82 (m, 12H, CH$_2$-adamantyl)

^{13}C NMR (CDCl$_3$) (δ,ppm): 129.3 (CH, NHC), 51.1 (CH,(COD)), 40.6(CH-adamantyl) 31.4(CH$_2$-adamantyl), 28.1 (CH$_2$-(COD)), 27.1(CH$_2$-adamantyl);

IR (ν, cm^{-1}): 3161 (m, CH aromatic), 2910 (m,CH), 1545 (m C=C aromatic), 1454 (s, CH$_2$), 1155 (s, C-N);

MS (FAB, *m/z* (%)):337.5 (100) [M$^+$-Rh-Cl-(COD)], 207.1 (35) [M$^+$-NHC-Cl].

2d: ^{1}H NMR (DMSO) (δ,ppm): 210.6 (Rh-C), 4.86 (s, 2H, CH-NHC), 3.45 (m,2H, CH-isopropyl), 2.34 (s,4H,CH-(COD)), 1.98 (s,8H, CH$_2$-(COD)) 1.5 (s,12H,CH$_3$-isopropyl)

^{13}C NMR (DMSO) (δ,ppm): 117.8 (CH, NHC), 66.7 (CH) 52.2 (CH,(COD)), 25(CH$_2$-(COD)), 22.5 (CH$_3$-isopropyl);

IR (ν, cm^{-1}): 3152 (m, CH aromatic), 2876 (m,CH), 1558 (w,m C=C aromatic), 1469,1426 (s, CH$_2$), 1387 (m, CH$_3$), 1048v (s, C-N);

MS (FAB, *m/z* (%)):254.2 (4) [M$^+$-Rh-Cl-(COD)], 153.3 (100) [M$^+$-NHC], 363.5 (7) [M$^+$- 2(CH3)], 289.3 (3.5) [M$^+$-(COD)], 339.6 (1) [M$^+$-Cl-CH$_3$].

2e: ^{1}H NMR (DMSO) (δ,ppm): 4.49 (s, 2H, CH-NHC), 3 (s,4H,CH-(COD)), 2.1 (s,8H, CH$_2$-(COD)), 1.41(m, 18H, CH$_3$)

^{13}C NMR (DMSO) (δ,ppm): 211.2 (Rh-C), 129 (CH, NHC), 64.1 (C-ditertbutyl), 50.2 (CH, (COD)), 28.1 (CH$_2$-(COD)), 27(CH$_3$);

IR (ν, cm^{-1}): 3141 (m, CH aromatic), 2980 (m,CH), 1634 (w,m C=C aromatic), 1374 (m, CH$_3$), 1033 (s, C-N);

MS (FAB, *m/z* (%)):183.2 (100) [M$^+$-Rh-Cl-(COD)], 326.9 (10) [M$^+$-Cl-4(CH$_3$)], 207 (35) [M$^+$- (COD)- 2(tertbutyl)], 221 (15) [M$^+$-(COD)-Cl-4(CH$_3$)], 281 (20) [M$^+$-Cl-(COD)].

5.7. GENERAL PROCEDURE FOR SYNTHESIS OF RHODIUM-*NHC*-CO COMPLEXES

The complexes **2a-2e** were dissolved in 50 ml of DCM. Carbon Monoxide was bubbled through this solution for 15 minutes. The yellow-white precipitate was filtered by cannular under vacuum, washed with hexane and dried overnight under vacuum. Physical data for the complexes is given in **Table 5.3**.

Table 5.3. Identification of rhodium-NHC-CO complexes.

Complex	NHC Complex	Colour	Yield (%)
3a	1,3-bis-(2,4,6-trimethylphenyl)-imidazol-2-ylidene	Yellow-white	89
3b	1,3-bis-(2,6-diisopropylphenyl)-imidazol-2-ylidene	Yellow-white	90
3c	1,3-bis(1-adamantyl)-imidazol-2-ylidene	Yellow-white	88
3d	1,3-diisopropyl-imidazol-2-ylidene	Yellow-white	87
3e	1,3-di-tert-butyl-imidazol-2-ylidene	Yellow-white	86

3a: ^{1}H NMR (CDCl$_3$) (δ,ppm): δ 6.93 (m, 4H, CH phenyl), δ 4.41 (d, 2H, CH-NHC), 2.34 (12 H, CH$_3$) 2.25 (6 H, CH$_3$);

^{13}C NMR (CDCl$_3$) (δ,ppm): 211.2 (Rh-C), 168.1, 159.2(CO), 139.7 (C, phenyl), 134.2 (C, phenyl), 129.2 (CH, phenyl), 92 (CH, NHC), 20 (CH$_3$), 17 (CH$_3$);

IR (ν, cm^{-1}): 3034 (m, CH aromatic), 2919 (m,CH), 2067, 1998 (s, Rh-CO), 1627` (w,m C=C aromatic), 1484,1464 (s, CH), 1380 (m, CH$_3$), 1262v(s, C-N), 852 (s, N-phenyl);

MS (FAB, *m/z* (%)):207 (100) [M^+- Cl - 2(CO) - 2(PhMe$_3$)], 307.2 (98) [M^+-NHC], 326.9 (40) [M^+- 2(CO) -PhMe$_3$], 340.9 (25) [M^+-CO -PhMe$_3$-CH$_3$], 281 (65) [M^+-2CO-PhMe$_3$-Me$_3$].

3b: ^{1}H NMR (CDCl$_3$) (δ,ppm): 7.34 (m, 12H, CH phenyl), δ 4 (d, 2H, CH-NHC), 3.33 (4 H, CH) 1.37 (24 H, CH$_3$);

^{13}C NMR (CDCl$_3$) (δ,ppm):   210.5 (Rh-C), 166.5, 146.2(CO)   134.2 (C,   phenyl), 128.5(CH, phenyl), 123.5 (CH, phenyl), 91.8 (CH, NHC), 67.8 (CH-isopropyl), 25.8 (CH$_3$);

IR (v, cm^{-1}): 3105 (w, CH aromatic), 2962 (m,CH), 2067, 1986v (s, Rh-CO), 1660, 1590` (w,m C=C aromatic), 1446,1419 (s, CH), 1384 (m, CH$_3$), 1261 (s, C-N), 801v (s, N-phenyl);

MS (FAB, *m/z* (%)):489.1 (100) [M^+- Cl - 2(CO)], 154 (98) [M^+-Cl-NHC], 387.2 (70) [M^+- Cl-Rh-2CO], 232.1   (35) [M^+-(diisopropylphenyl)-CO], 549 (25) [M^+-Cl].

3c: ^{1}H NMR (CDCl$_3$) (δ,ppm):   4.16 (d, 2H, CH-NHC), 2.24 (6 H, CH), 2.14 (12 H, CH$_2$), 1.71 (12 H, CH$_2$);

^{13}C NMR (CDCl$_3$) (δ,ppm): 210.2 (Rh-C), 162.3, 159.2 (CO), 117.6 (CH, NHC), 41.5 (C, adamantane),   34.2(CH,   adamantane),   32.5(CH$_2$, adamantane),   28.4   (CH$_2$, adamantane);

IR (v, cm^{-1}): 3167 (w, CH aromatic), 2910 (m,CH), 2064, 1987 (s, Rh-CO), 1623, 1547 (w,m C=C aromatic), 1454 (s, CH$_2$), 1156 (s, C-N);

MS (FAB, *m/z* (%)):337.1 (100) [M^+- Cl – Rh-2(CO)], 154 (30) [M^+-Cl-NHC].

3d: ^{1}H NMR (CDCl$_3$) (δ,ppm): 4.87 (s, 2H, CH-NHC), 3.52 (m,2H, CH), 1.9 (24, CH$_3$); **^{13}C NMR (CDCl$_3$)** (δ,ppm): 208.7 (Rh-C), 165.3, 146.1, CO), 123.4 (CH,NHC), 53.1 (CH-isopropyl),25.8 (CH$_3$);

IR (v, cm^{-1}): 3144 (w, CH aromatic), 2980 (m,CH), 2062, 1982 (s, Rh-CO), 1637 (s, C=C aromatic), 1466 (s, CH), 1374 (m, CH$_3$), 1033 (s, C-N).

3e: ^{1}H NMR (CDCl$_3$) (δ,ppm): 4.51 (s, 2H, CH-NHC), 1.38 (m,18 H, CH$_3$);

^{13}C NMR (CDCl$_3$) (δ,ppm): 208.9 (Rh-C), 166, 147.3 (CO), 128.1 (CH, NHC), 63.5 (C-ditertbutyl), 27.2 (CH$_3$-ditertbutyl);

IR (v, cm^{-1}): 3140 (w, CH aromatic), 2976 (m,CH), 2062, 1983 (s, Rh-CO), 1630 (s, C=C aromatic), 1380 (m, CH$_3$), 1036 (s, C-N);

MS (FAB, *m/z* (%)):183.2 (100) [M$^+$-Rh-Cl-(COD)], 289 (15) [M$^+$-CO-2(CH$_3$)], 203.1 (9) [M$^+$- CO- 2(tertbutyl)], 307 (15) [M$^+$-Cl-2(CH$_3$)].

5.8. CATALYTIC TESTING OF RHODIUM-PHOSPHINE AND RHODIUM-NHC COMPLEXES

Hydrogen was bubbled into the reaction vessel (pear shaped flask) attached to a 100 ml gas syringe for 30 minutes. The catalyst (**1a,1d,1e** and **2a, 2b, 2c, 2d and 2e**) was then dissolved in the solvent and the syringe was filled with H$_2$. The substrate was introduced using a microsyringe and H$_2$ consumption was recorded against time. Reactions were done in duplicate to ensure reliable results.Completion of reactions were confirmed by injecting 100 µl of the solution into a GC. Reaction conditions and Hydrogenation setup are presented in **Table 5.4**. and **Figure 5.1.** respectively.

Table 5.4. Hydrogenation reaction conditions

Subtrates	**1-hexene, 1-heptene, 1-octene, cyclohexene**
Quantity of catalyst	10 mg
Quantity of olefin	0.04 ml
Temperature	25 ºC
H$_2$ Pressure	1 atm
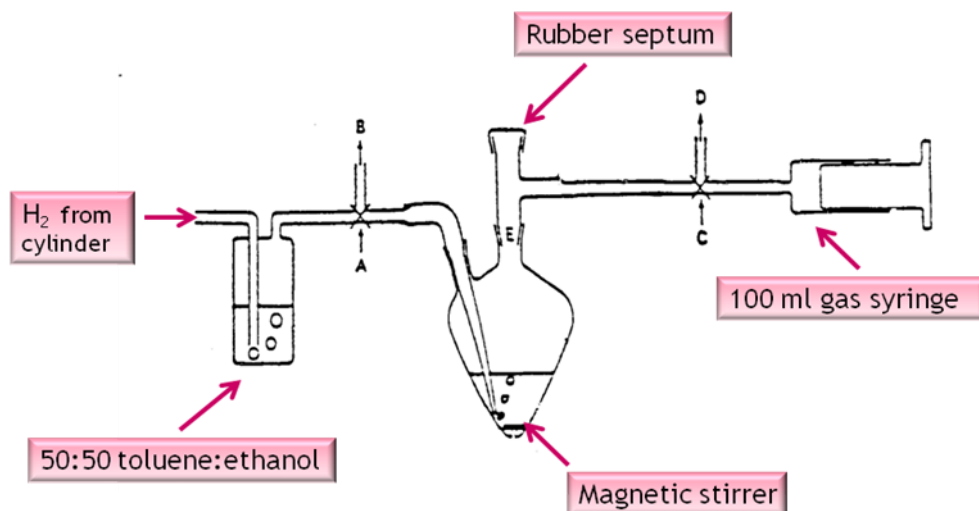
Figure 5.1. Simple hydrogenation setup.
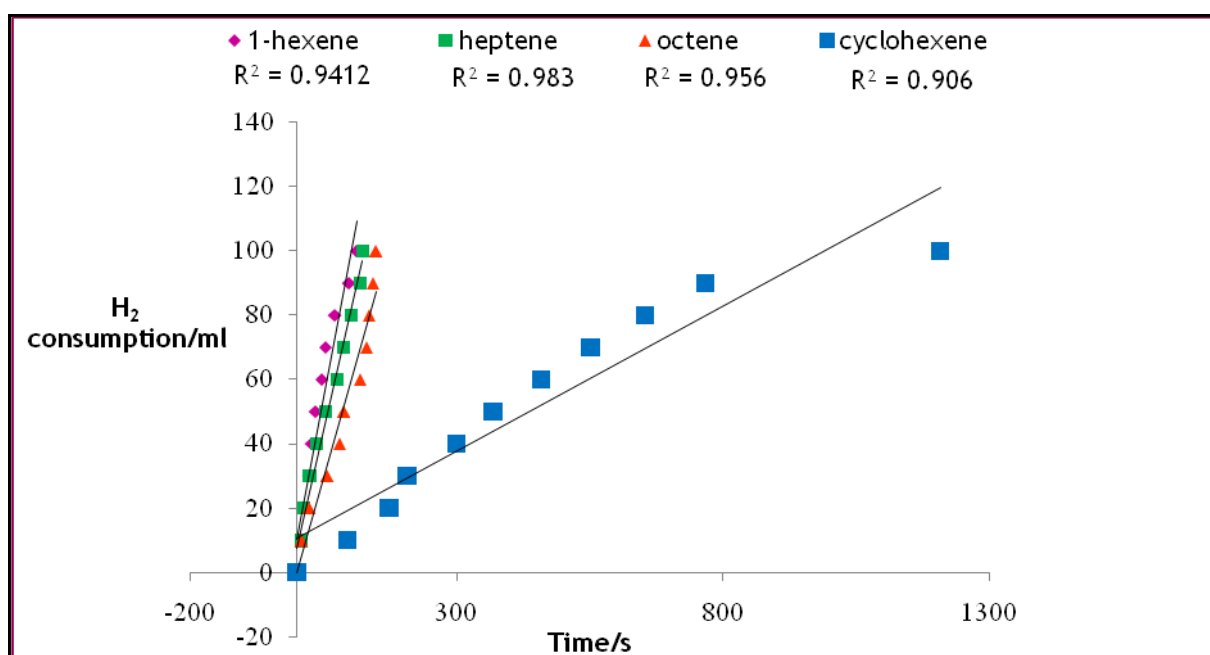
Figure 5.2. Graph of H_2 consumption against time for complex **1a**
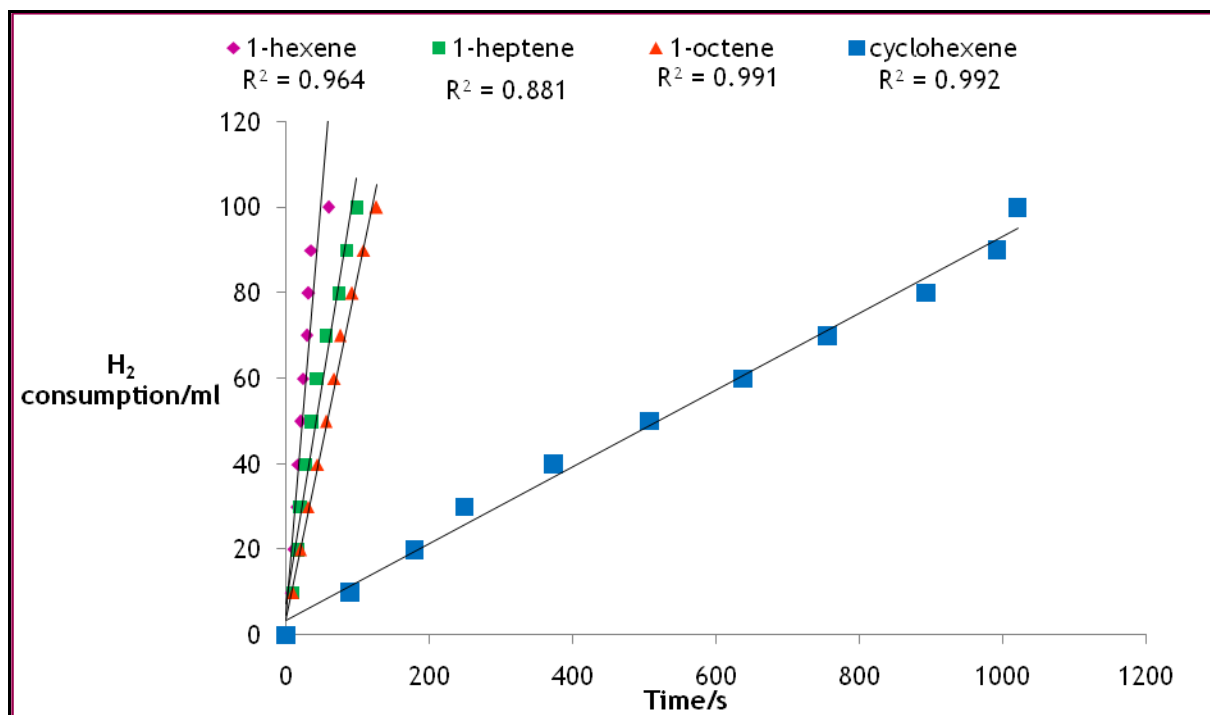
Figure 5.3. Graph of H_2 consumption against time for complex **1d**
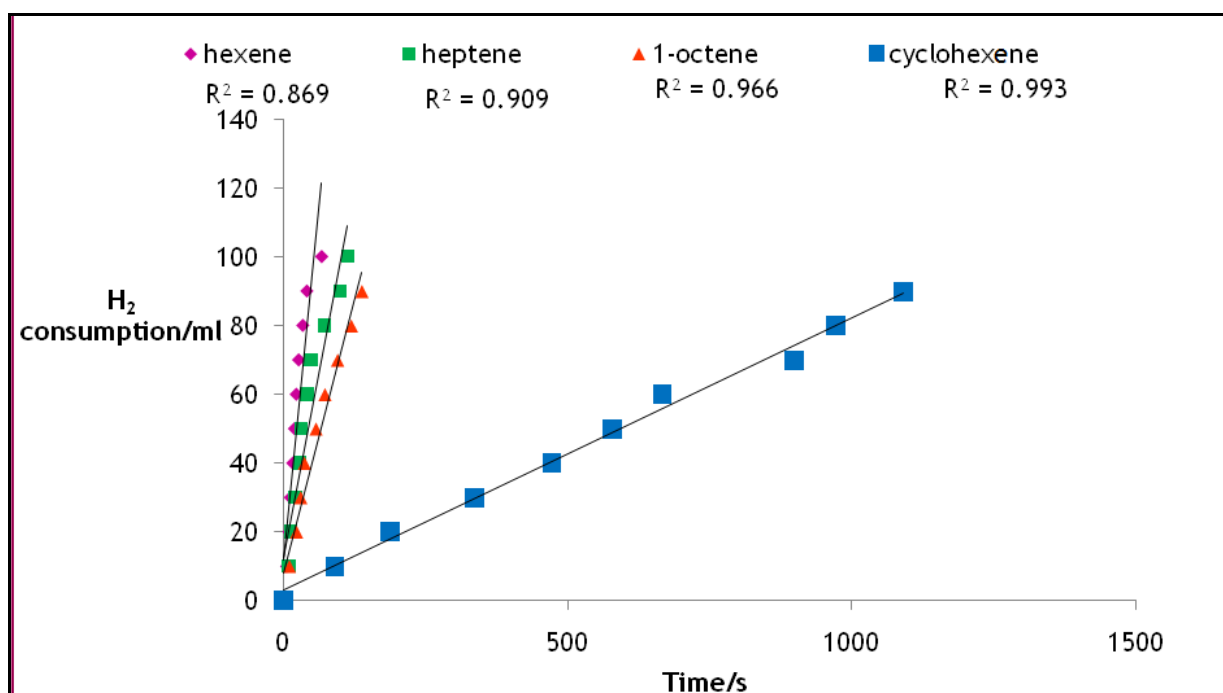
Figure 5.4. Graph of H_2 consumption against time for complex **1e**
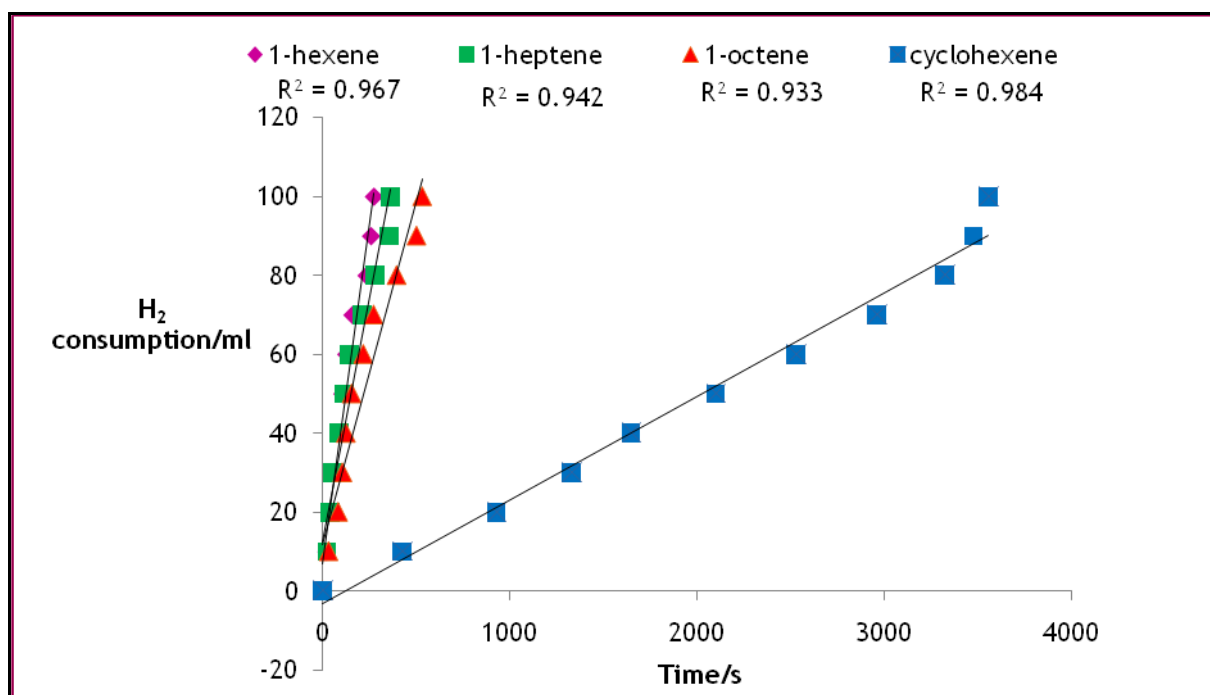
Figure 5.5. Graph of H_2 consumption against time for complex **2a**
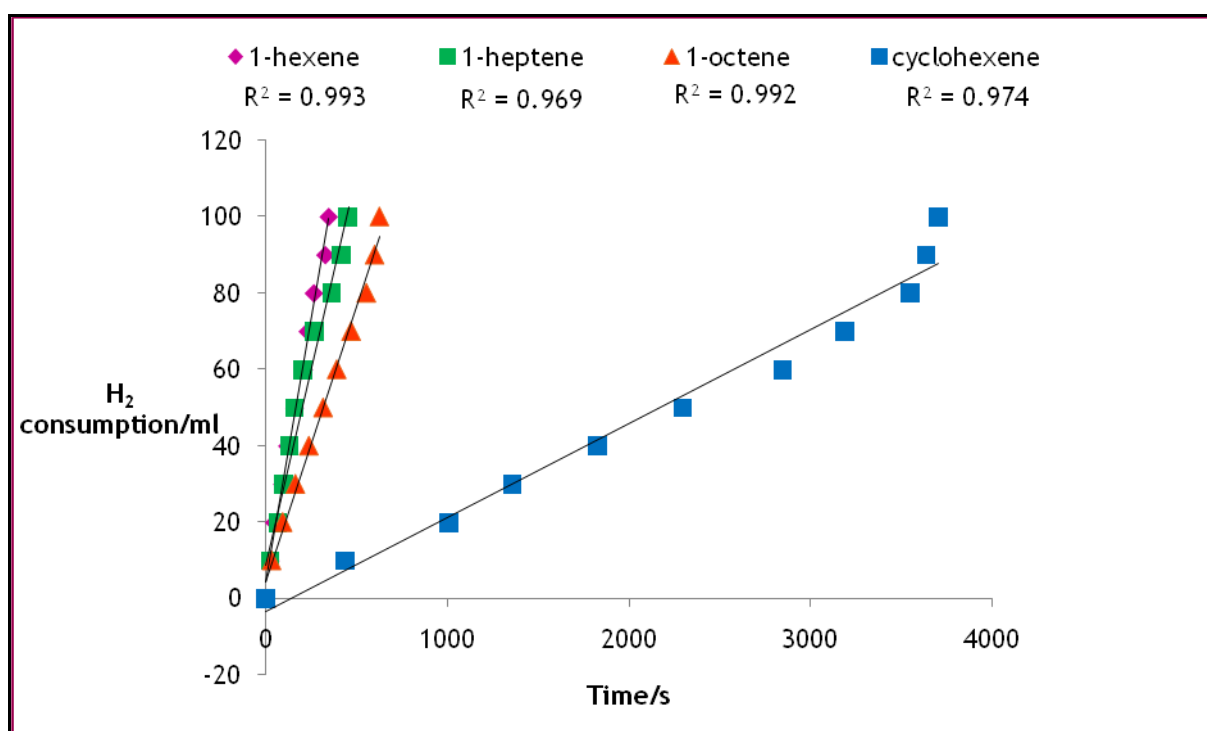
Fig 5.6. Graph of H_2 consumption against time for complex **2b**
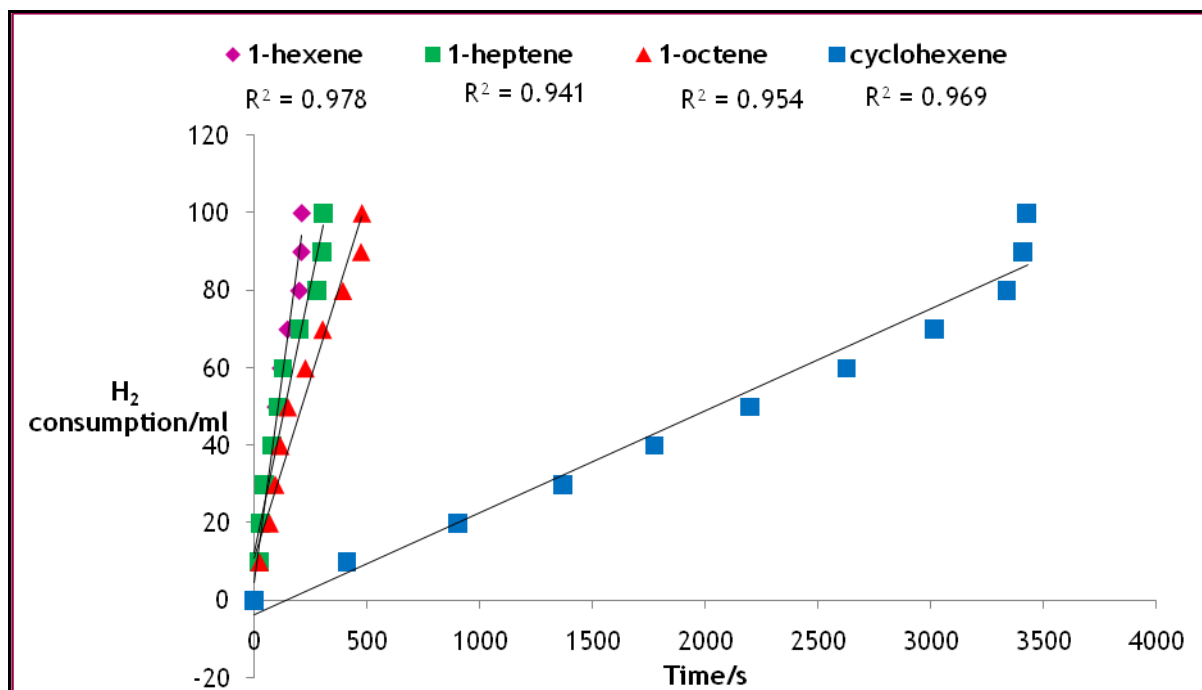
Fig 5.7. Graph of H_2 consumption against time for complex **2c**
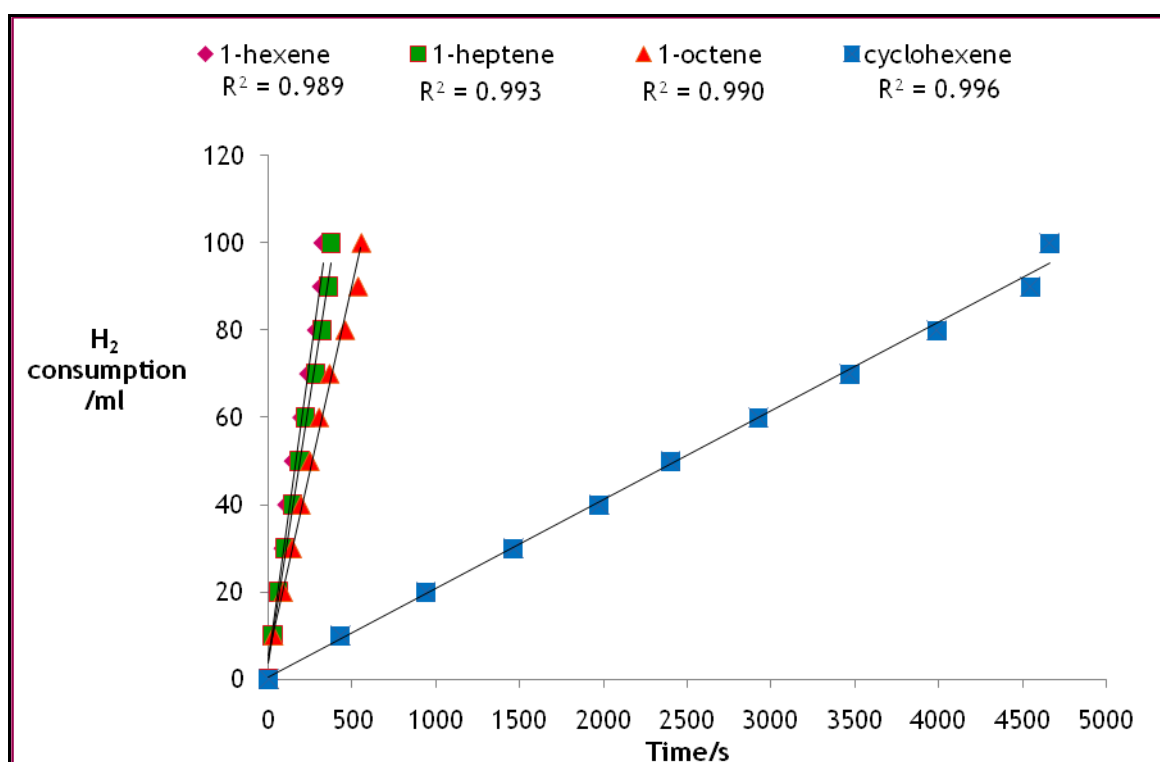
Figure 5.8. Graph of H_2 consumption against time for complex **2d**
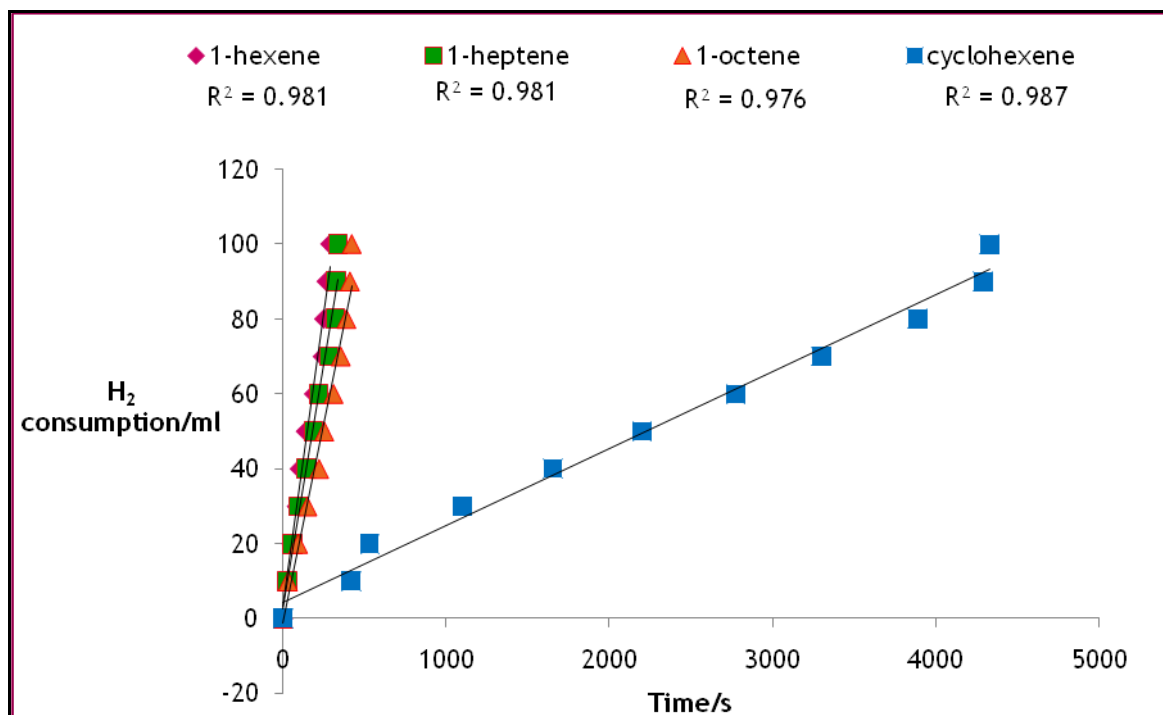
Figure 5.9. Graph of H_2 consumption against time for complex **2e**

5.9. REFERENCES

1) Bruker. *APEX2*. Version 2.0-1. Bruker AXS Inc., Madison, Wisconsin, USA, 2005.

2) Bruker. *SAINT+*. Version 6.0. (includes XPREP and SADABS) Bruker AXS Inc., Madison, Wisconsin, USA, 2005.

3) Bruker. *SHELXTL*. Version 5.1. (includes XS, XL, XP, XSHELL) Bruker AXS Inc., Madison, Wisconsin, USA, 1999.

4) L.J. Farrugia, *J. Appl. Cryst.*, 1997, **30**, 565.

5) A.L. Spek, *J. Appl. Cryst.*, 2003, **36**, 7.

6 CONCLUSIONS

Five rhodium-phosphine complexes **1a**: Rh(PPh$_3$)$_3$Cl, **1b**: Rh(PPh$_2$Me)$_3$Cl, **1c**: Rh(PPh$_2$Et)$_3$Cl, **1d**: Rh(PPhMe$_2$)$_3$Cl, **1e**: Rh(PPhMe$_2$)$_3$Cl have been successfully synthesised and characterised. Also, five rhodium-NHC-(COD) complexes **2a, 2b, 2c, 2d** and **2e** have been synthesised and characterised and five related rhodium-NHC-CO complexes **3a, 3b, 3c, 3d** and **3e** have been successfully synthesised and characterised. Complexes **1a-c** are Rh(I) products and Ccomplexes **1d** and **1e** are Rh(III) products.

Complexes **1a, 1d, 1e, 2a, 2b, 2c, 2d** and **2e** function as catalysts for the hydrogenation of alkenes. For the rhodium-phosphine complexes the catalyst efficiency based on TOF increases is in the following order: **1a > 1d > 1e**. For the rhodium-NHC-(COD) complexes catalyst efficiency based on TOF increases in the following order: **2d > 2b > 2e > 2a > 2c.**

While rhodium-phosphine complexes are far more active than rhodium-(COD)-NHC complexes, the latter seem to be active for a longer time and hence more stable under mild hydrogenation conditions.

APPENDIX

Crystal structure solution and refinement-Face indexed

Table 1. Atomic coordinates (x 10^4) and equivalent isotropic displacement parameters (Å^2x 10^3) for **1d**. U(eq) is defined as one third of the trace of the orthogonalized U^{ij} tensor.

	x	y	z	U(eq)
C(1)	1653(2)	1504(2)	3292(1)	19(1)
C(2)	2204(2)	1211(2)	3952(1)	23(1)
C(3)	1924(2)	448(2)	4579(1)	27(1)
C(4)	1109(2)	-38(2)	4555(1)	27(1)
C(5)	562(2)	245(2)	3911(1)	26(1)
C(6)	830(2)	1019(2)	3290(1)	23(1)
C(7)	1206(2)	2458(2)	1691(1)	27(1)
C(8)	2761(2)	1135(2)	2055(1)	31(1)
C(9)	1072(1)	4319(2)	3901(1)	18(1)
C(10)	894(2)	3682(2)	4621(1)	22(1)
C(11)	97(2)	3174(2)	4741(1)	25(1)
C(12)	-543(2)	3283(2)	4155(1)	26(1)
C(13)	-380(2)	3907(2)	3439(1)	25(1)
C(14)	415(2)	4428(2)	3317(1)	22(1)
C(15)	1804(2)	6784(2)	3739(2)	31(1)
C(16)	2695(2)	4861(3)	4678(1)	31(1)
C(17)	4073(2)	7042(2)	3521(1)	24(1)
C(18)	4635(2)	6404(3)	4065(1)	32(1)
C(19)	4899(2)	7022(3)	4775(2)	45(1)
C(20)	4606(2)	8244(3)	4949(2)	48(1)
C(21)	4061(2)	8879(3)	4428(2)	45(1)
C(22)	3793(2)	8283(3)	3707(2)	32(1)
C(23)	3456(2)	7486(2)	1887(1)	32(1)
C(24)	4779(2)	5656(3)	2258(1)	32(1)
P(1)	2070(1)	2396(1)	2442(1)	19(1)
P(2)	2101(1)	5066(1)	3732(1)	18(1)
P(3)	3757(1)	6195(1)	2592(1)	20(1)
Cl(1)	1736(1)	5616(1)	1853(1)	24(1)
Cl(2)	3381(1)	3878(1)	1332(1)	28(1)
Cl(3)	3844(1)	3297(1)	3353(1)	22(1)
Rh(1)	2779(1)	4429(1)	2608(1)	15(1)

Table 2. Anisotropic displacement parameters ($\text{Å}^2 \times 10^3$) for **1d**. The anisotropic displacement factor exponent takes the form: $-2\pi^2[h^2 a^{*2} U^{11} + \ldots + 2 h k a^* b^* U^{12}]$

	U^{11}	U^{22}	U^{33}	U^{23}	U^{13}	U^{12}
C(1)	23(1)	15(1)	19(1)	-2(1)	0(1)	1(1)
C(2)	19(1)	23(1)	27(1)	3(1)	-2(1)	-2(1)
C(3)	29(2)	27(2)	25(1)	4(1)	-3(1)	5(1)
C(4)	35(2)	21(1)	26(1)	3(1)	6(1)	-1(1)
C(5)	23(1)	24(1)	32(1)	-6(1)	6(1)	-4(1)
C(6)	26(1)	21(1)	21(1)	-5(1)	-2(1)	-2(1)
C(7)	33(2)	28(2)	19(1)	-1(1)	-6(1)	-4(1)
C(8)	37(2)	23(1)	32(1)	-5(1)	6(1)	4(1)
C(9)	17(1)	16(1)	21(1)	-2(1)	3(1)	2(1)
C(10)	24(1)	23(1)	20(1)	-1(1)	2(1)	1(1)
C(11)	29(2)	25(1)	22(1)	0(1)	8(1)	0(1)
C(12)	20(1)	24(1)	34(1)	-3(1)	7(1)	-3(1)
C(13)	18(1)	25(1)	32(1)	-1(1)	-2(1)	2(1)
C(14)	22(1)	20(1)	23(1)	4(1)	3(1)	4(1)
C(15)	30(2)	21(1)	42(2)	-9(1)	12(1)	-3(1)
C(16)	23(1)	50(2)	20(1)	-5(1)	0(1)	-7(1)
C(17)	21(1)	27(2)	23(1)	2(1)	1(1)	-10(1)
C(18)	34(2)	33(2)	30(1)	6(1)	-6(1)	-10(1)
C(19)	45(2)	58(2)	31(2)	8(1)	-12(1)	-25(2)
C(20)	49(2)	67(2)	28(2)	-13(2)	5(1)	-30(2)
C(21)	38(2)	49(2)	49(2)	-23(2)	11(1)	-13(2)
C(22)	26(2)	31(2)	39(2)	-7(1)	2(1)	-7(1)
C(23)	39(2)	27(2)	30(1)	10(1)	-5(1)	-4(1)
C(24)	22(1)	35(2)	38(2)	3(1)	10(1)	-3(1)
P(1)	21(1)	18(1)	17(1)	-1(1)	-2(1)	1(1)
P(2)	17(1)	22(1)	17(1)	-2(1)	2(1)	0(1)
P(3)	20(1)	20(1)	20(1)	3(1)	0(1)	-2(1)
Cl(1)	22(1)	27(1)	24(1)	7(1)	-4(1)	3(1)
Cl(2)	31(1)	36(1)	19(1)	-2(1)	7(1)	1(1)
Cl(3)	18(1)	23(1)	24(1)	3(1)	-3(1)	3(1)
Rh(1)	15(1)	17(1)	14(1)	1(1)	0(1)	1(1)

Table 3. Hydrogen coordinates (x 10^4) and isotropic displacement parameters ($Å^2$x 10^3) for **1d**.

	x	y	z	U(e
H(2)	2770	1537	3969	28
H(3)	2296	261	5028	32
H(4)	922	-570	4983	33
H(5)	-1	-94	3894	31
H(6)	445	1224	2854	27
H(7A)	1030	1564	1547	40
H(7B)	1396	2913	1211	40
H(7C)	724	2930	1909	40
H(8A)	2438	322	1972	46
H(8B)	3236	979	2442	46
H(8C)	2983	1423	1541	46
H(10)	1327	3599	5031	27
H(11)	-12	2745	5233	30
H(12)	-1091	2932	4242	31
H(13)	-816	3979	3030	30
H(14)	517	4868	2826	26
H(15A)	1477	6968	4216	46
H(15B)	1457	6986	3253	46
H(15C)	2319	7326	3752	46
H(16A)	3239	5322	4655	46
H(16B)	2799	3926	4776	46
H(16C)	2368	5222	5116	46
H(18)	4834	5548	3948	39
H(19)	5286	6593	5141	54
H(20)	4785	8656	5440	57
H(21)	3862	9731	4555	54
H(22)	3416	8733	3342	38
H(23A)	2946	7931	2070	48
H(23B)	3337	7106	1353	48
H(23C)	3922	8120	1858	48
H(24A)	5175	6398	2266	47
H(24B)	4715	5311	1709	47
H(24C)	5003	4967	2619	47

Table 4. Atomic coordinates (x 10^4) and equivalent isotropic displacement parameters ($\mathring{A}^2$x 10^3)

For **1e**. U(eq) is defined as one third of the trace of the orthogonalized U^{ij} tensor.

	x	y	z	U(eq)
				C(1)
C(2)	-2909(2)	7017(1)	1337(1)	22(1)
C(3)	-4224(2)	7119(1)	1286(1)	27(1)
C(4)	-4796(2)	7532(2)	784(1)	31(1)
C(5)	-4058(2)	7839(1)	329(1)	32(1)
C(6)	-2744(2)	7747(1)	378(1)	26(1)
C(7)	137(2)	7540(1)	246(1)	25(1)
C(8)	1528(2)	7302(2)	151(1)	31(1)
C(9)	-272(2)	5837(1)	975(1)	26(1)
C(10)	-1161(2)	5293(2)	539(1)	44(1)
C(11)	-1872(2)	9525(1)	1329(1)	18(1)
C(12)	-1270(2)	9822(1)	822(1)	24(1)
C(13)	-1966(2)	10237(1)	348(1)	31(1)
C(14)	-3265(2)	10382(2)	382(1)	34(1)
C(15)	-3865(2)	10109(2)	883(1)	32(1)
C(16)	-3176(2)	9676(1)	1356(1)	24(1)
C(17)	-224(2)	10245(1)	2240(1)	20(1)
C(18)	-1021(2)	11177(1)	2131(1)	25(1)
C(19)	-2074(2)	8675(1)	2507(1)	19(1)
C(20)	-2592(2)	9440(1)	2929(1)	24(1)
C(21)	833(2)	8590(1)	3387(1)	19(1)
C(22)	924(2)	9514(1)	3653(1)	26(1)
C(23)	209(2)	9733(2)	4139(1)	34(1)
C(24)	-595(2)	9044(2)	4362(1)	34(1)
C(25)	-682(2)	8123(2)	4108(1)	30(1)
C(26)	31(2)	7890(1)	3629(1)	23(1)
C(27)	2976(2)	9204(1)	2725(1)	24(1)
C(28)	4124(2)	8908(2)	2373(1)	32(1)
C(29)	2603(2)	7162(1)	3044(1)	25(1)
C(30)	3316(2)	7315(2)	3643(1)	39(1)
P(1)	-427(1)	7186(1)	971(1)	18(1)
P(2)	-924(1)	9076(1)	1972(1)	14(1)
P(3)	1755(1)	8251(1)	2750(1)	16(1)
Rh(1)	613(1)	7892(1)	1827(1)	13(1)
Cl(1)	2337(1)	6767(1)	1628(1)	22(1)
Cl(2)	1705(1)	9095(1)	1295(1)	20(1)
Cl(3)	-363(1)	6636(1)	2365(1)	19(1)

Table 5.   Anisotropic displacement parameters (Å^{2}x 10^3) for **1e**.   The anisotropic displacement factor exponent takes the form: -2$\square^2$[h^{2}a*^{2}U^{11} + ... + 2 h k a* b* U^{12}]

	U^{11}	U^{22}	U^{33}	U^{23}	U^{13}	U^{12}
C(1)	18(1)	22(1)	21(1)	-6(1)	1(1)	-4(1)
C(2)	19(1)	23(1)	24(1)	-2(1)	2(1)	-4(1)
C(3)	20(1)	29(1)	33(1)	-4(1)	5(1)	-6(1)
C(4)	16(1)	36(1)	42(1)	-5(1)	-3(1)	-3(1)
C(5)	28(1)	37(1)	30(1)	-4(1)	-10(1)	-1(1)
C(6)	26(1)	33(1)	19(1)	-4(1)	0(1)	-6(1)
C(7)	24(1)	34(1)	19(1)	-5(1)	6(1)	-5(1)
C(8)	27(1)	38(1)	29(1)	-8(1)	12(1)	-5(1)
C(9)	28(1)	21(1)	30(1)	-9(1)	6(1)	-4(1)
C(10)	38(1)	36(1)	57(1)	-27(1)	6(1)	-10(1)
C(11)	19(1)	16(1)	19(1)	0(1)	-1(1)	1(1)
C(12)	23(1)	26(1)	23(1)	4(1)	1(1)	-1(1)
C(13)	38(1)	31(1)	24(1)	9(1)	-1(1)	-1(1)
C(14)	38(1)	32(1)	31(1)	7(1)	-13(1)	4(1)
C(15)	22(1)	36(1)	38(1)	2(1)	-7(1)	6(1)
C(16)	21(1)	29(1)	23(1)	0(1)	1(1)	2(1)
C(17)	19(1)	16(1)	25(1)	-2(1)	1(1)	0(1)
C(18)	28(1)	15(1)	32(1)	-2(1)	2(1)	2(1)
C(19)	17(1)	19(1)	20(1)	1(1)	4(1)	2(1)
C(20)	22(1)	26(1)	24(1)	-4(1)	7(1)	2(1)
C(21)	20(1)	21(1)	16(1)	-1(1)	-1(1)	4(1)
C(22)	33(1)	23(1)	20(1)	-1(1)	-3(1)	3(1)
C(23)	47(1)	32(1)	23(1)	-6(1)	-3(1)	15(1)
C(24)	37(1)	47(1)	19(1)	1(1)	4(1)	17(1)
C(25)	26(1)	42(1)	21(1)	7(1)	4(1)	5(1)
C(26)	24(1)	26(1)	20(1)	0(1)	1(1)	2(1)
C(27)	20(1)	24(1)	28(1)	-3(1)	1(1)	-5(1)
C(28)	17(1)	36(1)	41(1)	-1(1)	4(1)	-5(1)
C(29)	23(1)	24(1)	26(1)	3(1)	-2(1)	7(1)
C(30)	38(1)	48(1)	29(1)	1(1)	-8(1)	16(1)
P(1)	16(1)	20(1)	17(1)	-4(1)	3(1)	-4(1)
P(2)	13(1)	14(1)	16(1)	0(1)	2(1)	1(1)
P(3)	14(1)	16(1)	18(1)	-1(1)	1(1)	0(1)
Rh(1)	11(1)	12(1)	16(1)	-1(1)	3(1)	0(1)
Cl(1)	18(1)	20(1)	29(1)	-3(1)	5(1)	4(1)
Cl(2)	18(1)	20(1)	23(1)	3(1)	6(1)	-3(1)
Cl(3)	20(1)	15(1)	22(1)	1(1)	4(1)	-3(1)

Table 5.   Hydrogen coordinates (x 10^4) and isotropic displacement parameters (Å^2 x 10^3) for **1e**.

	x	y	z	U(eq)
H(2)	-2522	6727	1683	26
H(3)	-4730	6902	1597	33
H(4)	-5694	7606	751	38
H(5)	-4452	8115	-19	38
H(6)	-2246	7963	64	31
H(7A)	-396	7203	-65	30
H(7B)	9	8258	193	30
H(8A)	2071	7674	435	47
H(8B)	1734	7484	-252	47
H(8C)	1673	6595	210	47
H(9A)	615	5666	889	32
H(9B)	-426	5596	1378	32
H(10A)	-2044	5399	643	65
H(10B)	-968	4587	553	65
H(10C)	-1044	5542	138	65
H(12)	-377	9740	801	28
H(13)	-1553	10422	0	37
H(14)	-3740	10670	59	41
H(15)	-4753	10215	907	39
H(16)	-3600	9484	1699	29
H(17A)	-37	10184	2671	24
H(17B)	598	10337	2052	24
H(18A)	-1162	11280	1704	38
H(18B)	-569	11745	2306	38
H(18C)	-1842	11102	2313	38
H(19A)	-2808	8379	2282	22
H(19B)	-1671	8144	2750	22
H(20A)	-1883	9754	3153	36
H(20B)	-3152	9115	3204	36
H(20C)	-3074	9940	2701	36
H(22)	1477	9997	3502	31
H(23)	277	10366	4317	41
H(24)	-1088	9201	4690	41
H(25)	-1236	7645	4263	36
H(26)	-24	7248	3462	28
H(27A)	2590	9806	2546	29
H(27B)	3275	9368	3134	29
H(28A)	4615	8401	2591	47
H(28B)	4663	9485	2316	47
H(28C)	3828	8647	1986	47
H(29A)	1982	6621	3083	30
H(29B)	3221	6949	2753	30
H(30A)	3996	7800	3600	58
H(30B)	3686	6688	3780	58
H(30C)	2723	7555	3931	58

Table 6. Torsion angles [°] for **1e**.

_____

C(6)-C(1)-C(2)-C(3)	-1.2(3)
P(1)-C(1)-C(2)-C(3)	-179.67(13)
C(1)-C(2)-C(3)-C(4)	0.5(3)
C(2)-C(3)-C(4)-C(5)	0.6(3)
C(3)-C(4)-C(5)-C(6)	-1.0(3)
C(4)-C(5)-C(6)-C(1)	0.3(3)
C(2)-C(1)-C(6)-C(5)	0.8(3)
P(1)-C(1)-C(6)-C(5)	179.20(14)
C(16)-C(11)-C(12)-C(13)	-1.7(3)
P(2)-C(11)-C(12)-C(13)	-174.89(14)
C(11)-C(12)-C(13)-C(14)	1.7(3)
C(12)-C(13)-C(14)-C(15)	-0.5(3)
C(13)-C(14)-C(15)-C(16)	-0.7(3)
C(12)-C(11)-C(16)-C(15)	0.6(3)
P(2)-C(11)-C(16)-C(15)	173.68(14)
C(14)-C(15)-C(16)-C(11)	0.6(3)
C(26)-C(21)-C(22)-C(23)	-1.4(3)
P(3)-C(21)-C(22)-C(23)	-179.60(14)
C(21)-C(22)-C(23)-C(24)	0.0(3)
C(22)-C(23)-C(24)-C(25)	0.8(3)
C(23)-C(24)-C(25)-C(26)	-0.1(3)
C(24)-C(25)-C(26)-C(21)	-1.3(3)
C(22)-C(21)-C(26)-C(25)	2.0(3)
P(3)-C(21)-C(26)-C(25)	-179.72(13)
C(6)-C(1)-P(1)-C(7)	-6.09(17)
C(2)-C(1)-P(1)-C(7)	172.33(13)
C(6)-C(1)-P(1)-C(9)	-113.28(15)
C(2)-C(1)-P(1)-C(9)	65.14(15)
C(6)-C(1)-P(1)-Rh(1)	125.42(13)
C(2)-C(1)-P(1)-Rh(1)	-56.15(15)
C(8)-C(7)-P(1)-C(1)	-169.21(13)
C(8)-C(7)-P(1)-C(9)	-63.38(15)
C(8)-C(7)-P(1)-Rh(1)	59.63(15)
C(10)-C(9)-P(1)-C(1)	39.84(16)
C(10)-C(9)-P(1)-C(7)	-67.29(16)
C(10)-C(9)-P(1)-Rh(1)	165.33(13)
C(16)-C(11)-P(2)-C(19)	11.44(16)
C(12)-C(11)-P(2)-C(19)	-175.53(13)
C(16)-C(11)-P(2)-C(17)	-100.27(15)
C(12)-C(11)-P(2)-C(17)	72.76(15)
C(16)-C(11)-P(2)-Rh(1)	138.00(12)
C(12)-C(11)-P(2)-Rh(1)	-48.98(15)
C(20)-C(19)-P(2)-C(11)	-86.20(14)
C(20)-C(19)-P(2)-C(17)	19.77(15)
C(20)-C(19)-P(2)-Rh(1)	143.37(11)
C(18)-C(17)-P(2)-C(11)	30.96(15)
C(18)-C(17)-P(2)-C(19)	-79.16(14)
C(18)-C(17)-P(2)-Rh(1)	157.24(11)
C(28)-C(27)-P(3)-C(21)	160.27(13)
C(28)-C(27)-P(3)-C(29)	55.02(15)
C(28)-C(27)-P(3)-Rh(1)	-68.10(14)
C(22)-C(21)-P(3)-C(27)	14.56(16)
C(26)-C(21)-P(3)-C(27)	-163.66(14)

C(22)-C(21)-P(3)-C(29)	122.73(15)
C(26)-C(21)-P(3)-C(29)	-55.48(15)
C(22)-C(21)-P(3)-Rh(1)	-115.85(13)
C(26)-C(21)-P(3)-Rh(1)	65.93(14)
C(30)-C(29)-P(3)-C(27)	56.14(16)
C(30)-C(29)-P(3)-C(21)	-51.79(16)
C(30)-C(29)-P(3)-Rh(1)	-177.81(13)
C(11)-P(2)-Rh(1)-Cl(3)	-114.77(6)
C(19)-P(2)-Rh(1)-Cl(3)	8.74(6)
C(17)-P(2)-Rh(1)-Cl(3)	129.93(6)
C(11)-P(2)-Rh(1)-Cl(2)	66.29(6)
C(19)-P(2)-Rh(1)-Cl(2)	-170.20(6)
C(17)-P(2)-Rh(1)-Cl(2)	-49.01(6)
C(11)-P(2)-Rh(1)-P(1)	-27.98(6)
C(19)-P(2)-Rh(1)-P(1)	95.54(6)
C(17)-P(2)-Rh(1)-P(1)	-143.28(6)
C(11)-P(2)-Rh(1)-P(3)	160.01(6)
C(19)-P(2)-Rh(1)-P(3)	-76.47(6)
C(17)-P(2)-Rh(1)-P(3)	44.71(6)
C(1)-P(1)-Rh(1)-P(2)	-24.36(6)
C(7)-P(1)-Rh(1)-P(2)	100.21(7)
C(9)-P(1)-Rh(1)-P(2)	-140.67(6)
C(1)-P(1)-Rh(1)-Cl(3)	71.34(6)
C(7)-P(1)-Rh(1)-Cl(3)	-164.09(7)
C(9)-P(1)-Rh(1)-Cl(3)	-44.96(6)
C(1)-P(1)-Rh(1)-Cl(2)	-112.02(6)
C(7)-P(1)-Rh(1)-Cl(2)	12.55(7)
C(9)-P(1)-Rh(1)-Cl(2)	131.68(6)
C(1)-P(1)-Rh(1)-P(3)	114.10(9)
C(7)-P(1)-Rh(1)-P(3)	-121.33(9)
C(9)-P(1)-Rh(1)-P(3)	-2.20(10)
C(1)-P(1)-Rh(1)-Cl(1)	160.99(6)
C(7)-P(1)-Rh(1)-Cl(1)	-74.43(7)
C(9)-P(1)-Rh(1)-Cl(1)	44.69(6)
C(27)-P(3)-Rh(1)-P(2)	-88.89(7)
C(21)-P(3)-Rh(1)-P(2)	35.92(6)
C(29)-P(3)-Rh(1)-P(2)	151.64(7)
C(27)-P(3)-Rh(1)-Cl(3)	175.35(7)
C(21)-P(3)-Rh(1)-Cl(3)	-59.84(6)
C(29)-P(3)-Rh(1)-Cl(3)	55.88(7)
C(27)-P(3)-Rh(1)-Cl(2)	-1.43(7)
C(21)-P(3)-Rh(1)-Cl(2)	123.38(6)
C(29)-P(3)-Rh(1)-Cl(2)	-120.90(7)
C(27)-P(3)-Rh(1)-P(1)	132.50(9)
C(21)-P(3)-Rh(1)-P(1)	-102.70(9)
C(29)-P(3)-Rh(1)-P(1)	13.03(10)
C(27)-P(3)-Rh(1)-Cl(1)	85.72(7)
C(21)-P(3)-Rh(1)-Cl(1)	-149.47(6)
C(29)-P(3)-Rh(1)-Cl(1)	-33.75(7)